THE CONTRIBUTION OF FLUVIAL PROCESSES TO THE FORMATION OF CRYOPLANATION TERRACES: THE ROLE OF PERIGLACIAL SORTED STRIPES

By

Raven Jezell Mitchell

A THESIS

Submitted to
Michigan State University
in partial fulfillment of the requirements
for the degree of

Geography – Master of Science

2020

ABSTRACT

THE CONTRIBUTION OF FLUVIAL PROCESSES TO THE FORMATION OF CRYOPLANATION TERRACES: THE ROLE OF PERIGLACIAL SORTED STRIPES

By

Raven Jezell Mitchell

The mechanisms of material excavation and removal from large periglacial landforms known as cryoplanation terraces (CTs) have been debated for over a century. These unknowns hinder acceptance of a unified understanding of CT formation. The research reported in this thesis links sorted stripes—a type of periglacial patterned ground frequently encountered on CT treads—to the hydrologic connectivity of periglacial hillslopes, which has not been considered in the context of CT development. Traditional interpretations hold that the presence of sorted patterned ground indicates geomorphic quiescence, a view that has contributed to the dismissal of these features as a factor in the creation of periglacial topography. This thesis addresses the geomorphic role of sorted stripes as fluvial features by investigating their hydrologic effectiveness in removing weathered material from CT treads.

Process-focused investigations and watershed morphometric analysis were conducted on thee cryoplanation terraces in an active upland periglacial environment near Atlin, British Columbia, Canada. Results demonstrate the landscape-scale spatial organization and geomorphic effectiveness of sorted stripe networks for transporting water and suspended sediment across CT surfaces. A qualitative model of sediment production and transportation is presented that: 1) outlines erosional processes responsible for CT formation; and 2) defines the distinct hydrologic-geomorphic imprint imparted by sorted stripes on periglacial hillslopes.

ACKNOWLEDGMENTS

The thesis is the culmination of two years of hard work, exciting adventures, and new experiences, and represents my most rigorous academic pursuit to date. Without the help from many, this work would have been entirely impossible and significantly less fulfilling.

I would like to thank the members of my committee, Drs. Alan Arbogast and Ashton Shortridge for their careful and patient editing and for their willingness to lend a helping hand when needed. A special acknowledgment goes to my advisor, Dr. Fritz Nelson, who championed me throughout my degree and whose unwavering support and advising I will cherish for the rest of my life. To Dr. Kelsey Nyland, thank you for your patience, your mentorship, your help during my very first field season, and most of all, thank you for your continued belief in me. I also acknowledge Dr. Randall Schaetzl for the use of his laboratory facilities, Christopher Baish and Jarrod Knauff for help in the lab, and my fellow geography students for their comradery.

Acknowledgment is extended to the Department of Geography, Environment, and Spatial Sciences and to the College of Social Science for their generous funding over the years. Thank you to the Circumpolar Active Layer Monitoring (CALM) program, for affording me the opportunity to travel to some of the most beautiful and remote parts of the Arctic, for exposing me to permafrost research, and especially for the beautiful friendships forged through the months of fieldwork. I would also like to express my gratitude to the Juneau Icefield Research Program for use of their research facilities in British Columbia, which has enabled the work of myself and others since the 1970s.

Lastly, I would like to acknowledge my family. To my mother, grandmother, and little sister: thank you all for being my very own support team, offering encouragement when I needed it most. To my partner, Ally: thank you for wearing the hats of thesis editor, life coach, cheer team, and for always supporting my dreams. The love from you all was limitless.

Countless others assisted me over the last two years in innumerable ways—to them and to those named above, thank you!

TABLE OF CONTENTS

LIST OF TABLES

LIST OF FIGURES

Chapter 1 Introduction

Cryoplanation terraces (CTs) are large upland periglacial landforms resembling giant staircases, with series of gently sloping treads bounded by ascending steep risers (Figure 1.1). Although the formative mechanisms related to CT development are better understood today than they were at the onset of the 20th century when CTs were first documented, some aspects of CT formation and development remain mired in confusion (Ballantyne, 2018,   221)

Recent research has confirmed the importance of CT tread expansion through parallel retreat of scarps, demonstrating the time-transgressive nature of CT formation (Matthews et al., 2019; Nyland & Nelson, 2020). The most widely accepted hypothesis of tread expansion is the nivation hypothesis, which emphasizes the role of perennial snow cover in scarp erosion and subsequent transportation of snowbank meltwater and weathering products (Ballantyne, 2018, 221). Weathering near the snowpatch margin has been substantiated in recent years, and qualitative models of time-transgressive scrap retreat have been proposed (e.g. Kelsey E. Nyland & Nelson, 2020a) while the mass movement/transportation component of nivation on CT slopes has received little more than cursory investigation (Queen, 2018, 41; Nyland, 2019, 59; Thorn & Hall, 2002a, 545). Some geomorphologists have argued that, under the nivation hypothesis of CT formation, rampart-like accumulations of sediment should exist on subjacent treads near the scarp-tread junctions, representing past scarp positions. No such accumulations have been documented on cryoplanation terraces in unglaciated Beringia (Ballantyne, 2018, and references therein) and the absence of such ramparts has been used to question the nivation hypothesis of CT formation.

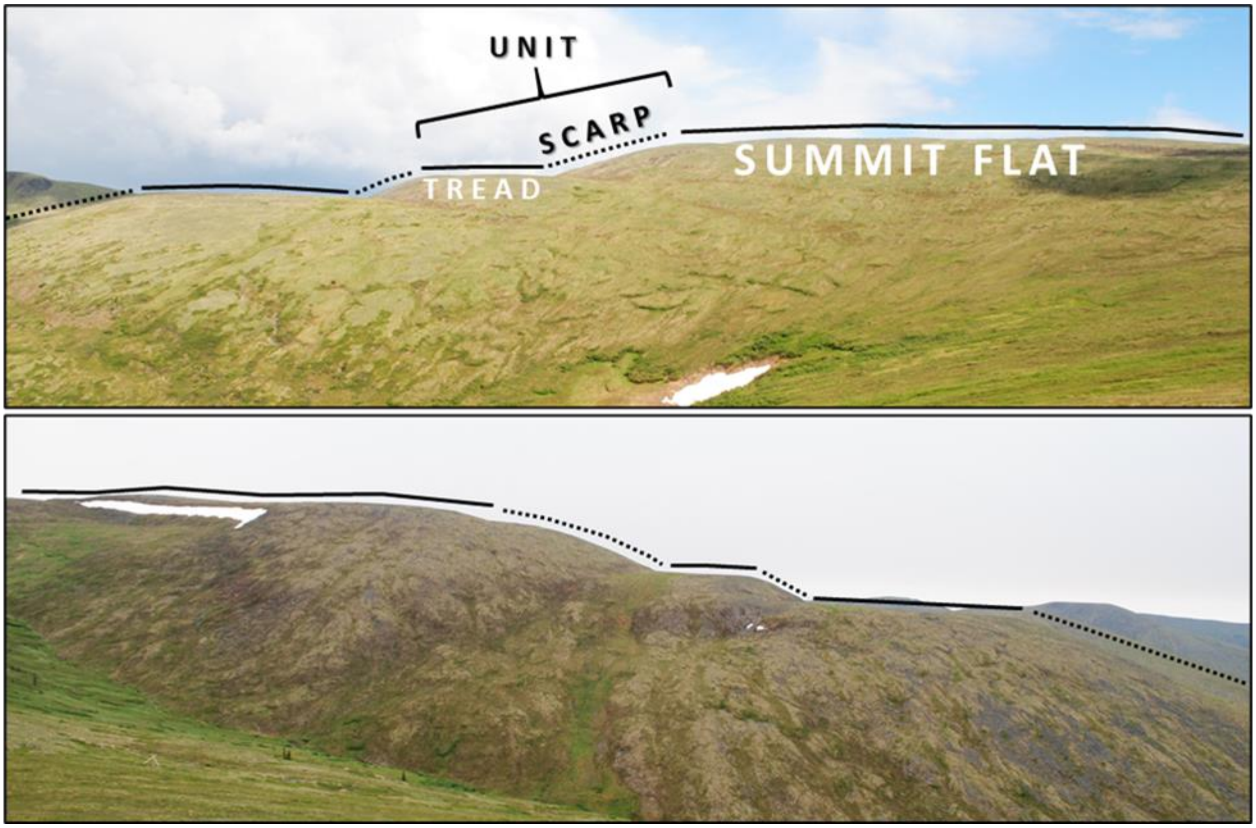

Figure 1.1 Examples of characteristic cryoplanation terraces at Eagle Summit, AK. Cryoplanation terraces (top and bottom) typical of upland, unglaciated Beringia. One tread (solid black lines) and its accompanying scarp (dotted black lines) comprise a cryoplanation terrace unit, labeled. Treads range in size from 10 to several hundred meters in both length and width, with slopes between 1-5°; scarp height ranges between 1-75 meters, with slopes between 15-40° (Reger & Péwé, 1976; Ballantyne, 2018, 220). Here, one CT unit is approximately 200 m in the horizontal dimension. Photos taken in July 2018 by R.J. Mitchell.

Some workers have alluded to the removal of eroded material in sorted stripes—a type of periglacial patterned ground—(e.g., Taylor, 1955; Demek, 1969; Thorn & Hall, 2002b; Queen, 2018; Nyland, 2019;) over lateral terrace margins, but few quantitative data exist to substantiate this proposition. Competing opinions within the literature assert the presence of patterned ground as being indicative of geomorphic quiescence (e.g., Karte, 1979, 1981; Thorn & Hall, 2002, 545), while others (Paquette et al., 2017a, 2018; Wilkinson & Bunting, 1975) emphasize the dynamic hydrologic and geomorphic controls implied by the presence of sorted patterned ground, although not in the context of cryoplanation. Given these diametrically opposing views, it is imperative that sorted stripes, which abound on CT treads (Nyland, 2019, 57), be made an investigative focal point about the mode of sediment transport on CT treads and side slopes.

1.1 Brief History of Cryoplanation Research

Across the spectrum of periglacial environments, CTs are some of the largest and most widespread landforms, giving rise to entire upland landscapes. Assemblages of periglacial microfeatures made up of frost-fractured rock, geometrically arranged ground, and solifluction lobes, characterize cryoplanated ridges. Despite the pervasiveness of CTs throughout periglacial regions and their distinct geomorphic imprint, workers since the opening of the 20th century have struggled to relate specific periglacial processes to CT formation, a trend that contributes to the current contention surrounding the origin of these features.

1.1.1 First encounters. Observational accounts of cryoplanation terraces in North America were first recorded in the early 1900s in the course of surveys by the United States and Canadian Geological Surveys (e.g., Prindle, 1905; Cairnes, 1912; Eakin, 1916; Mertie, 1937). These workers, who were trained under the dominant paradigm of W.M. Davis' *normal cycle of erosion*, struggled to reconcile their observations with Davisian principles.

Davis' "normal cycle of erosion" in humid temperate regions, conceived by creating an analogy with the life cycle of biological organisms, was based on the concept of geomorphic landscapes going through young, mature, and old stages. A cycle culminates in leveled surfaces of regional extent at low elevation, which Davis called *peneplains*. Following epeirogenic uplift or a drop in base level, which signals the beginning of a new geographic cycle, these peneplain surfaces are dissected by fluvial processes, leaving discontinuous remnants of former peneplains at relatively high elevation. However, the flat elevated surfaces observed in northwestern North America by early surveyors displayed non-accordant summit elevations at the local scale and were topped with angular clasts rather than the alluvium specified in Davis' criteria for identifying elevated peneplain remnants (see Thornbury 1969, 182-185). Davis (1909) also recognized the imprint of other climatic conditions on geomorphic landscapes, referring to them as the results of "climatic accidents." These include aridity and glaciation, for which he developed alternative cycles of erosion. Davis himself, however, did not develop a modification to the normal cycle that adjusted for periglacial climatic conditions and geomorphic processes.

1.1.2 Introduction of periglacial geomorphology. Around the time that CTs were first encountered, periglacial studies gained relevance in the European literature with the introduction of foundational periglacial terminology. Lozinski (1909) coined the term *periglacial* (*near glaciers*), the study of landforms formed under cold but nonglacial conditions, a concept expanding Andersson's (1906) work focused on solifluction (slow soil flow over frozen ground).

F.E. Matthes, working in the Big Horn Mountains of Wyoming, introduced the concept of *nivation*. The process suite invoked by the term begins when snow accumulates within topographic hollows on north-facing slopes, persists late into the summer or, in some cases, the entire year. As these snow accumulations achieve greater densities and ablate, intensive freeze-thaw, chemical weathering, slopewash, and solifluction occur in the vicinity of the snowpatch. The recurring weathering and transportation processes excavate small depressions known as nivation hollows. In the context of CT formation, ridgecrests occupied by perennial snowpatches promote headward scarp retreat, widening nivation hollows so that the ridge profile resembles a giant staircase of ascending treads and scarps.

Early work by Matthes (1900), Andersson (1906), and Lozinski (1909) contributed to the nascent field of *climatic geomorphology*, which gained traction as a continental European reaction to Davisian geomorphology (see Penck 1905; Martonne 1913; Büdel 1948a; Tricart & Cailleux 1972; Büdel 1977; Beckinsale & Chorley 1991, Chapter 12). Periglacial studies formed an important component of climatic geomorphology. Early work by Troll (1944) and Büdel (1948b) attempted to subdivide Earth's periglacial regions and eventually led to development of the "Göttingen school" of periglacial geomorphology, led by Hans Poster (e.g., Hövermann & Oberbeck 1972; Poser, 1977; also see Karte, 1979, 1982). The International Geographical Union facilitated interactions between periglacial scientists of the Eastern and Western blocs through its long-standing Periglacial Commission, particularly through its journal *Biuletyn Peryglacjalny*, founded in Poland by Jan Dylik in 1954.

1.1.3 Early conceptions of the nivation hypothesis. In the early 1900s, Prindle (1913) and Cairnes (1912) made genetic inferences about CT development that were consistent with the nivation process-suite set forth by Matthes a decade earlier. Like Davis' peneplain concept, Cairnes emphasized widespread leveling of the ground surface, a process he called *equiplanation*. Under equiplanation, erosion occurs by nivation and solifluction where the surface is ultimately lowered by freeze-thaw action and the movement of weathered ramparts to the level of the underlying permafrost table. Prindle (1913), without using the term, indirectly connected the processes of nivation to scarp retreat of "step-cut benches" in east-central Alaska. Other scientific generalists operating in Alaska in the early 1900s interpreted CTs as a consequence of geologic structure (see Nyland, 2019, 25). Following these initial observations in the early 1900s, very little work was published about CTs until the 1960s, using the term *altiplanation terraces* Eakin, 1916). The literature on nivation, although more voluminous, remained deductive and descriptive until the 1970s.

1.1.4 Periglacial geomorphology gains traction. An augmentation to Davis' normal cycle of erosion was presented to the Anglophone audience in *"The Geographic Cycle in Periglacial Regions as it Related to Climatic Geomorphology"* by Louis Peltier (1950). Peltier's geographic cycle holds that morphogenetic regions, delineated by regional prevailing climatic regimes, progress geomorphically through climate-specific erosional processes. Erosional stages were demarcated using Davisian nomenclature—youth, maturity, and old age—but emphasis was placed on climatically induced landscape development. As such, climates are not viewed as "accidents" but rather as naturally occurring sets of controls over geomorphic processes.

Peltier (1950) proposed the periglacial realm as one of nine morphogenetic regions (cf. Büdel 1948a). Nivation and solifluction, concepts proposed years earlier, are emphasized under Peltier's stages of erosion, in which the generation of frost-shattered material contributes to material accumulation and mass movement processes—solifluction, slopewash, and congeliturbation—that promote scarp retreat. *Cryoplanation surfaces* characterize Peltier's cycle and are achieved as rampart accumulations eventually rise to a level at which further denudation is limited, giving way to the formation of broad erosional surfaces. Cryoplanation, a term first coined by Bryan (1946), was adopted by Peltier (1950) and became used widely in reference to the long-term generation of cryoplanation terraces via scarp retreat in cold regions (Demek, 1968; Ballantyne, 2018, 220). Peltier (1950) was successful in incorporating periglacial relief generation into Davis' cycle of erosion, bringing periglacial geomorphology into the mainstream of Anglophone geomorphology.

1.1.5 Definitive studies on cryoplanation terraces. The first comprehensive studies concerning cryoplanation terraces were conducted by Demek (1969) and Reger (1975). These works drew on all the available information (e.g. stratigraphy, climate, sedimentology, and morphology) to characterize CTs and to map their extent across the Northern Hemisphere. One of the significant findings of these works was their documentation of CTs cutting across geologic structure, a major blow to the geological-control hypothesis of CT formation. Both authors embraced the nivation hypothesis of CT formation, in which scarp retreat is related to the mass-balance of large and persistent banks of snow (Figure 1.2). Both authors understood the limitations of their works, which relied on classification and mapping, and made poignant calls for process-based studies, dating of CT surfaces, and investigations on transportation of weathered material. Specifically, these authors highlighted the importance of tracing the fate of weathered material on CT slopes to explain the stepped appearance of CT profiles. Ultimately these works would not be highly influential, however, largely because their distribution was severely limited. Calls for process-based investigations would remain unaddressed for many years.

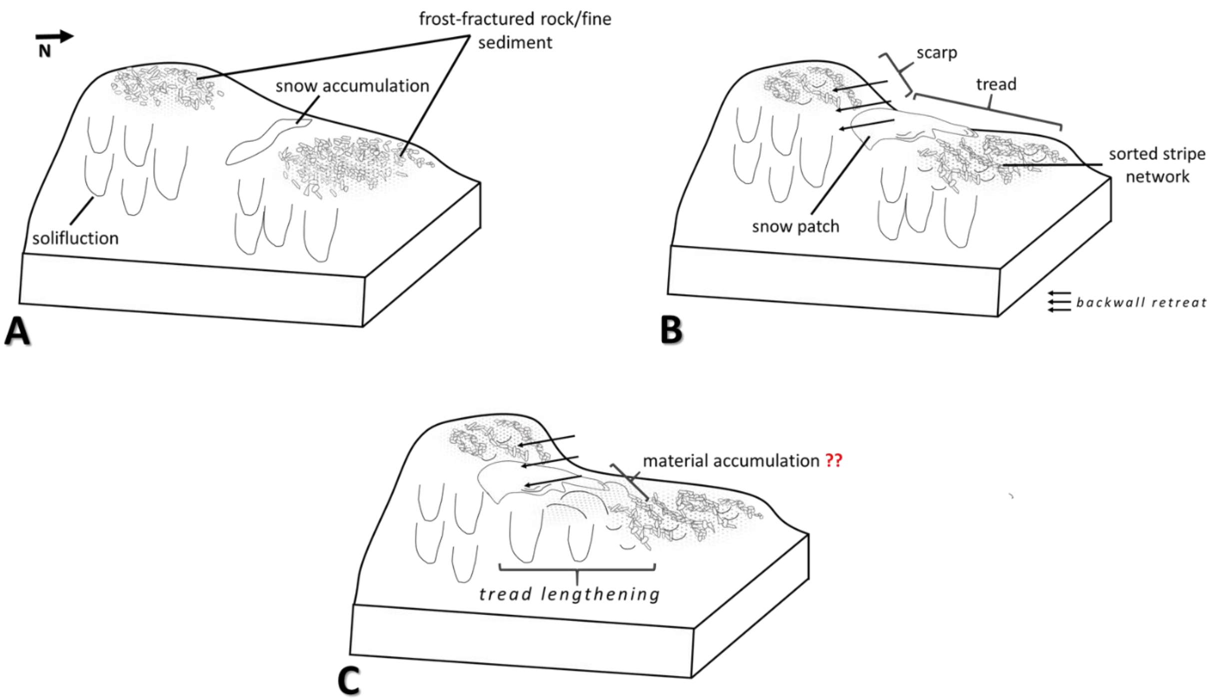

Figure 1.2 Diagrammatic model of nivation-driven scarp retreat of cryoplanation terrace formation. *The stages of CT development are characterized by (A) the accumulation of snow within a topographic irregularity on a north-facing slope. (B) the elongation of the topographic hollow through backwall retreat which forms a visible break in slope between the CT tread and tread. The formation of sorted patterned ground from available snow melt water occurs on the CT tread. (C) The CT tread continues to lengthen via scarp retreat but material accumulations representing past scarp position are not visible. Figure after Nyland (2019, Figure 18).*

1.1.6 Quantitative studies ensue. Process studies focusing on nivation would not be undertaken until the mid-1970s following the field research conducted by Thorn (1976) who worked in the alpine periglacial environment of the Colorado Front Range. This work quantitatively substantiated the intensified weathering and transportation of material in the vicinities of late-lying snowpatches but ultimately, Thorn concluded that his observed erosion rates by nivation were inconsistent with the size of cirque-scale features and argued forcefully against the concept of a continuum between nivation hollows and glacial cirques. Nelson (1989), working with Reger's (1975) data set, confirmed that the size of CTs is significantly smaller than cirques, but also established that Thorn's (1976) nivation rates were consistent with the dimensions of CTs, providing some support for the nivation hypothesis of CT formation. Nelson (1989, 1998) and Nelson and Nyland (2017) argued that CTs are periglacial analogs of glacial cirques; both features form as a consequence of the mass balance of bodies of snow and ice, both show poleward-facing orientation, and both follow the climatically defined regional snowline.

Thorn & Hall (1980) have raised concerns about the efficacy of the nivation process suite and took issue with its terminology. Although their concerns had been tempered by the turn of the 21st century (Thorn & Hall 2002), their earlier objections were translated into textbook form by H.M. French, who recommended that the term nivation be abandoned altogether (French, 2017, 233 and references therein). By the early 2000s only indirect lines of evidence continued to attribute CT formation to nivation. Process-based studies on the landforms remained entirely lacking.

1.2 Revisiting the Nivation Hypothesis

A recent trend in periglacial research highlights the transference of water, fine clastic sediment, and weathered solutes within sorted patterned ground and associated periglacial water tracks (e.g., Paquette et al., 2017, 2018). In these studies, sorted patterned ground, specifically sorted stripes, were found to be responsible for the initiation of periglacial water tracks, and thus the widespread hydrologic connectivity of the hillslope. This research trend informs an important line of investigation that has profound implications in the context of CT formation hypotheses.

1.2.1 Scrutiny. The most widely invoked scrutiny of the nivation hypothesis of CT formation states that moraine-like deposits, representative of past scarp positions, should accumulate on CT inner treads (Ballantyne, 2018, 221). No such accumulations have been observed in characteristically periglacial regions, a situation supposedly indicative of the absence of processes that remove weathered products from CT treads. In the absence of another widely supported hypothesis, the nivation explanation for CT formation seems the most appropriate but rampart accumulations must be accounted for before the hypothesis can be widely embraced.

1.2.2 The missing "link" from the nivation hypothesis. The networks of sorted patterned ground and solifluction lobes frequently encountered on CT treads and side slopes are potentially important features for the transmission of weathering products across CT treads. A record of work that notes the presence of running water within sorted stripes on CT treads exists (e.g., Taylor, 1955; Caine, 1963; Smith, 1968; Nelson, 1979) and provides impetus for investigations into the hydrology of sorted patterned ground. However, no study has related sorted patterned ground to landscape-scale evolution, specifically cryoplanation terraces, although previous work has indicated the ability of sorted stripes to exert major hydrologic controls over large extents of the hillslope (Paquette et al., 2018). An exploration into the hydrologic and geomorphic significance of sorted stripes on CT treads is required to reveal the information necessary to explain the absence of ramparts on the inner (proximal) areas of CT treads.

This study attempts to address the absence-of-ramparts issue by examining the role of flowing water in the coarse "gutters" of sorted stripes through two avenues of research: (1) process-related studies; and (2) fluvial geomorphometric analysis of a sorted–stripe network.

The results of this study are used to specify the nature of the missing “link” that addresses the issue of the absence of ramparts on CT treads, thereby addressing Thorn and Hall’s (2002) call for scrutiny of the nivation hypothesis. In doing so, it has potential to remove two of the last major objections to the nivation hypothesis of cryoplanation-terrace formation: (1) demonstration of a mechanism for transporting large volumes of sediment over and off CT treads; and (2) growth and maintenance of the characteristic step-like CT form.

Chapter 2 Hydrologic Significance of Sorted Patterned Ground

Prior to the 1970s, the role of water in periglacial landscape was rarely addressed in the literature. This research deficit has been overturned by the documentation of fluvial features such as gullies, rivers, and V-shaped valleys abounding in periglacial landscapes (Ballantyne, 2018, 253). In arid periglacial environments, hydrologic activity is largely determined by the occurrence and distribution of perennial snowpatches and ice, which are responsible for the prolonged release of moisture to slopes (Ballantyne, 2018, 253). Underlying ice-bonded permafrost also exerts a hydrologic control by limiting vertical water percolation and by concentrating hydrologic activity in the seasonally thawed active layer (Slaughter & Kane, 1979; Woo, 1986). Fluvial action, in association with periglacial hydrologic-related constituent processes, is one of the most important geomorphic processes in periglacial regions (Ballantyne, 2018, 253).

A recurring theme in periglacial literature of the past several decades hints at the hydrologic controls imposed by the minor periglacial features known as patterned ground (Nelson, 1975; Wilkinson & Bunting, 1975; Paquette et al., 2017a, 2018). Some writers regard patterned ground as “embroidery on the landscape” (Ballantyne, 2018, 145), a phrase that implies a trivial relationship between patterned ground and the underlying topography. Further opposition is presented through the interpretation of patterned ground as an indication of geomorphic dormancy (e.g., Thorn & Hall, 2002b, 545), underscoring notions about the hydrologic insignificance of the features.

Research by Paquette et al., (2018) explicitly attributes enhanced channeling of water within areas of patterned ground to the formation of periglacial water features known as water tracks. The connectivity of this patterned ground-water track complex provides striking evidence that favors the interpretations about the geomorphic and hydrologic significance of patterned ground. This thread is exemplified in a thesis by Queen (2018), who applied the concept of feature assemblages to periglacial landscapes, demonstrating that repeating assemblages of minor periglacial features such as patterned ground are the elemental building blocks of larger units that are recognizable and operational at the landscape scale, i.e., cryoplanation terraces.

The conception of patterned ground as being of minor or no geomorphic significance is at odds with literature that documents patterned ground hydrology. On the one hand, the reader is led to believe that patterned ground is nothing more than periglacial décor, while on the other hand, substantial evidence demonstrates its hydrologic and geomorphic significance. An understanding of slope development in a periglacial setting warrants consideration of patterned ground as a fluvial feature. This approach to assessing the hydrology of a periglacial setting permits the exhaustive exploration of associated geomorphic development.

2.1 Periglacial Hydrology

Peltier (1950, 215) opined that mass movement and moderate to strong wind action are important generators of relief in the periglacial morphogenetic region. Under the geographic (geomorphic) cycle as it relates to periglacial environments, the impact of water is given little mention, conveying a sense of insignificance regarding periglacial hydrology. Major contributions to periglacial hydrology were made beginning only in the 1970s, revealing the unique runoff regime in periglacial regions, which is characterized by the cessation of runoff in winter, the dominance of water storage as ice and snow, and underlying permafrost conditions.

2.1.1 Increasing interest in periglacial hydrology. One of the first serious considerations of hydrology in the periglacial literature was published by McCann et al. (1972), a paper in which the lack of studies focusing on periglacial hydrology is noted very explicitly. The dearth of information on periglacial hydrology at that time was accentuated by the fact that of the few published works on periglacial catchments—mostly focused in Alaskan tundra basins—most were qualitative (McCann, et al., 1972). The late 1970s brought about a marked change in interest about periglacial hydrology, with extensive research by Ming-ko Woo, working in Canadian watersheds in the late 1970s and 1980s, (e.g., Woo, 1976; Woo, 1986). Woo's research focused on tundra rivers and on the oddities of periglacial rivers such as the influence of snow-choked channels (Woo, 1976; Woo & Sauriol, 1980). Research on the hydrology of periglacial regions advanced rapidly thereafter, as reflected by an in-depth review by Clark (1988), who nonetheless lamented that the subject was still in its infancy. Progress has continued unabated in the intervening years, and the subject was treated comprehensively in a recent volume by Woo (2012). Today, active areas of research in periglacial hydrology apply field-based monitoring efforts and modeling techniques to modern issues such as the response of the periglacial hydrologic regime to warming global temperatures (Woo et al., 2008).

2.1.2 Characteristics of periglacial watersheds. Arid and semi-arid periglacial watersheds are typified by a snowfed, or *nival regime* (Woo, 2012, 475–477). Under this regime, rivers and other water features are controlled primarily by snowmelt water (Christiansen, 1996) confining most hydrologic activity to the spring, when snow begins to melt in the Northern Hemisphere.

Threshold-like melting is achieved in snowpatches at the onset of above-freezing temperatures, which cause the snowpatches to "ripen" until the entire entity is isothermal at 0°C (Quinton & Marsh, 1999). Vertical percolation of water into the substrate underlying the snowpatch is at first inhibited due to the formation of basal ice, which induces lateral flow between the ground surface and the overlying snowpatch (Ballantyne, 2018, 255). In the early spring, limited groundwater storage due to frozen ground, rapid melting of snowpatches, and dominantly lateral flow on the hillslope all contribute to intense hydrologic activity in periglacial watersheds. Irregular accumulations of snow concentrate hydrologic activity and erosive power in those areas proximal to snowpatches, invoking the influence of nivation in periglacial watersheds.

2.1.3 Sorted patterned ground. Patterned ground is the term given to "the more or less symmetrical forms, such as circles, polygons, nets, steps, and stripes, that are characteristic of, but not necessarily confined to, mantle subject to intensive frost action" (Washburn, 1956). A subgrouping of patterned ground, *sorted* patterned ground—"sorted" refers to the concentrated presence of coarse fragments bordering fine-textured areas—is frequently encountered occupying broad areas extending downslope from perennial snow-patch margins (Ballantyne, 2018, 145 and references therein). Sorted patterned ground imparts a distinctive imprint on local hydrology by establishing microtopographic variation, material sorting, and channelization of water.

2.2 Sorted Stripes as Fluvial Features

Underlying permafrost conditions inhibit fluvial incision of water features into mature channels so that in some periglacial settings, smaller and less accentuated periglacial hydrologic features may be the only indications of water transportation on the ground and represent substantial caches of water (Woo, 2012, 242–249). The initial focus of periglacial hydrology on rivers contributed to some degree of dismissal of the hydrologic control of other features and processes such as rillwash and gullying (Embleton & King, 1975). Recent research has linked patterned ground and other periglacial features to significant hydrologic activity (e.g., Levy et al., 2011; Paquette et al., 2017a, 2018), marking a resurgence of research on these features.

2.2.1 Sorted patterned ground formation. Modeling efforts aimed at establishing the origins of sorted patterned ground demonstrate that differential frost heave occurring at the interface between unfrozen and frozen ground causes uplift of coarse fragments, a process known as *frost sorting* that leads to squeezing and confinement of stones along their margins (Hallet, 1990; Kessler & Werner, 2003). Macrofabrics from the coarse borders of sorted circles (Nelson 1982a) and sorted stripes (Nelson 1982b) reflect this process; tabular clasts lie with their long axes parallel to borders and are frequently on edge. Under recurrent freeze-thaw cycles within a soil medium composed of unsorted coarse and fine-textured material, particles migrate toward areas of similarly sized particles, i.e., large clasts migrate toward higher concentrations of similar particles, invoking a self-organizing formation scheme related to continued patterned ground development (Kessler & Werner, 2003). Sorted patterned ground is further altered under the influence of slope, where the greater the slope, the more elongate the forms; i.e., stripes (Washburn, 1956). The self-propagation of sorted patterned ground formation ensures the maintenance of textural boundaries, which are the defining components of water movement.

2.2.2 Overlooked features. Sorted stripes appear on the ground surface as repeating linear bands of coarse fragments alternating with bands of fine sediment oriented parallel to slope and always occurring in groups (Washburn, 1956). Sorted stripes occupy slopes between 4-11° and have been associated with efficient water transportation, which flows in the large interstitial spaces of the coarse stripes (e.g., Nelson, 1975; Wilkinson & Bunting, 1975). Solifluction, literally "slow soil flow" is associated with the downward movement of intervening fine-textured material (Washburn, 1956). That water flows within coarse sorted stripes is not controversial and is well-documented e.g., (Wilkinson & Bunting, 1975). The hydrologic *significance* of sorted patterned ground is less well recognized (Paquette et al., 2017a). Goldthwait (1976, 31) described the flow of water through a sorted patterned ground landscape:

"these are openwork boulder gutters between soil centers where one hears water trickling in the early summer"

Woo (2012, 245-246) noted that hydrologically, sorted stripes direct runoff from snowmelt into surface drainage networks, indicating that when present sorted stripes comprise the rudiments of an informal drainage network. Qualitative documentation of sorted stripe hydrology provides a foundation for their consideration as fluvial features, but in the absence of quantitative data, leaves the concept open to question.

2.2.3 Previous work. Hydrologic activity within sorted stripes was tangentially outlined by Taylor (1955) who noted the occurrence of "stone lines"—interpreted here as sorted stripes—superimposed on terraces off the coast of Tasmania. Taylor (1955, 136) noted that the stone lines trended downslope and that they “provide rapid drainage for the water table when it approaches the surface”. Caine (1963, 178) postulated the origin of sorted stripes in northern England and qualitatively deduced that drainage of water from a heavily saturated field site was directed through the coarse portions of sorted stripes. He observed:

“As thawing progresses most of the drainage from the [sorted] stripes was found to take place through the coarse stripes or the grooves of thawed material just below them as long as an extensive layer of impervious frozen ground remained.”

Work conducted by Wilkinson and Bunting (1975), focused on the movement of water as overland flow in a periglacial setting via subtle water features, known as rills, demonstrating that a system of rills—fed by snow meltwater—were hydrologically connected to other water sources on the hillslopes through effective transport of water and sediment. Nelson (1975) outlined the geomorphic and hydrologic character of sorted stripes at an alpine periglacial site, describing the preferential flow of water through coarse stripes (16). Nelson (1975), following Ule (1911), Cairns (1912), Salomon (1929), Mortenson (1930), Poser (1931), Czeppe (1961), and Washburn (1969), also hypothesized that the sorted stripes originate from snow meltwater rillwash (Nelson, 1975, 20). Troll (1944) rejected this explanation on grounds that many stripes lie parallel to one another and/or do not occupy depressions in the soil matrix, arguing instead that solifluction is responsible for stripes through elongation of sorted nets or circles. This view has become a standard explanation for sorted stripes (e.g., Embleton and King 1975, 91). Goldthwait (1976) also argued against a rillwork origin on the basis that rill networks do not exhibit the geometric regularity he perceived, without quantitative characterization, in patterned ground fields he investigated. The similarities between the network characteristics of a field of sorted stripes and those of low-order fluvial networks is the subject of detailed investigation in Chapter 6 of this thesis.

Nelson (1975) used two diagrams depicting water flow through a sorted stripe and sorted net landscape to summarize his observations (Figure 2.1). Hodgson & Young (2001) found the hydraulic conductivity within coarse sorted stripes to be three orders of magnitude higher than in intervening frost-mound centers; hydraulic conductivity values for coarse stripes were between 90-1000 m/day whereas frost mound values ranged from 0.1- 1.0 m/day.

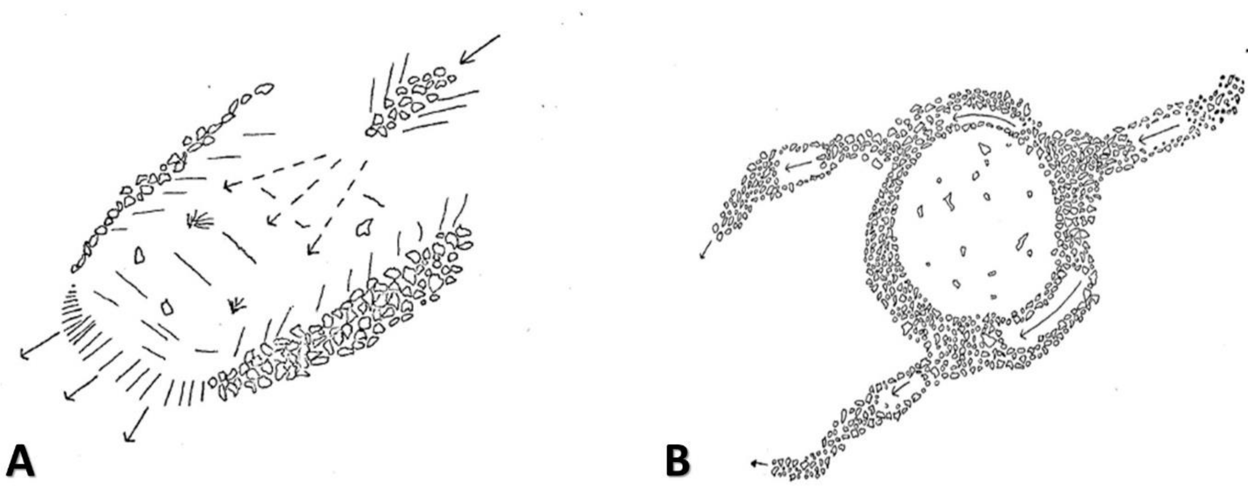

Figure 2.1 Sketch of water movement through sorted patterned ground. (A) Water movement from a sorted stripe to and through a solifluction lobe downslope; (B) Sorted patterned ground features on Frost Ridge, showing pathways of running water through interstitial space in coarse portions of the patterns. The direction of water movement in both sketches is indicated by arrows. Sketches from Nelson (1975). Local late-lying snowbanks supplied meltwater to these areas throughout the summer season. This thesis explores the hypothesis that movement of water through a sorted patterned ground environment prevents the formation of accumulative ramparts on subjacent treads.

2.2.4 Hillslope connectivity. Recent studies have suggested that poorly incised water features, known as water tracks, exert a dominant role in linking terrestrial and aquatic systems in upland periglacial regions (Levy et al., 2011; Paquette et al., 2017a, 2018). Water tracks, which appear as linear bands of rich vegetation that alternate with bands of sparse vegetation (Figure 2.2), have been shown to control nutrient transportation, vegetation establishment, and water fluxes from upland slopes in hillslopes underlain by permafrost (Levy et al., 2011). In periglacial catchments that lack formal river systems, water tracks are in some instances the only evidence of drainage pathways (Woo, 2012, 242–243). McNamera et al. (1998) found that water tracks occupying hillslopes in the Kuparuk River basin in Alaska were responsible not only for basin drainage, but also for significant water storage. Although water tracks do not achieve the organization of a mature drainage network, their drainage and storage characteristics make them significant components of the catchment hydrologic system (McNamara, et al., 1998). Observations by Levy et al (2011) in Antarctica demonstrate that within water tracks, which were composed of silt, sand, and pebbles, solute transport was two orders of magnitude faster than in adjacent soils, indicating the prominent transportation pathways imparted by water tracks.

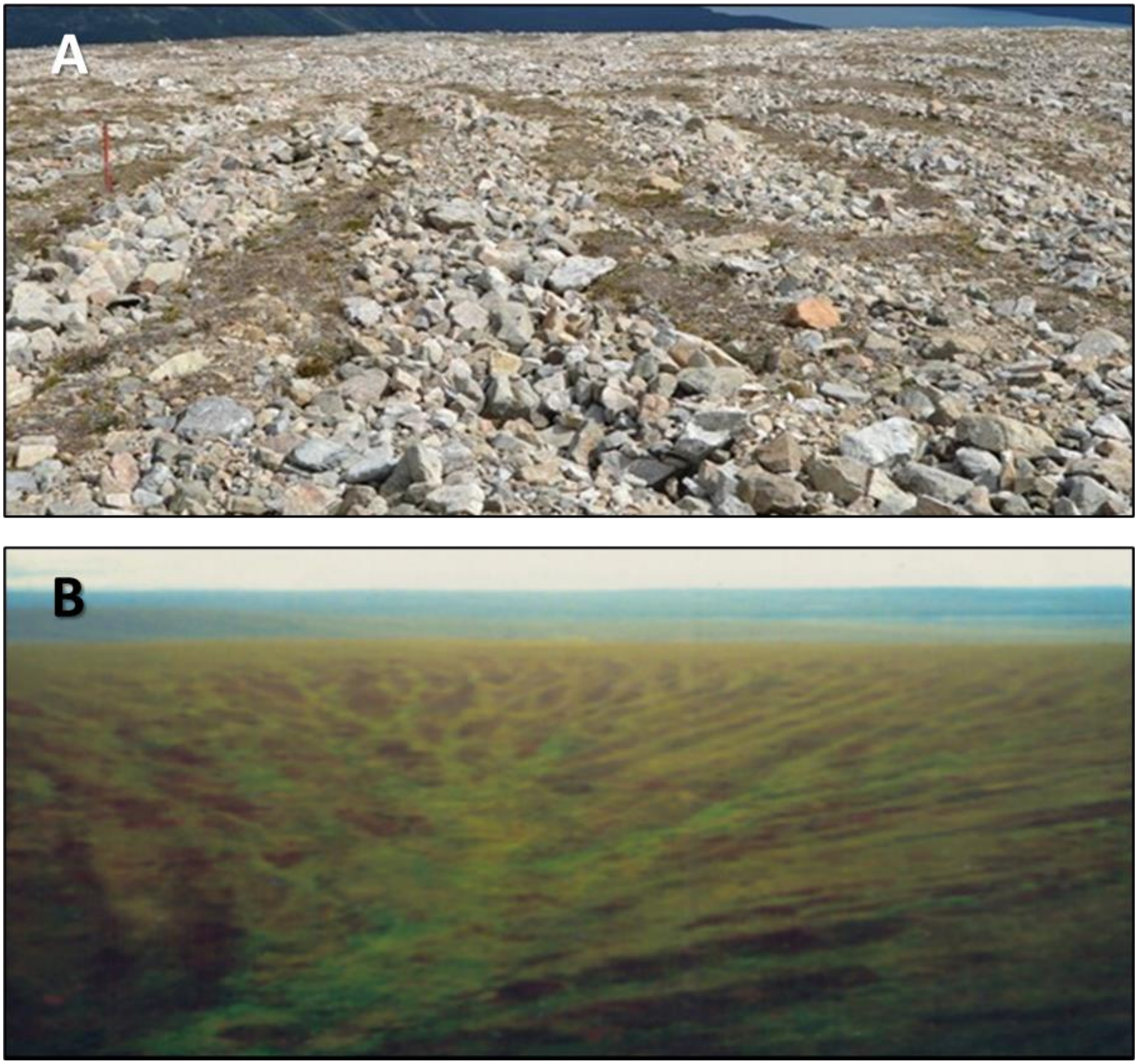

Figure 2.2. Organizational similarities between sorted stripes and water tracks. *(A) sorted stripes near Atlin, British Columbia, Canada. Here, stripes are downslope trending and extend towards the slope margin in the background of this photo. Photo taken by C.W Queen 2017. (B) Water tracks extend from upslope in the background and converge in the foreground of the photo. Photo taken in the Arctic Foothills, AK, by A.E Klene.*

A series of works by Paquette et al., (2014, 2017, 2018) demonstrated the importance of patterned ground in water-track initiation. Presented at the Fourth European Conference on Permafrost in 2014, this research introduced the hypothesis of patterned-ground-initiated water track formation (Paquette, et al., 2014). Preferential sorting, eluviation of fine material, and channelized water flow associated with patterned ground were attributed to downslope water track formation, defining the hydrologic connectivity of the hillslope. Papers published by the same authors in 2017 and 2018 expand on the concept of hillslope-scale connectivity, establishing that the patterned ground-water track complex tended to dominate the local hillslope hydrology, and that patterned ground increased hillslope connectivity to the principal water sources, snow patches. The resonating theme of these contemporary studies lies in their compelling evidence that patterned ground increases connectivity between upland water sources (in this case, snowpatches) and lowland water features, e.g., lakes, through the exertion of geomorphic and hydrologic control. These findings challenge the notion that patterned ground indicates geomorphic quiescence and further demonstrate that when moisture conditions permit, patterned ground is a critical component in periglacial hydrology.

2.3 Conclusion: Sorted Stripes, Nivation, and Cryoplanation Terraces

It is evident that where present, sorted stripes and water tracks represent preferential flow pathways on periglacial hillslopes. The hydrologic significance of these features is especially prominent in arid and semi-arid periglacial regions, where snow meltwater constitutes a major hydrologic input. The linkages between patterned ground, water tracks, and hydrology have been documented since the 1950s (Taylor, 1955), but have seldom been embraced widely in the literature (Paquette et al., 2014, 2017a).

Work by Queen (2018) established cryoplanation terraces as foundational units in a periglacial setting. Inherently related to the basic CT unit is the operation of periglacial assemblages, whose repeating morphologic signatures link micro-scale periglacial features and processes to landform- and landscape-scale geomorphic activity. Patterned ground, solifluction lobes, and perennial snow patches favor CT profiles owing to the poleward orientation of CTs (Nelson, 1998), and the rubble mantle cover that typifies CT treads (Ballantyne, 2018, 220). The co-location of patterned ground and perennial snowpatches atop cryoplanation terraces is an arrangement that has not been explored previously in the context of CT formation. Allusion to evacuation of sediment from CT treads via sorted patterned ground (e.g., Nelson 1975; Nyland, 2019, 59; Queen, 2018, 41), is only an initial step in recognizing the importance of low-order fluvial networks in the formation and maintenance of cryoplanation terraces.

Chapter 3 Study Area

The Juneau Icefield is the fifth largest expanse of continuous upland ice in North America (Miller, 1975, 1), covering an area of about 1,800 km^2 in the 1950s (Field & Miller, 1950, 180). The icefield extends from the Taku River Valley, AK in the south, to the vicinity of Skagway, AK in the north. The northern and eastern flanks of the icefield extend into Canada, covering a confluence area across the Alaska, British Columbia, and Yukon Territory borders. The Juneau Icefield remained largely unexplored until the establishment of the Juneau Icefield Research Project (JIRP), under the auspices of the American Geographical Society (Heusser, 2007). The first research-motivated reconnaissance mission was conducted in 1948 (Field & Miller, 1950). A series of research camps established at the onset of icefield explorations form a northeast-southwest transect extending from the coastal side of the Boundary Range in Alaska to the northeast into British Columbia, Canada (Miller, 1975, 1). Most periglacial work in the interior of the icefield has been conducted on nunataks (e.g., Hamelin, 1964; Nelson, 1979, 101-102; Dixon et al., 1984). The research camp transect terminates at Camp 29 near the village of Atlin, British Columbia, which is the site where the research for this thesis was conducted in the summer of 2019 (Figure 3.1). The glacial history of this area, among other environmental conditions, has promoted the development of a wealth of both relict and active periglacial features (Nelson, 1979, 8), making it a highly unusual site for periglacial investigations.

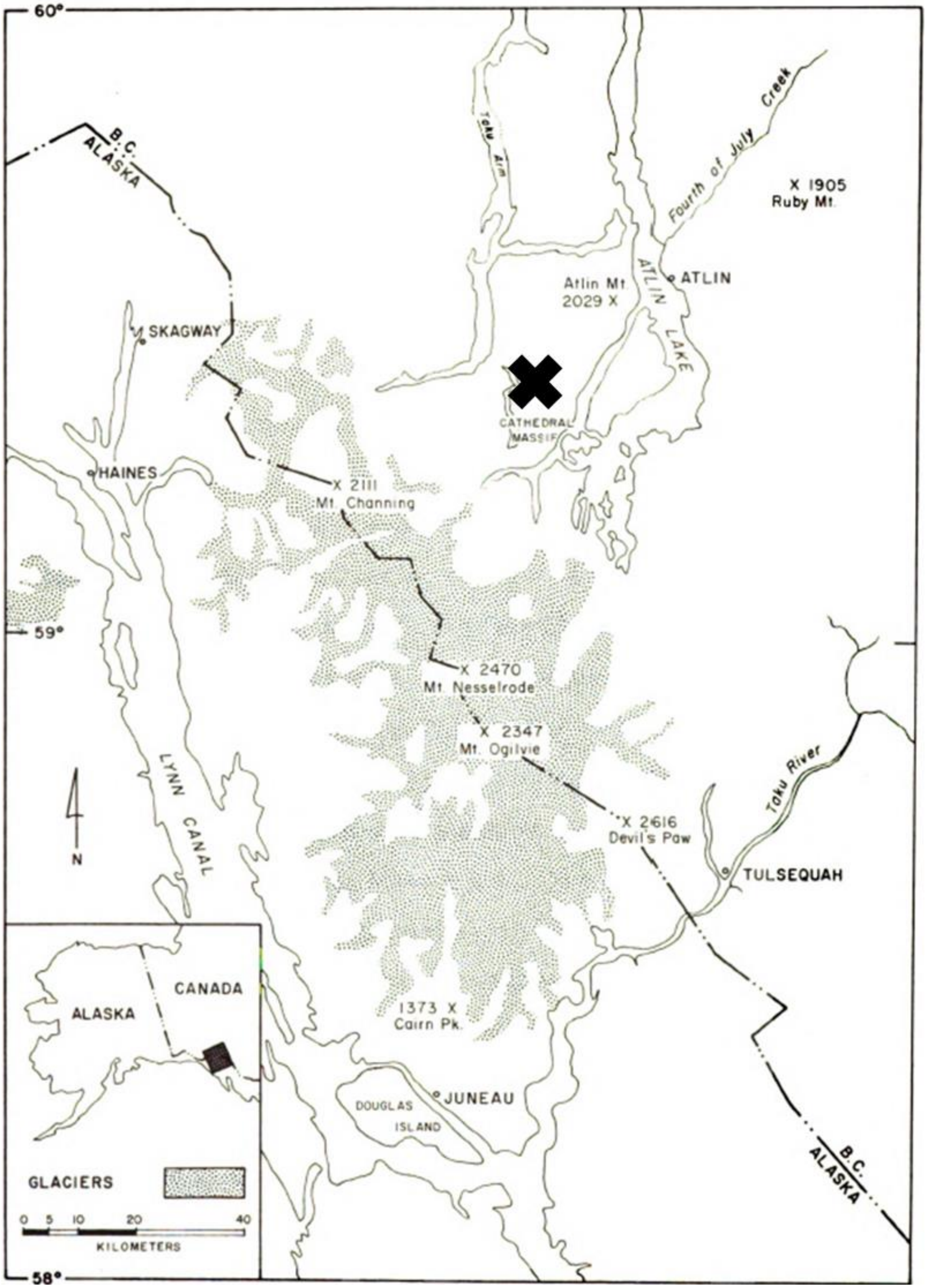

Figure 3.1 The Juneau Icefield. *The extent of the Juneau Icefield with the approximate location of Camp 29, the study site for this thesis, denoted with a black "x". Map modified from Nelson (1979), map after C.J. Cialek.*

3.1 The Greater Atlin Area

3.1.1 Geographic description. The village of Atlin is situated along the eastern shore of Atlin Lake and lies within the Atlin/ Téix'gi Aan Tlein Provincial Park (59°31'21"N 133°45'35"W) Stikine Region of northwest British Columbia (Statistics Canada, 2018). Atlin Lake, like many of the lakes in this region, occupies a glacial valley that is a relic of the region's glacial activity (Slupetzky & Krisai, 2009a, 192).

3.1.2 Geology. The geology of northwestern British Columbia is composed of a complex mosaic of terranes—fragments of crustal material that have coalesced due to tectonic rifting (Monger et al. 1972). As such, the geology of the area invokes a multitude of geologic discontinuities representing distinct geologic and physiographic boundaries (Monger et al., 1972, 577–579). Atlin lies within the fault-bounded westernmost limit of the Atlin Terrane and is composed of little-metamorphosed upper Paleozoic rocks belonging to the Cache Creek Group (Monger, 1975, 2; Colpron & Nelson, 2011).

3.2 The Cathedral Massif

3.2.1 Physical description. The Cathedral Massif—an isolated, rocky highland—is located approximately 35 km southwest of Atlin. The highest point of the massif, Cathedral Peak, (2314 m.a.s.l.), is flanked to the west by Mount Edward Little (1932 m.a.s.l.) and to the east by Splinter Peak (1925 m.a.s.l.) (Figure 3.2). The Cathedral Glacier occupies two glacial cirques. This glacier, sometimes referred to as the *Cathedral Massif Glacier* (e.g., Slupetzky & Krisai, 2009a), occupies the north-facing side of the Cathedral Massif, immediately downslope from Cathedral Peak. Slupetzky & Krisai (2009, 194) reported the terminus of Cathedral Glacier to be at 1615 m.a.s.l. (in 1999), though the current terminus elevation is likely much higher as the glacier has receded substantially in recent years (Nelson, 2018, personal communication). Two major flow units are derived from the Cathedral glacier: flow from the eastern cirque drains eastward into the southern reaches of Atlin Lake, while flow from the western lobe drains directly downslope, resulting in a proglacial lake at its base. Downslope from the present terminus of the Cathedral glacier, a glacial valley is occupied by a terminal and several recessional moraines, which represent past glaciations that occurred during the Little Ice Age (Slupetzky & Krisai, 2009b, 196).

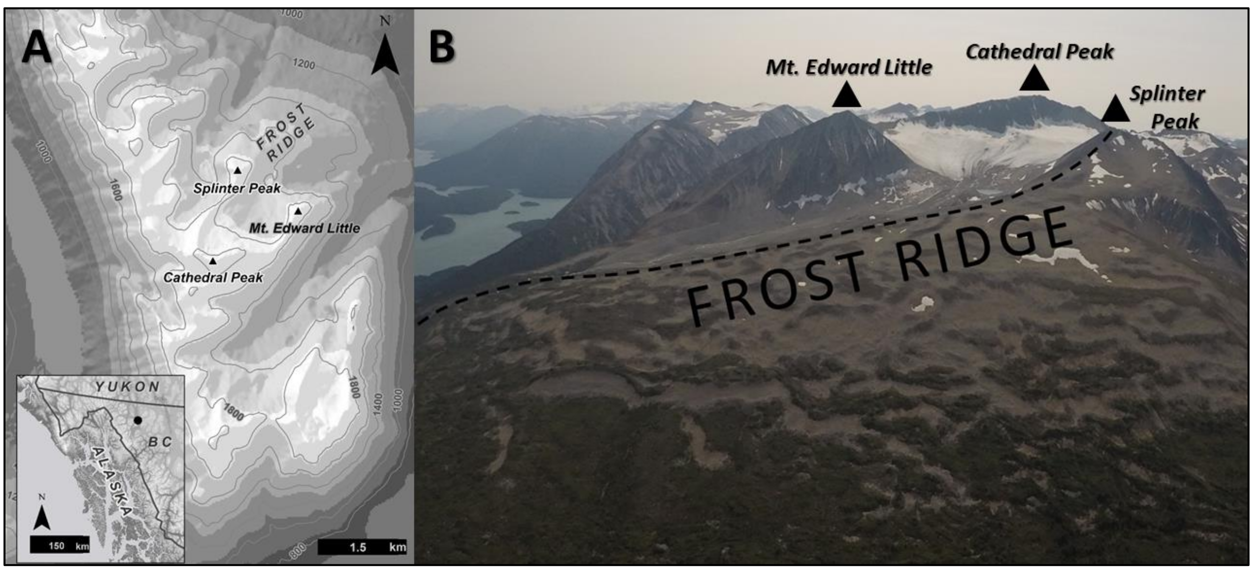

Figure 3.2 Orientation of Frost Ridge. *(A) Site map of Frost Ridge and relevant features. (B) Oblique view of Frost Ridge facing south. The Cathedral Glacier can be seen between Splinter Peak and Mt. Edward Little. The western lobe of the Cathedral Glacier is located between Cathedral Peak and Splinter Peak. The eastern lobe is located between Mt. Edward Little and Cathedral Peak. Photo taken July 2018 by R.J. Mitchell.*

3.2.2 Geology. Jones (1975) provided reconnaissance-level geologic data for the Cathedral massif region, which lies immediately outside the western border of the Atlin Terrane, within a narrow strip of the Stikinia Terrane (MacIntyre et al., 2001; Colpron & Nelson, 2011). The geology of the area is composed predominantly of volcanic, plutonic, and sedimentary rock of Late Triassic to Early Jurassic age (Colpron & Nelson, 2011). A dark, heavily stressed, fine-grained granodiorite intrusion characterizes most of the Cathedral Massif (Jones, 1975, 22–23). Near and above the Neoglaciation limit, Splinter Peak is composed of highly weathered metamorphic rock (Jones, 1975, 25).

3.2.3 Climate. The climate of the Cathedral Massif region is classified as continental, semi-arid, and sub-polar (Miller, 1975, 6)., The climate is influenced by its location on the continental side of the Boundary Range, which inhibits penetration of moist air from the Pacific Ocean to the southwest (Jones, 1975, 39). The continental climate of the Cathedral Massif and greater Atlin area is characterized by cold and dry conditions, with the Atlin area receiving 285 mm of precipitation per year (Jones 1975, 39; Nelson 1979, 12). Owing to the climatic continentality, much of the unglaciated parts of the Cathedral Massif are classified as periglacial (Tallman, 1975a, 106; Johnson, 1983, 2;).

3.2.4 Glacial history. The glacial history of the Cathedral Massif is revealed by a network of moraines that occupy the glacial valley downslope from Cathedral Peak. Rounded peaks, glacial scouring, fields of glacial till and proglacial lakes also reflect glacial activity within the area. Pre-Wisconsinan glaciation from the ancestral Hobo-Llewellyn glacier deposited a large terminal moraine over 1.5 km north of Cathedral peak (Tallman 1975, chap.6; Miller 1975 131-132, Slupetsky & Krisai 2009). Ice flowing north and northeast around the Cathedral deeply scoured the southern flanks of the massif, creating the Atlin Lake basin (Jones, 1975b, 31; Tallman, 1975b, 32; Slupetzky & Krisai, 2009). Late Pleistocene glaciation resulted in the deposition of an impressive lateral moraine found on the eastern flank of Frost Ridge (Slupetzky & Krisai, 2009). Later, Neoglacial-period ice deposited minor recessional moraines that are well-confined within the Cathedral glacier valley. In addition to glacial alteration of the Cathedral Massif, periglacial processes have contributed to alteration of local geomorphology (Jones, 1975; Nelson, 1979).

3.3 Frost Ridge

3.3.1 Physical description. Frost Ridge (FR) is a northeast trending linear feature extending from Splinter Peak to the southern end of Atlin Lake. FR is flanked to the east by a large lateral moraine and to the west by the unoccupied Snowdrift Cirque (Jones, 1975). Hummocky, vegetated terrain characterizes the lower reaches of FR while well-expressed patterned ground—sorted nets, circles, and stripes— and other periglacial features abound in its upper reaches.

3.3.2 Climate. The same continental climate described for the Cathedral Massif area prevails on Frost Ridge. Topographic irregularities and minimized solar radiation on north-facing slopes contribute to the accumulation of what little snow does fall on the ridge. Late-lying snowpatches occur on FR where snow accumulations persist into the summer months, supplying prolonged moisture to the slope.

3.3.3 Glacial history. During the Wisconsinan glaciation the upper reaches of Frost Ridge remained above the glacial margins (Nyland 2018, 82). Further downslope, ice contact from the ancestral Hobo-Llewellyn glacier carved marginal drainage features on the north-facing side of FR (Nyland 2019, 84). Above these marginal drainage scars, the upper reaches are characterized by an abundance of periglacial features formed within the frost-shattered mantle cover since the waning stages of the Wisconsinan (Queen, 2018, 57).

3.3.4 Hydrology. Late-lying snowpatches are common on Frost Ridge and permit the relatively moist substrate conditions necessary for patterned ground formation, mechanical and chemical weathering, and overland flow. Frost Ridge constitutes an alpine nival regime (Woo 2012, 475–477) in which snow and ice are the primary suppliers of moisture to the area. Runoff from the snowpatch margins facilitates observable overland flow, slopewash, and rillwash. The only indications of appreciable water flow atop FR are solifluction lobes and sorted patterned ground, through which the preferential flow of water has been documented (Nelson, 1975).

3.3.5 Periglacial features. Relict and active periglacial features abound in the frost-shattered mantle of Frost Ridge. Nelson (1979) provided a description of the well-developed patterned ground field occupying the uppermost reaches of FR. Notable features here are well-developed coarse stripes, sorted circles, and solifluction lobes composed primarily of silty material (Nelson, 1979, 32). The occurrence of inactive sorted stripes has also been reported (Nelson 1979). Inactivity of stripes is indicated by the subdued appearance of the coarse lineations relative to intervening fines, which had been penetrated by vertical plant roots (Nelson, 1979, 43). Since the time of that research the periglacial features have undergone modifications (Nelson, 2018, personal communication) owing to complex relationships between snow mass balance and climate trends. For example, a snowpatch on the upper reaches of FR used to persist until early September in the mid-1970s, which is no longer the case. The resulting loss of moisture has resulted in widespread inactivity of the well-developed patterned ground field, which seems to have undergone a “tipping point” over the last four decades.

At the landscape scale, a series of incipient cryoplanation terraces, or nivation hollows, impart a notched appearance to Frost Ridge. These terraces, which were incised into the ridge by the ancestral Hobo-Llewelyn glacier, have been modified under the influence of nivation since deglaciation of the area. Today, the incipient terraces are comparable in scale to characteristic cryoplanation terraces found throughout unglaciated Beringia (Nyland, 2019, 81). Field reconnaissance during the summers from 2017-2019 confirm active periglacial processes operating on these incipient terraces, evidenced by the occurrence of late-lying snowpatches that persist into mid-July, and by the burgeoning or "puffed up" appearance of the sorted patterned ground.

3.4 Previous Work on Frost Ridge

Detailed periglacial investigations on Frost Ridge were first recorded in an open file report by Nelson (1975), in which he postulated the origins and formation of patterned ground. Nelson (1975) presented a rill-initiated hypothesis of patterned ground formation on Frost Ridge, emphasizing channelization by snow meltwater-fed rivulets, the obstruction of vertical percolation by the frozen substrate, and annual freezing to perpetuate ground sorting. Trenching of stripes normal to their axes by Nelson (1975) revealed the occurrence of anchored sorted stripes on FR whose depth of sorting (~80 cm) appeared to coincide with the position of the permafrost table, thereby fixing stripe positions on the slope. A thesis by Nelson (1979), which focused on the distribution and internal structure of sorted patterned ground on Frost Ridge, revealed that the distribution and form of patterned ground is related to both the moisture of the substrate, clast shape, slope, and local climate conditions. Nelson (1982) also addressed clast fabric within the coarse stripes, which he attributed to the squeezing of clasts along their axes oriented away from intervening bands of fine-textured sediment.

Periglacial studies on FR lapsed for more than 40 years. Work of this nature was resumed in 2017 by Michigan State University personnel (Queen 2018; Nyland 2019) and has focused largely on the role of nivation in the development of the FR incipient terraces. This body of work has contributed an understanding of cryoplanation terrace formation rates (Nyland & Nelson, 2020) and the characterization of a periglacial morphometric signature (Queen, 2018).

3.5 Conclusion

The glacial history, geology, and geomorphic activity of the Cathedral Massif region are well understood. Detailed studies conducted on Frost Ridge in the 1970s, in addition to the recent resurgence of research at the site have contributed knowledge pertaining to nivation, cryoplanation terrace development, and periglacial activity. The existence here of actively developing cryoplanation terraces provides an unusual opportunity to focus on the relationship between cryoplanation terrace development and the fluvial characteristics of sorted patterned ground.

Chapter 4 Statement of Problem and Hypothesis

Process-based investigations on CT formation are required before the nivation hypothesis can be widely embraced (Nyland, 2018, 96-97). Research points to the importance of snow patches in the generation of the characteristic stepped profiles (e.g., Nelson, 1989; Nelson & Nyland, 2017; Nyland & Nelson, 2020) but direct lines of evidence linking snow erosion to CT tread expansion are absent.

4.1 Statement of Problem

Cryoplanation terraces have been the subject of two genetic interpretations: (1) geologic structure; and (2) the nivation process suite. Geologic structure has been ruled out by some workers (e.g., Demek, 1969; Reger, 1975) because in many instances, CTs are observed to have no relation to foliation, faults, or compositional layering, and have been observed cutting across geologic structure.

The erosive efficacy of nivation has been scrutinized in recent years (e.g., Thorn & Hall, 2002; French, 2017), calling into question the role of nivation in land-forming processes. Recent literature has been more accepting of the nivation hypothesis (e.g., Nyland & Nelson, 2020a), but only indirect evidence exists to link nivation with CT formation. A fault in the nivation concept is that it fails to explicitly account for the absence of constructional ramparts on the inner (proximal) parts of CT treads.

Little effort has been made throughout the history of cryoplanation-terrace research to address the hillslope hydrology of CT treads and side slopes. The fluvial role of sorted patterned ground, specifically sorted stripes, has been documented qualitatively (e.g., Taylor, 1955;

Nelson, 1975, 1979; Queen, 2018; Nyland, 2019), and quantitatively (e.g., Hodgson & Young, 2001; Paquette et al., 2014, 2017a, 2018). Aside from short treatments in theses by Queen (2018) and Nyland (2019) no studies have leveraged the well-documented role of fluvial activity within sorted stripes in periglacial environments to better understand landscape-scale geomorphic evolution, specifically that of cryoplanation landforms.

Queen (2018) confirmed the existence of a characteristic periglacial landscape, describing the presence of periglacial landform assemblages, which he suggested are "form communities" of minor periglacial features such as sorted stripes and solifluction lobes. Queen suggested that these features operate as integrated, functional units. Paquette et al. (2018, 1087), demonstrated that the hydrologic influence of sorted stripes and water tracks can extend outside of their immediate hydrologic zone. The conception of sorted stripes operating on the landform assemblage scale, as demonstrated by Queen (2018) and Paquette et al. (2018), counters the dismissal of patterned ground as mere periglacial "embroidery" and highlights these features' potential influence on geomorphic evolution.

This thesis directly challenges opposition to the nivation hypothesis through a single research question: *"what is the fate of snowbank-weathered material on cryoplanation terrace profiles?".* If an adequate answer to this question can be constructed it will be among the first studies to unambiguously link CT morphology with periglacial processes.

4.2 Hypothesis

The above-stated research question is summarized by a hypothesis accounting for sediment transport from the location of weathering at scarp-tread junctions across CT treads:

Fluvial processes operating within the coarse portions of sorted stripes provide a mechanism for removal of weathered sediment from cryoplanation terrace scarps and treads, thereby preventing development of ramparts on treads below. Solifluction assists in the removal of sediment in the intervening fine stripes.

This thesis examines processes operating atop Frost Ridge through two distinct but complementary lines of investigation: (1) analysis of field data collected on two incipient cryoplanation terraces (Chapter 5); and (2) geomorphometric analysis of the network formed by sorted stripes in a large patterned ground field, based on high-resolution remotely sensed imagery (Chapter 6). Chapter 7 synthesizes this material to provide a new qualitative model of cryoplanation terrace development. This work is motivated by the apparent high degree of organization of sorted stripes on CT treads, their prevalence in these positions, the demonstrated hydrologic significance of coarse sorted stripes within the literature, and the failure of past work to account for the absence of weathered material accumulations on CT inner treads.

Chapter 5 Process Investigations on Two Incipient Cryoplanation Terraces

In some areas where well-developed cryoplanation terraces exist, e.g., throughout unglaciated Beringia, periglacial processes are more subdued than during past glacial periods, contributing to the interpretation that CT are inactive (Ballantyne, 2018, 221). Many studies conducted on cryoplanation terraces have been focused on geomorphically dormant CTs so that the processes responsible for CT formation are deduced from form (Ballantyne, 2018, 221). Contention exists within the literature surrounding the origins and formation of CTs because no studies have been conducted that explore periglacial process that may be related to CT formation.

Recent work on cryoplanation terraces has provided support for the nivation hypothesis of CT formation (Nyland & Nelson, 2020b). Other work has emphasized the importance of permafrost groundwater seepage in the localized weathering of CT scarp-tread junctions to maintain CT profiles (Matthews et al., 2019). Both studies implemented chronologically based methods to confirm the time-transgressive nature of CT treads but neither study confirms the processes responsible for scarp retreat.

5.1 Process-focused Geomorphology

Contemporary research on cryoplanation terraces has implemented relative and absolute age-determination techniques to define the origins and development of CTs (Matthews et al., 2019; Nyland & Nelson, 2020a,b; Nyland et al. 2020). Sufficient evidence now exists to unambiguously recognize the time-transgressive nature of CT treads through scarp retreat, and the resulting stepped CT profiles. Rates of CT formation have also been defined using sophisticated remote sensing techniques (Nyland & Nelson, 2020). With the integration of dating, remote sensing, mapping, and cirque-analog characterization of CTs, the case for causal association between late-lying snow patches and cryoplanation terraces has been reinforced. It is still the case, however, that the processes responsible for scarp retreat have not been confirmed through field-based investigations.

5.1.1 Process work in geomorphology. Process-based work in geomorphology emphasizes explanations of operational geomorphic processes to better understand landform development (Bradshaw, 1982). Adoption of process-based investigative strategies as replacements for qualitative theories of landscape evolution began in the late 1950s and have been attributed to the quantification of geomorphology (Sack, 1992). The quantitative characterization of drainage basins presented by Horton (1945), Strahler (1952), and Schumm (1956) serve as examples of studies that were some of the first to relate geomorphic form to process. Similarly, modeling efforts rely on the relation between landform and process to predict landform development (Goudie, 1990, 15). Nested within the process study paradigm is the systems theory approach as an explanatory model of geomorphic processes (Goudie, 1990, 6). Under the systems approach, landscapes form through interrelated processes that result in the maintenance of a stable form as opposed to processes resulting in greater change (Goudie, 1990, 7). Landforms are then viewed as inherent end members of models that are driven by underlying land-forming processes.

Process investigations are difficult in many periglacial environments because, in regions where CTs are well-expressed, periglacial processes are not as dominant as they were during cold climatic intervals (Reger, 1975, 202). Research on relict CTs has confirmed important characteristics such as elevation trends, dominant aspect, and the time-transgressive nature of tread development, but further work is needed to synthesize the qualitative models of CT formation that have been outlined by workers such as Demek (1969), Reger (1975), and Nyland (2019, 59).

5.1.2 Suggestions for process-based investigations on cryoplanation terraces. Calls for process studies on cryoplanation terraces have been made by Demek (1969), Reger (1975), and Thorn & Hall (1980; 2002). Assessments of erosion rates, morphological characterization, and the study of active CTs have been produced in recent years (Queen, 2019; Nyland, 2019; Nyland & Nelson 2020b). Still, data concerning 1) the hydrological regime of CTs (Demek, 1969, 70), 2) over-tread transportation of weathering products (Reger, 1975,.202), and 3) monitoring of climate conditions (Reger, 1975) are absent. Although CTs have been extensively mapped (Demek, 1969; Reger, 1975; Queen, 2018), the general remoteness of CTs and logistical constraints have hampered attempts to verify periglacial activity in all the locations where CTs are known to occur. As such, the ability to directly measure the processes thought to be associated with CT formation, specifically nivation, has been negatively impacted.

Specific attention should be paid to the investigation of material displacement in the generation of the characteristic stepped CT profile. The installation of mass movement pillars can be used to assess rates of sediment movement via solifluction (Benedict, 1970). Such features are known to occupy CT treads. Gerlach troughs have been utilized to estimate rates of erosion in inter-rill and rill zones (Roels & Jonker, 1983), which are similar in spatial distribution to the coarse and fine-textured sorted stripes in periglacial regions. Miniature temperature loggers can be programmed to collect and store climate data at varying temporal scales, and are easily deployable, and economical (Humlum, 2008, 22). Similarly, temperature loggers with external sensors can be used to collect air and ground temperature data for long-term monitoring investigations.

The need for process-based studies of CT formation has been indicated over the past four decades. Past work has eliminated some previously advanced CT formation hypotheses, but work remains to be conducted that relates periglacial processes to the existing qualitative models of CT formation. The availability and advancement of field equipment and techniques employed in periglacial regions facilitates process-based investigation of CTs. Cryoplanation terraces that are in a state of active scarp retreat are ideal locations to conduct process-based work.

5.2 Field Investigations on Frost Ridge

Two active incipient terraces are the sites of study for this chapter. At both sites, sorted stripes extend from snowpatch margins to the CT tread toes. In the coarse “gutters,” sediment is carried by running water, while the intervening fine stripes function as solifluction lobes. In early summer, running water can be heard flowing within the interstitial spaces of coarse stripes. Water is channeled through the sorted patterned ground landscape, moving sediment across CT tread surfaces. Some coarse stripes terminate near the margins of CT treads with silty deposits reminiscent of alluvial fans (Figure 5.1). Water running as overland flow from the termini of sorted stripes has been observed. Sediment transfer is the result of preferential flow of water through the coarse stripes over the gently sloping CT treads. The source of the water is the snowpatch upslope. The hydrologic activity occurring within sorted stripes atop FR was summarized by Nelson (1979, 32): “*Stone stripes are slightly sinuous and serve as channels for meltwater from perennial snowbanks upslope.”*

Figure 5.1 Oblique photo of Frost Ridge sorted stripe with silt fan. *From left to right; Frost Ridge and an extent box outlining sorted stripes downslope from a perennial snow patch with an extent box outlining a silt fan, forming at a coarse stripe terminus. Left photo taken July 9th, 2019, middle and right photos taken July 14th, 2019 by R. Mitchell.*

The occupation of CT treads and scarp backwalls by active periglacial features provides an unusual opportunity to study contemporary processes related to CT formation. The methodology presented in this chapter utilizes climatic monitoring and data collection to investigate the role of water and sediment transmission via sorted patterned ground and solifluction to assess CT formation, thereby addressing decades-old calls for such investigations. Results and data gleaned from this study are used to assess qualitative models of CT formation. The duration of the observation period reported here was necessarily very short, owing to logistical and scheduling limitations during the summer of 2019. The automated instrumentation described below was programmed to operate for up to two years and the resulting records are expected to span the period from July 2019 to July 2021.

5.2.1 Field methods. Field samples were collected over a week in mid-July 2019 from two incipient cryoplanation terraces (transverse nivation hollows). The incipient terraces, Terraces 2 and 4, are located on Frost Ridge at approximately 1622 and 1525 m.a.s.l., respectively (Figure 5.2). The terrace nomenclature adopted here follows terminology used by

Nyland (2019) and Queen (2018) to maintain consistency and to avoid confusion. To assess the microclimate-related characteristics of coarse and fine-textured patterned ground features, a series of temperature loggers were installed. On Terrace 2, Station 1 was established to characterize the subaerial and ground temperature profiles of areas occupied by solifluction lobes. Station 1 was instrumented with S-TMB-M0xx 12-bit air and ground temperature sensors (Onset Computer Corporation, Bourne, MA; see Appendix), stabilized by a tripod mast. The air temperature sensor was installed within a radiation shield, 2 m above the ground surface, while the ground temperature sensors were installed within a solifluction lobe. Excavating a pit within the solifluction lobe, the ground temperature sensor was installed 10 cm below the ground surface within the upslope wall of the pit. S-SMC-M005 soil moisture sensors (Onset Computer Corporation, Bourne, MA) were installed at 10 cm and 30 cm below the ground surface, accompanying the temperature sensor at Station 1. A similar instrumental array was established downslope on Terrace 4 (Station 2). Here, a mast with air and ground temperature sensors was accompanied by an additional ground temperature sensor placed 30 cm below the ground surface. Soil moisture sensors were placed at 10 cm and 30 cm depths. Ground temperature logging equipment on Terrace 4 was installed within a solifluction lobe, mirroring the instrument setup on T2.

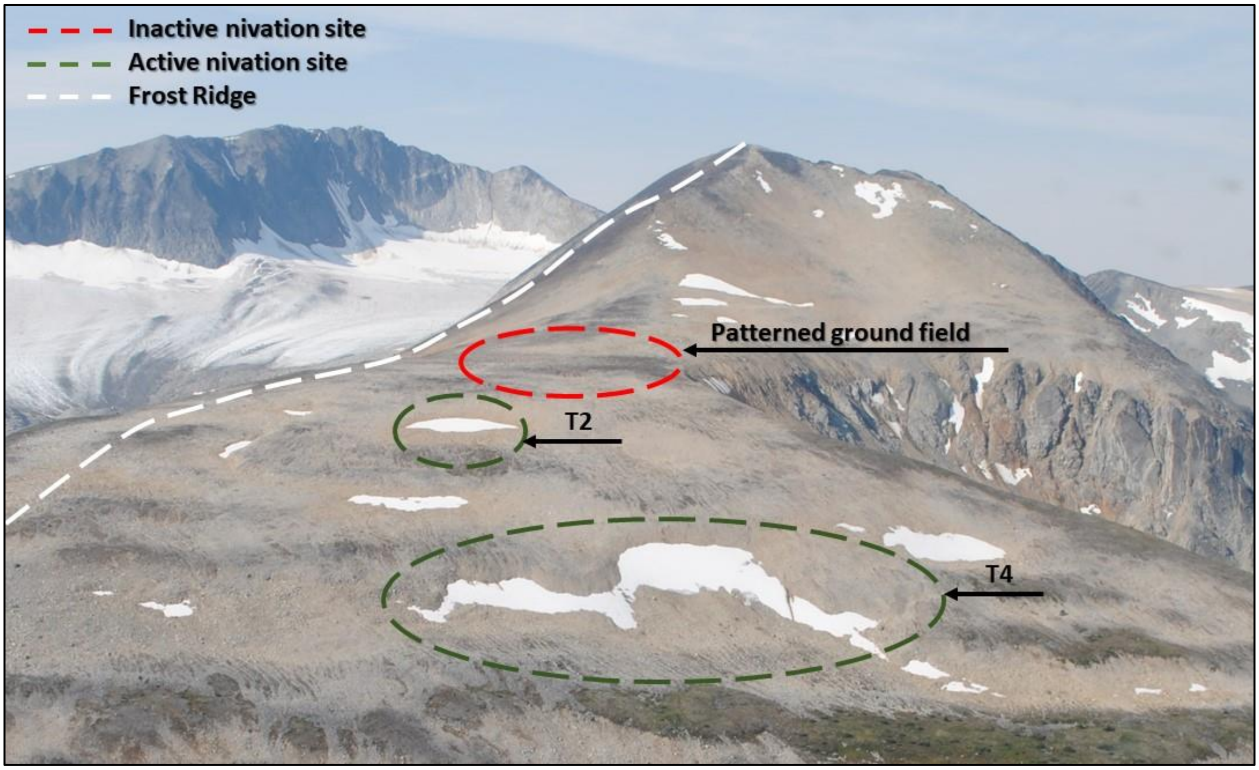

Figure 5.2 Site arrangement on Frost Ridge. *Field sites are indicated by dashed circles. T2 and T4 are active periglacial sites evidenced by the occurrence of late lying snowpatches occupying the incipient terrace scarp backwalls. The patterned ground field is considered inactive because snow no longer persists late into the summer. Frost Ridge faces north. Photo taken July 9th, 2019 by R. Mitchell.*

Six MX2203 TidbiT® (Onset Computer Corporation, Bourne, MA) miniature temperature data loggers were installed in two transects extending from the mast on Terrace 4 (located near the toe of the CT tread) upslope towards the CT scarp. At the time of data collection, the CT scarp backwall was occupied by a receding snowpatch. To monitor one coarse sorted stripe, coarse fragments were removed to excavate small, shallow (<10 cm) spaces within which loggers were deployed. These cavities were loosely covered with the excavated blocky material. The three loggers comprising the coarse-stripe monitoring transect were placed at approximately 1528, 1532, and 1546 m.a.s.l on the slope. The logger at the highest position on the slope was placed at the snowpatch margin on Terrace 4. To monitor fine-textured areas moving as solifluction lobes, three of the miniature temperature sensors were deployed on the ground surface directly upslope from the mast on Terrace 4 at approximately 1523, 1526, and 1529 m.a.s.l on the slope. All climate monitoring equipment on both terrace study sites was programmed to log data at 5-minute intervals for the duration of the field campaign. Miniature temperature sensor data were collected and stored using HOBOmobile® software. Ground, air, and soil moisture data were collected and stored using H21-USB Micro Station data loggers (Onset Computer Corporation, Bourne, MA) and Hoboware® graphing and analysis software (Appendix, 107).

5.2.2 In lab calculations. Calculation of thermal diffusivity was made using temperature data from Terrace 4 to indicate characteristics of the ground thermal regime. Thermal diffusivity, an index of a material's ability to change temperature (Williams & Smith, 1989, 94), has been used to discern the operation of non-conductive forms of heat transfer in the substrate (Nelson et al., 1985; Rajeev & Kodikara, 2016). In a purely conductive system, it is assumed that within a homogenous medium, heat flows only by conduction in the vertical direction (Williams & Smith, 1989, 85). Non-conductive heat transfer within the thermal regime is introduced through variations in soil moisture and texture, and through phase changes of water within the ground profile (Williams & Smith, 1989, 106). Apparent thermal diffusivity, $\propto'$, a non-laboratory method for calculating thermal diffusivity, can be used to detect phase change or other non-conductive modes of heat transfer occur. Two sinusoidal temperature records from varying depths within the material of interest can be treated with the apparent thermal diffusivity equation, which takes the form

$$\propto' = \frac{\omega}{2}\left[\frac{Z_2 - Z_1}{ln(A_1/A_2)}\right]^2 \qquad (5.1)$$

where Z refers to temperature sensor depths (m), A is thermal amplitude (C°) at depths Z_1 and Z_2, and ω is the angular frequency of oscillation given by

$$\omega = 2\pi/P, \qquad (5.2)$$

where P is the period of the temperature wave (s).

Equation 5.1 yields a quantity expressed in units of length squared per unit time (m^2 s^{-1} in SI units). An unreasonably large value would imply rapid and large changes in temperature (Williams & Smith, 1989, 104). In the case on Frost Ridge, apparent thermal diffusivity was used to assess the impacts of water on heat transfer at the feature level.

Water and transported sediment from the termini of three sorted stripes were captured using Gerlach Trough Runoff Sediment Samplers (Rickly Hydrological Co., Inc.) (Figure 5.3). The basin of each trough collects sediment that settles to the bottom of the trough while transported water is routed to a collection receptacle downslope. The design of the sediment trough facilitates separate measures of transported water and sediment samples. Clear nylon piping was used to connect troughs to 19-liter (5-gallon) jugs placed downslope from the trough to capture transported water. Overflow holes were drilled into the jugs to accommodate excess water flow. Troughs were installed at the terminus of a coarse sorted stripe by excavating some coarse fragments, digging a pit approximately the size of the trough beneath the stripe terminus, and inserting the trough into the pit. The lips of each trough were inserted beneath some coarse fragments of the sorted stripe to direct water and sediment flow into the trough (Figure 5.4B). Troughs were anchored using large fragments from surrounding areas. Two sediment troughs were instrumented for two separate coarse stripes on T2. One trough was instrumented at the base of a coarse stripe on T4, while another trough was installed at the base of a solifluction lobe, also on T4. Owing to the rocky substrate, troughs could not be installed flush with the coarse stripe termini. As such, some water and sediment were assumed to flow beneath and around the sides of the troughs. Volumes of transported sediment and water collected using the troughs are used as relative measures of sorted stripe hydrology.

Figure 5.3 Sediment trough and mast installation on cryoplanation terrace. *(Center) mast with sensors measuring soil temperature and moisture conditions in intervening fine area. (Right and left) sediment traps collecting transported water and sediment from the termini of sorted stripes. Sediment trap locations are indicated by dashed red circles.*

Figure 5.4 Field activities. *(A) Mast on T4. (B) Sediment trough installed on T4 at the terminus of a coarse sorted stripe (not pictured). (C) Location of miniature logger within a coarse stripe, outlined by a white dashed circle. (D) Ground temperature sensors within a solifluction lobe on T2. (E) Collection of transported water and sediment from the snowpatch margin in July during the summer 2018. (F) Organization of a sediment trough at a coarse stripe terminus and 5-gallon collection jug downslope. All photos except for photo E (taken in July 2018 by K. Nyland), were taken during the week of July 9th-14th, 2019.*

5.2.3 Laboratory methods. Transported sediment from the sediment troughs were collected and textures analyzed. During the summer of 2018, transported water and sediment were collected from the base of the snowpatches that occupy the nivation hollows on T2 and T4 (Nyland & Nelson, 2020). Snowpatch samples were compared to material collected from sediment troughs. Sediment trough samples were analyzed using laboratory facilities at Michigan State University during the early spring following the field campaign. Wet samples were oven dried at 40°C to remove all moisture. Samples were gently disaggregated by mortar and pestle and material sieved to separate coarse (>2mm), fine, and organic fragments. Fine samples were passed 3 times through a sample splitter to ensure a representative and homogeneous sample. 10mL of dispersant solution ($[NaPO_3]_{13} \cdot Na_2O$) and ~10mL of deionized water were added to 20mL vials containing ~0.5g of fine sediment sample. Vials were shaken for at least 30 minutes. Laser diffraction using a Malvern Mastersizer 2000E unit generated a particle size analysis report containing detailed textural information for each sample. Maps of the field arrangements on both terraces are presented in Figure 5.5.

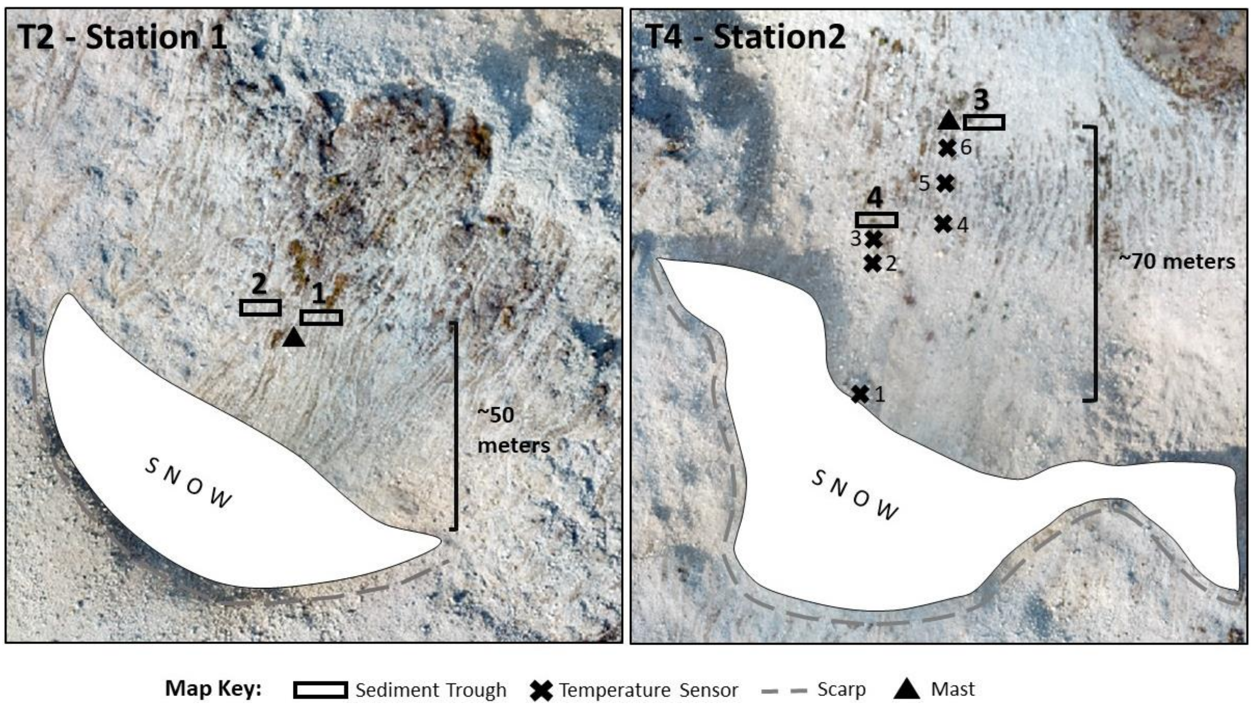

Figure 5.5 Equipment orientation on Frost Ridge. *(Left) Terrace two instrumented with a mast and two sediment troughs. (Right) Terrace 4 with six miniature temperature loggers, a mast and two sediment troughs. Small numbers next to the temperature sensor symbols indicate the miniature logger number. Larger numbers on top of the sediment trough symbols indicate trough number. Relative locations and distances between features are represented in this map.*

5.3 Results

The length of the record from all monitoring equipment spans approximately 3 days (Figure 5.6). Data logging began for each sensor around midday on July 11th and ceased midday on July

14th. During the logging period, a general decrease in temperature was observed in all logger records.

5.3.1 Monitoring data. Recorded air temperatures at the Terrace 4 station tended to be higher (8.19 °C) than those at Terrace 2 (7.09 °C), which is located at a higher elevation on Frost Ridge than Terrace 4. Ground temperatures at both sites tended to be higher than the recorded air temperatures. For example, on Terrace 4, at 10 cm depths, the average temperature was 12.84 °C compared to the average air temperature of 8.19 °C. In the fine soil, phase lags and progressively subdued thermal amplitude with depth were observed (Figure 5.6), as would be expected in a conductive heat-transfer system. Within the coarse stripe, the logger labeled *TB_1* was positioned closest to the snowpatch margin on Terrace 4 (Figure 5.5). Increasing logger numbers indicate progressively lower logger positions on the slope, with logger *TB_6* occupying the lowest position on Terrace 4. A numerical breakdown of the miniature and mast temperature data records is presented in Table 5.1.

Within the miniature temperature logger data, warmer temperatures were recorded from the loggers instrumented on fine sorted stripes. Within the fine-textured stripe closest to the CT tread margin, average temperatures were recorded at 12.85 °C. Generally, higher maximum and minimum temperatures were recorded for the fine stripes. From TB5, the miniature logger placed mid-CT tread, maximum and minimum temperatures were 19.04 °C and 5.79 °C, respectively. The greatest fluctuations in temperature were recorded from TB_1, located nearest the snowpatch margin, where the temperature amplitude was 14.12 °C, and from TB_6, located nearest the CT toe tread, where the temperature amplitude was 20.82 °C. Within all temperature data records, peak temperatures were achieved just after midday when the sun is at its highest position in the sky and receipts of solar radiation are greatest on the hillslope. Temperatures dip sharply near the end of the day and continue to decrease until the sun rises. Observable water flow, which occurred from the 12th to the 13th, corresponds with recorded temperatures. On the last day of the logging interval, no observable water flow was observed on the hillslope.

Higher soil moisture conditions were recorded at the 30 cm depth versus conditions at 10 cm depths. Soil moisture conditions recorded at 10 cm depths generally follow temperature trends. Soil moisture tends to be higher at midday than later in the day. The soil moisture sensor on Terrace 4 depicts this diurnal trend in soil moisture conditions clearly.

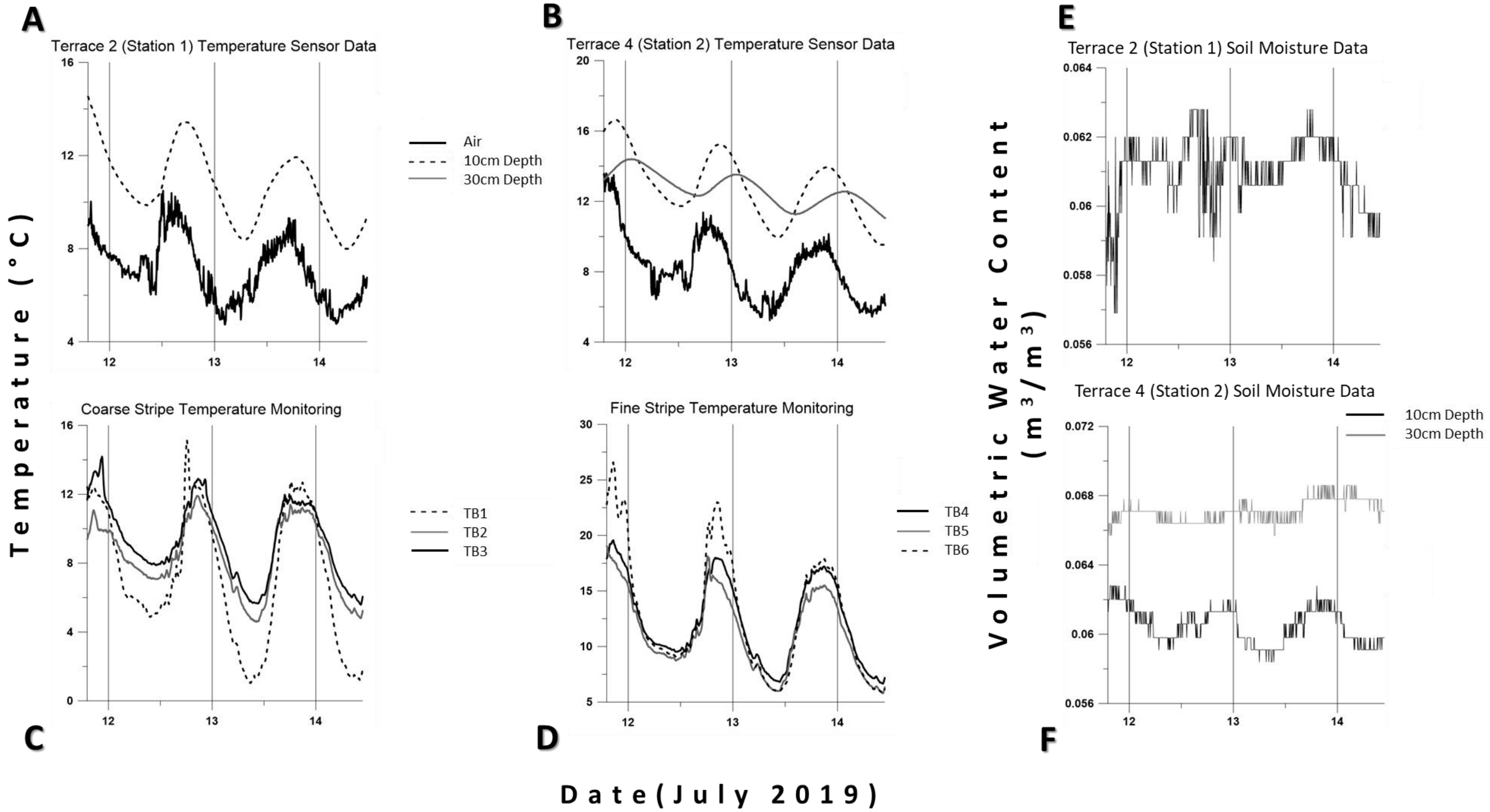

Figure 5.6 Field data logger records. *(Fig. 5.6A-B) Terrace 2 and Terrace 4 station temperature sensor data display a systematic diminution of thermal amplitude with depth, and a progressive lag in thermal response with depth. The diurnal variation of temperature is also depicted. (Fig. 5.6C-D) Coarse and fine stripe temperature monitoring records depict temperature variations induced by position on the slope and substrate material. (Fig.5.6E-F) Soil moisture data from both terraces depict the same diurnal variances as indicated in the temperature records. Amplitude increases are shown at depth, attributable to enhanced soil moisture conditions at depth and the leaching of surface moisture through vertical water percolation.*

Table 5.1 Temperature logger data breakdown. *Temperature indices are shown below for temperature sensors on masts and for the miniature temperature loggers. Mast sensor names refer to the station number and the depth at which the sensors were placed. Air sensors are labeled with the station number and "air". Flux temperatures were calculated as the difference between the maximum and minimum temperatures for each sensor.*

Position	**Sensor**	**Average Temperature (°C)**	**Minimum Temperature (°C)**	**Maximum Temperature (°C)**	**Temperature Amplitude (°C)**
	Mast				
Station 1	**TS1_air**	7.09	4.74	10.49	5.75
	TS1_10	10.68	8.00	14.53	6.53
	TS2_air	8.19	5.23	13.59	8.36
Station 2	**TS2_10**	12.84	9.53	16.63	7.10
	TS2_30	12.70	11.05	14.41	3.36
	Miniature Data Loggers				
	TB1	7.23	1.03	15.15	14.12
Coarse Stripe	**TB2**	8.39	4.59	11.91	7.32
	TB3	9.32	5.58	14.19	8.61
	TB4	12.30	6.66	19.57	12.92
Fine Stripe	**TB5**	11.29	5.79	19.04	13.26
	TB6	12.85	5.77	26.58	20.82

5.3.2 Thermal diffusivity calculations. The temperature record for Station 2 on Terrace 4 (Figure 5.6) was used to obtain a value of apparent thermal diffusivity (α') for the first full 24-hour period of observation. Values of the input parameters are given in Table 5.2. Equations 5.1 and 5.2 yield a value for α' much larger than those expected for a moderately wet silt in which heat transfer occurs entirely by conduction (Johnston et al. 1981, 119-123). Although the temperature record shows decreasing amplitude and a temporal lag with depth, the large variation in soil moisture (Figure 5.6) on this day contributed a significant nonconductive component to the ground-thermal regime. Variations in soil moisture, attributable to the arrival of snow meltwater on this day, depressed soil temperature rapidly. Over the course of a summer, snow meltwater also acts to decrease soil strength and encourage sediment transport by solifluction.

Table 5.2 Input parameters for determination of apparent thermal diffusivity.

P (s * day^{-1})	Z_1 (m)	Z_2 (m)	A_1 (°C)	A_2 (°C)	α' (m^2 s^{-1})
86,400	0.1	0.3	7.1	3.36	30.0 x 10^{-7}

5.3.3 Transported water/sediment data: Installation occurred on July 11th and material from all four sediment troughs was collected on July 14th. Particle-size analysis was conducted on all samples in the lab the following January. Results from this analysis are presented in Figure 6.8. Trough 3_4, which was installed within a solifluction tongue on Terrace 4, collected very little material, all of which was assumed to have blown/saltated in as opposed to having flowed in via solifluction. Texture curves in Figure 5.7 show the dominance of silt-textured material within samples collected from coarse stripe termini. Jugs collecting water from all three troughs installed at coarse stripe termini were found completely full after the first day following their installation. Based on observations of the overflowed jugs, more than 19 liters of transported water is inferred to have flowed through each coarse stripe. The transported sediment/water collection methodology implemented in this study yielded only relative volumetric measures; however, mass-movement pillars installed within one fine-textured stripe during the field campaign will yield data sufficient for volumetric estimates of sediment removal upon annual visits to the site. Texture size percentages are expressed numerically by sample in Table 5.3. Textural classifications presented in Table 5.3 confirm the silty texture of sediment transported in the coarse stripes.

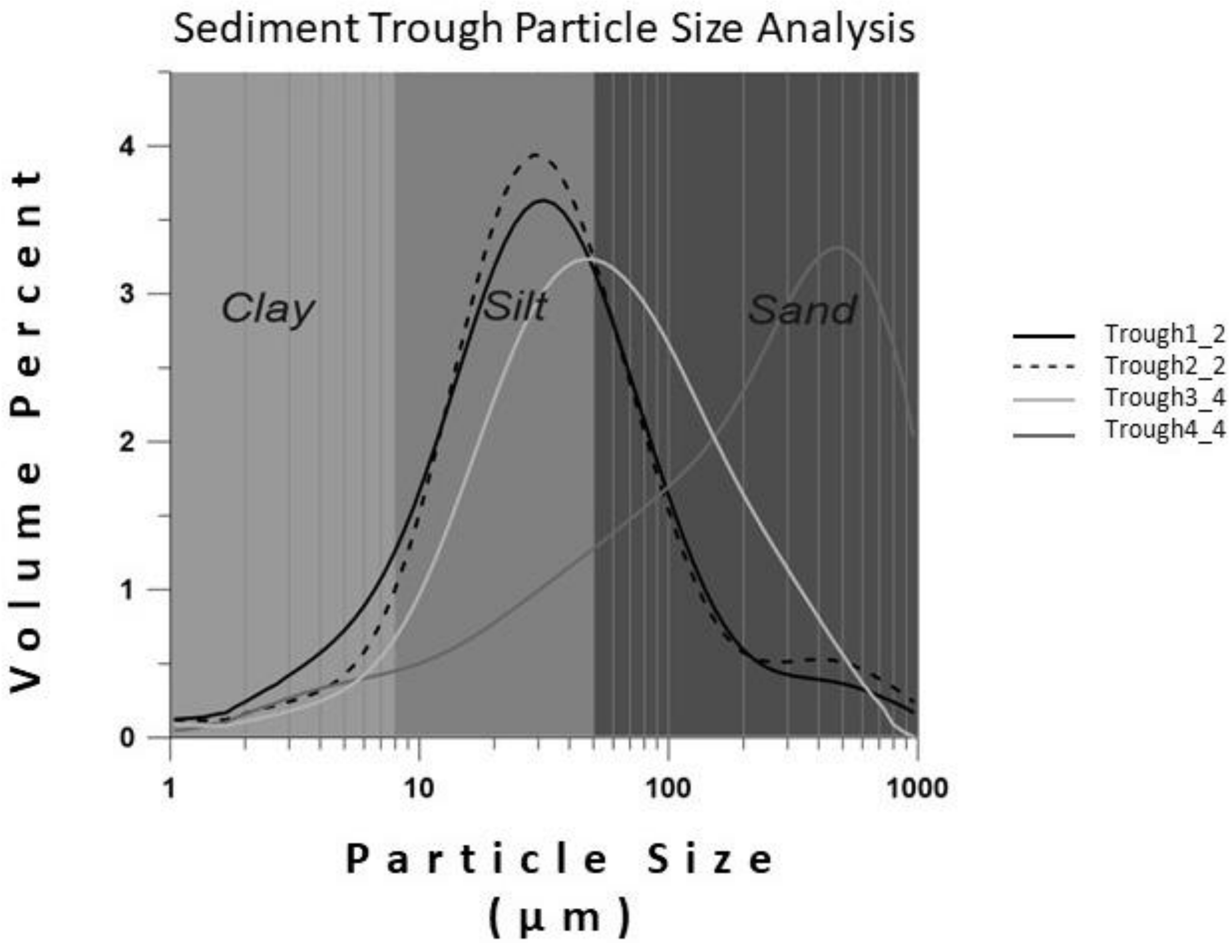

Figure 5.7 Particle size analysis of sediment trough data. *Particle size curves above are expressed as a percentage of each individual sample volume. Higher curves indicate a higher occurrence of a given soil texture within the sample. Particle sizes define the texture of the soil. Trough names indicate the number of the trough first, followed by the terrace on which the trough was instrumented.*

Particle size analysis was also conducted on transported sediment collected from the snowpatch margins on both Terraces 2 and 4 by Nyland (Nyland & Nelson, 2020). On both Terraces 2 and 4, samples collected from snowpatch margins were dominantly of sandy texture. As indicated in Table 5.2, transported sediment textures collected at coarse sorted stripe termini are dominantly silty.

Table 5.3 Sediment trough numerical particle size analysis results. *Texture classifications based on the data presented in Figure 5.7. Troughs 1, 2, and 4 were installed at the base of coarse stripe termini while Trough 3 was installed at the base of a fine stripe.*

Trough	% Clay	% Silt	% Sand	Texture
1_2	11.7	57.5	30.8	Silt Loam
2_2	7.9	60.4	31.7	Silt Loam
3_4	5.8	16.6	77.7	Loamy Sand
4_4	5.7	44.6	49.7	Very Fine Sandy Loam

5.4 Discussion

Results from the climate and soil monitoring equipment identify strong diurnal trends in conditions on both terraces and scale-based temperature gradients. Phase lags and subdued temperature amplitudes observed in soils at mast locations is indicative of conductive heat transfer at depth. A slope-scale temperature gradient is inferred from temperature records between Terraces 2 and 4—warmer conditions are present at lower positions on the slope. A terrace-level gradient is implied from the sorted stripe temperature monitoring equipment where the highest temperatures were recorded from the loggers operating closest to the CT toe. Substrate albedo seemed to impact recorded temperatures—temperatures on average were higher on fine stripe material compared to temperatures recorded within coarse material. Differences in temperature occurred between loggers that were placed next to one another on the CT tread—TB_3 and TB_4—but were placed within contrasting stripe material, indicating the presence of micro-scale topoclimatic influences on the hillslope. The largest fluctuations of sorted stripe temperatures were observed at the location closest to the snowpatch margin and closest to the CT toe. Large fluctuations at the location nearest the snowpatch demonstrate non-conductive heat transfer induced by diurnal pulses of water through the coarse stripes. Pronounced fluctuations in temperatures near the snowpatch margin may also be attributed to localized cool, dense air descending from the snowpatch. Near the CT tread margin, temperature variability may be related to contrasts in albedo between the darker solifluction lobes and the lighter-colored coarse stripes.

A feature-level temperature gradient is indicated by the air, 10 cm depth, and 30 cm depth temperature sensors, where temperature fluctuation was less pronounced. Soil moisture monitoring confirms the presence of moisture within fine stripes and displays a vertical gradient of soil moisture in which moisture increases with depth. Soil moisture conditions, especially near the ground surface, display a diurnal trend that follows diurnal temperature fluctuations. The presence and behavior of soil moisture within the fine stripes at both sites promotes solifluction and frost creep.

Silty material collected from the base of coarse-stripe termini and the overflowed 19-liter collection jugs confirm the active transport of silt-sized material suspended in water via the coarse stripes. Differences in textures from material collected at sorted stripe termini and snowpatch margins could be attributable to the fluvial sorting of material as it is transported away from the snowpatch margin towards the CT tread. Fluvial sorting as water and sediment is transported across the CT tread would help to explain the occurrence of silt fans that extend from the termini of coarse sorted stripes, as illustrated in Figure 5.1.

5.5 Conclusion

Climate monitoring records and soil texture analysis characterize periglacial processes operating on Terraces 2 and 4. Strong diurnal temperature fluctuations were observed on both terraces at three distinct spatial scales; slope level, terrace level, and feature level. At the slope level, a gradual increase in air temperature exists. The occurrence of snowpatches at both—the snowpatch on the lower terrace being the larger of the two—demonstrates that snow mass balance is influenced by the relationship between snow accumulation and topographic hollows that shield the snow from incoming solar radiation. At the terrace level, increases in temperature were observed as one moves from the snowpatch margin toward the CT tread margin, a consequence of water being warmed as it travels across the terrace. At the feature-level, marked differences were observed within coarse and fine stripes. Temperature amplitudes achieved in the coarse stripes closest to the snow margin demonstrate the non-conductive transfer of heat attributable to pulses of water flowing through coarse stripes. Temperature amplitudes within coarse stripes at progressively downslope positions indicate the flow of water in the large interstitial boulder spaces.

A system of sediment transportation driven by the onset of warm temperatures is indicated through the analysis of the quantitative data presented in this chapter. With the onset of warmer temperatures early in the day, snowpatches warm and release meltwater downslope, which is demonstrated clearly by large temperature fluctuations recorded by the temperature logger placed at the snow patch margin. The lag in temperature peaks within coarse stripe temperature loggers further downslope reflect the propagation of water through coarse stripes, reflecting the hydrologic connectivity that exists within coarse stripes. As water flows downslope through coarse stripes, coarser-textured material is deposited higher on the slope while finer-textured material continues to flow within coarse stripes. Near the CT tread toe, sorted stripes terminate in large silt fans sometimes burying their lower reaches and resulting in the formation of turf-banked solifluction lobes. Solifluction and flowing water both contribute to the efficient transport of water and sediment across CT treads. Diurnal decreases in temperature likely influence the potential of snowmelt water contributions. In this interpretation, nivation is responsible for much of the transport of material on the hillslope, a phenomenon that can be used to infer the lack of material ramparts on subjacent CT treads. Sediment transport on the hillslope is strongly influenced by both temperature and moisture availability. Underlying permafrost conditions and depth of sorting within the patterned ground network limit the vertical percolation of water, providing a maximum depth of hydrologic activity attributable to CT flatness.

Chapter 6 Network analysis of a Sorted Patterned Ground Field

The patterned ground field occupying the majority of the T1 cryoplanation tread atop Frost Ridge is comprised primarily of sorted stripes, although sorted circles, sorted nets, and turf-banked solifluction lobes are also found within the field. Sparse vegetation overlying a fine-textured substrate is also present in the sorted patterned ground field. Fieldwork conducted at this site in the mid-1970s confirmed that snowmelt water from a late lying snow patch upslope used to flow within the coarse segments of the patterned ground field throughout the summer (Nelson, 1975). Proximity to a perennial snow patch, snow meltwater, and cool climatic conditions promoted the development and maintenance of the patterned ground. Today, the patterned ground field, although seemingly geomorphically dormant owing to earlier disappearance of the snowpatch, is still intact and in fact, bears resemblance to a drainage network. This conceptualization has not previously been explored in the context of CT formation.

The methodology used in this thesis to address a network of well-developed sorted patterned ground atop a cryoplanation tread explores: 1) the efficacy of hydrologic modeling in a remote upland periglacial environment; 2) the comparison of manual versus automated channel detection; and 3) quantification of the characteristics of a sorted patterned ground channel network. Results of the channel network analysis will be used to infer local hydrology, an approach that has not previously been attempted in the context of sorted patterned ground (cf. Godin et al. 2019). Network analysis may provide insight into a system of features that operates to evacuate water and sediment from snowpack margins near CT scarp backwalls, thereby clarifying some of the problematic aspects of the nivation hypothesis raised by Hall (1998) and others, and contributing to enhanced understanding of CT formation.

6.1 Remote Sensing in Geomorphology

Remote sensing is a standard tool in geomorphic investigations (Rhoads, 2004). Geomorphology, a subdiscipline of physical geography, is the study of landforms and landscapes (Short & Blair, 1986) and is concerned primarily with surface morphology and composition (Smith & Pain, 2009). When available, remotely sensed data provide useful information if a site is difficult to access due to physical restrictions, enabling geomorphic studies. Utilization of remote sensing is particularly helpful when research topics are focused in remote realms such as Arctic and alpine regions. The bird's-eye-perspective of satellites and other unmanned aerial vehicles permit analysis of processes that operate over wide areas, revealing relationships not clearly visible from the ground (Short & Blair, 1986). Advances in computer technology, storage capacity, and the amount and availability of remote sensing data have added to the utility of such data in physical geography (Rhoads, 2004; Short & Blair, 1986; Smith & Pain, 2009). When remote sensing data are integrated with field-based validation, geomorphic studies benefit from increased accuracy and testing of previously untestable hypotheses (Smith & Pain, 2009). The state of remote sensing data acquisition and products as they relate to the methodology of this chapter is presented below.

6.1.1 Data acquisition. The term remote sensing refers to the acquisition of data from a distance (Colwell, 1966, 1; Campbell et al., 2011, 6). The process of remotely acquiring information about the land surface involves the physical object of study, a sensor such as a camera, and a platform on which the sensor is mounted, e.g., an unmanned aerial vehicle

(UAV). Sensors are responsible for capturing and recording the electromagnetic energy being emitted from the ground surface acquired during a survey, or the period of data acquisition (Brunn et al., 2004, 112). A temporal record of aerial imagery is achieved when an area is repeatedly surveyed by a sensor at different times. The most commonly derived data from a remote sensing survey are aerial images, or photos of the Earth's surface taken from above (Smith & Pain, 2009). Electromagnetic information (sunlight reflected from the ground surface) recorded from the Earth's surface is then converted into information that reflects the physical properties of the features of interest. For this reason, remotely sensed imagery is a model or representation of the Earth's surface (Brunn et al., 2004, 119).

6.1.2 Data. Aerial images, photos of the ground surface taken aloft, are converted to geographically rectified maps known as orthoimages. Orthoimages are models of the Earth's surface that depict details as imagery and have been adjusted to a standard datum and map projection (Jensen, 1995; Brunn et al., 2004, 124). Orthoimages reflect the positional and electromagnetic characteristics of objects on the ground. Orthomosaic maps, which are particularly useful products, are produced when two or more orthoimages are stitched together, giving the impression of one continuous image (Fernandez, Garfinkel, & Arbiol, 1998). Orthomosaic maps have the benefit of a seamless appearance, as well as having large spatial extent.

Digital Elevation Models (DEMs) are another type of model of the Earth's surface generated from aerial imagery (Zhang & Montgomery, 1994). DEMs reflect the topography of a given area of the Earth's surface and are often summarized as a grid of regularly spaced elevation information. A continuous elevation surface is created through interpolation methods such as kriging. Together, orthoimages and DEMs offer a strong visualization tool that can be used qualitatively for visual analysis and quantitatively as data inputs for modeling efforts implemented in a geographic information system (GIS) (Kamp et al., 2005; Smith & Pain, 2009).

6.1.3 Applications of remote sensing models in periglacial geomorphology. Physical geographers and other earth scientists benefit from the spatial and temporal coverage offered by remote sensing (Short & Blair, 1986; Boyd, 2009, 456 & 645). In certain cases, data of interest may be difficult to access or difficult to measure, e.g., remotely located sites, and tree canopies. A sensor mounted on aerial craft capture images covering large swaths of land in a fraction of the time that would be required for a human to trek across the same terrain. Similarly, the spatial coverage offered by aerial surveys encompass landform-size data (Singh, 2018). Numerous satellites that monitor the Earth's surface at varying spatial resolutions and scales (Short & Blair, 1986, ix), in addition to open-source data repositories, e.g., Google Earth, provide easy access to remotely sensed information at temporally robust scales (Smith & Pain, 2009).

Remotely sensed data products have been used in periglacial regions to assess the overall spatial organization of features, to test previously untestable hypotheses, and to map hard-to-access features. A study conducted by Nyland and Nelson (2020) used high-resolution DEMs to estimate denudation rates by nivation. Volumetric comparison of marginal drainage features and incipient cryoplanation terraces was conducted to estimate rates of erosion attributable to nivation (Nyland, 2019, 86-87). Results indicate that a nivation-altered hillslope had achieved the appearance and size of other cryoplanation terraces found in unglaciated Beringia since deglaciation of the area (Nyland, 2019, 87). Working in the same study area, Queen (2018) used large-scale geomorphometry to map periglacial features across Alaska and in northwestern British Columbia. Using elevation data from the Arctic DEM- Polar Geospatial Center (Porter et al., 2018) and field observations, Queen constructed local-scale maps of periglacial assemblages at several sites distributed across eastern Beringia, documenting the existence and structure of "periglacial form communities" (e.g., Poser 1977) and indicating the presence of characteristic periglacial landscapes. Similar efforts to map periglacial features were conducted by Grosse et al. (2005). Automated identification of features and manual digitizing were used and the results of the two methods compared to assess the accuracy of using remotely sensed imagery in feature extraction. High-resolution maps of periglacial features produced from the automated extraction of features using satellite imagery and DEMs underline the utility of such data inputs in periglacial geomorphology. Kamp et al. (2005) used elevation data from the ASTER (Advanced Spaceborne Thermal Emission and Reflection Radiometer) sensor to produce a map of periglacial features including solifluction lobes and patterned ground. The results of that study provide support for the use of remotely sensed elevation data to map periglacial features. Other inventories of periglacial features using air photographs, digital elevation models, or remote sensing products include Evans et al. (2017), Křížek et al. (2019), Mithan et al. (2019), and Eichel et al. (2020).

Results from studies using remotely sensed imagery as data input indicate that use of such data is feasible and yield useful applications in periglacial environments. The integration of remote sensing into periglacial research broadens the spatial extent of the studies (e.g., Queen 2018) and enables testing of hypotheses that are otherwise difficult to evaluate because of field limitations (e.g., Nyland, 2019).

6.2 Drainage Network Analysis

A drainage network is comprised of paths on the land surface along which water flows (Tarboton, 1989, 11). Sorted patterned ground features often occur as an interconnected system of boulder-filled gutters on the ground surface. Such patterned ground fields resemble drainage networks but have not been quantitatively explored as such. Quantitative methods to characterize drainage networks are abundant in the literature and provide useful metrics to define drainage networks past general qualitative assessment.

6.2.1 Sorted patterned ground drainage channels. All sorted patterned ground forms are comprised of boulder/stone gutters and areas of fine soil cells (Goldthwait, 1976). Sorted patterned ground forms often develop as networks of interconnected circles, polygons, and stripes (Washburn 1956), and are prominent periglacial features. Boulder gutters, which are the defining boundaries of sorted forms, connect to one another, unifying the individual forms. Elongated sorted stripes display this arrangement on slightly sloping surfaces and serve as a shallow drainage system on hillslopes (Goldthwait, 1976). Within this sorted network, water flows through the large interstitial spaces of the boulder gutters, promoting removal of fines from the gutters. The interconnectedness of sorted stripes and the available interstitial space offered by boulder gutters facilitate a system of water and sediment movement, a phenomenon that has been documented over the past half century (Caine, 1963; Smith, 1968; Nelson, 1975; Goldthwait, 1976; Queen, 2018, 57). Although sorted patterned ground has been documented as effective water channels for removal of sediment, (e.g., Nelson, 1975), no study has been conducted that assesses the geometric or topological arrangement of such networks.

6.2.2 Drainage network Analysis. River network characteristics were first quantified in terms of stream order by R.E. Horton in 1945 (Melton, 1957, VIII). Previously, drainage networks had been qualitatively classified based on pattern (e.g., Thornbury, 1969). The stream-ordering methods presented by Horton were later revised by Strahler (1952) to produce the widely known Horton/Strahler stream ordering method (Smart, 1978). The methodology presented by Horton involved identification of basin stream order, the most fundamental drainage basin assessment. Stream ordering gives rise to other quantitative drainage-basin parameters, such as stream length and number of streams. Horton related stream order and length through a series of ratios known as "Horton's laws" to characterize drainage basins.

The bifurcation ratio (R_b) is the ratio of the number of stream lengths of a given order (N) to the number of stream lengths of the next highest order (N+1). Bifurcation ratios generally range from 3.0-5.0 and indicate degree of structural influence (Pareta & Pareta, 2011). Stream length ratio (R_L) is the ratio of the stream length of segments of a given order 'L' to the mean stream segment lengths of the next lower order (L-1). Stream length ratio varies at the basin and sub-basin levels, and indicates the relationship between flow discharge and the erosional stage of the basin (Hajam, Hamid, & Bhat, 2013). Drainage density (D_d) is the ratio of the total length of all streams in a drainage network (L_T) to the drainage basin area (A). Drainage density is an indicator of drainage basin dissection, where a high value of D_d is related to a highly dissected basin (Melton, 1957, 35; Hajam et al., 2013). Drainage density also indicates relief — steep basins tend to have a low drainage density ratio value (Melton, 1957, 37). The above-stated morphometric calculations are given by the formulae:

Bifurcation Ratio $$R_b = \frac{N}{(N+1)} \qquad (6.1)$$

Stream Length Ratio $$R_L = \frac{\bar{L}}{(\bar{L}-1)} \qquad (6.2)$$

Drainage Frequency $$D_f = \frac{N_T}{A} \qquad (6.3)$$

Drainage Density $$D_d = \frac{\bar{L}_T}{A} \qquad (6.4)$$

Relief Ratio $$R_r = \frac{R}{L_P} \qquad (6.5)$$

The Strahler stream ordering method (Strahler, 1952) is used in this study. The Strahler ordering method assigns an order N = 1 to all streams that do not have tributaries. Downstream from the first-order streams, when two or more streams of the same order N meet, an order of N + 1 is assigned. If stream order N is met by a stream order less than N, no change to the downstream section occurs. All sediment and water flow out of the highest order stream lengths. A higher stream order is associated with a higher basin discharge (Hajam et al., 2013). Horton's laws are useful metrics to characterize drainage networks (Smart, 1978) and are still implemented (e.g., Pareta & Pareta, 2011; Hajam et al., 2013).

Commonly accepted analyses of drainage networks involve calculation of Horton's laws, as well as parameters suggested by other workers. Hajam et al., (2013) and Pareta & Pareta (2011) used quantitative metrics presented by Horton (1945) and others, e.g., Schumm (1956) and Strahler (1954), to quantitatively detail their drainage basin study areas and to assess hazards such as flood risk. The work done by Horton (1945) confirmed that numeric data can be related to form. From form, processes can be inferred. Calculation of quantitative parameters can confirm field conditions on the ground and reveal relationships that are not observable from maps.

6.2.3 Hydrologic flow models. Numeric hydrologic modeling involves prediction of hydrologic activity through implementation of algorithms within computer software (Martz & Garbrecht, 1992). Algorithms are usually parameterized by data derived from field measurements (Jayawardena, 2014, 16) because field measurements promote accurate prediction of hydrologic responses (Beven & Kirkby, 1979). Models representing natural features include digital elevation models (DEMs), which are gridded representations of the Earth's surface topography, also help to characterize drainage basin properties (Martz & Garbrecht, 1992). Hydrologic models are useful because outputs of algorithms such as stream number and order are often difficult if not impossible to accurately measure in the field. Because drainage characterization is critical in land/water management, hydrologic modeling has become an integral component in such management strategies (Arnold, Srinivasan, Muttiah, & Williams, 1998). Stream modeling is commonly used as base data to quantify drainage basin morphology, (e.g., Hajam et al., 2013) The advent and ongoing development of computers and geographic information systems (GIS) since the 1960s have enhanced processing ability and storage of hydrologic data, spurring advances in hydrologic modeling (Arnold et al., 1998; Singh, 2018).

Various models have been developed and used since the 1850s, (e.g., Mulvaney 1851) to predict surface runoff, subsurface flow, and groundwater storage (Singh, 2018). Flow models use assumptions about the influence of topography on the flow of water to digitally represent flow paths based on the individual cells in the DEM grid (Martz & Garbrecht, 1992). Most flow models are adapted for DEMs, which are the primary data input for flow-model algorithms. Flow models have applications in channel identification and can aid in the quantitative analysis of channel networks because the digital representations produced by flow models are easily analyzed within a tabular interface

A flow model developed by O'Callaghan and Mark (1984), the D8 flow algorithm, uses a series of steps implemented with a GIS to extract or identify stream channels within a DEM. The D8 algorithm assumes that water from one cell of the DEM flows completely into one of eight neighboring cells (hence the "8" in D8), separated by 45° angles. Broadly, the D8 algorithm implementation can be broken down into three steps: 1) artificial pit removal and flow direction computation DEM, 2) flow accumulation calculation, and 3) definition of channels based a user-defined threshold of flow accumulation cells (Tarboton, 1989, 56). The result of the D8 application over a DEM is the identification of streams where stream channels represent those connected cells with the largest flow accumulation values. The D8 flow algorithm is a useful method to map networks of channels when a DEM grid is available. Other flow models developed, e.g., the multiflow direction algorithm from Quinn et al. (1991), are based on the conceptual framework of the D8 model but adjust the generation of flow direction to reflect the ability of water to flow in multiple directions, or into multiple adjacent cells. The main conceptual difference between the D8 and multiflow direction algorithms is that the D8 model assumes that flow is directed only in the direction of the steepest slope, i.e., convergence while the multiflow algorithm assumes that flow is directed into all downslope directions, i.e., divergence (Wolock & McCabe, 1995). The D8 model is implemented in this study because the effects on channel extraction using either D8 or multiflow algorithms are minimal (Wolock &

McCabe, 1995). In the case of the patterned ground field on Frost Ridge, both the D8 and multiflow channel detection methods produced similar channel identification results, highlighting the prominence of convergence on the hillslope.

6.2.4 Applications of flow modeling in geomorphology. McNamara et al. (1999) utilized flow modeling with a DEM as data input to locate water tracks at a high-latitude site. Through the identification of water tracks at Imnavait Creek, Alaska (68°37'N, 149°17'W), they explored the organizational characteristics of a drainage basin underlain by permafrost. The results of McNamara's study indicate that a network of water tracks forms a rudimentary drainage network, probably due to underlying permafrost conditions that inhibit incision. They postulate that as underlying permafrost conditions are compromised under warming trends in climate, incision of water tracks will commence, contributing to hillslope erosion. Water tracks in Antarctica have also been identified using flow modeling infer groundwater activity (Levy et al., 2011). The identification of water tracks in that study, in conjunction with field observations, revealed that water tracks were efficient transporters of meltwater and rock-weathering-derived solutes, indicating their geomorphic significance. Flow model algorithms have been used to parameterize TOPMODEL (Beven & Kirkby, 1979), a hydrologic model that has been used in a wide array of hydrologically based predictions and simulations. Flow models can be used to infer depth to water table, which is parameter in TOPMODEL (Beven & Kirkby, 1979; Wolock & McCabe, 1995).

Flow modeling uses assumptions about water flow and elevation inputs to predict flow paths. Identification of drainage networks using flow models produce outputs, e.g., stream order, stream length, and number of streams, that can be used as numerical input to characterize the morphology of the drainage basin (e.g., Gleyzer et al., 2004; Pareta & Pareta, 2011; Hajam et al., 2013). Modeling of flow pathways is an important tool to predict the distribution of moisture in the subsurface, to understand the organization of water features, and to infer geomorphic processes. Understanding the distribution of such features is especially important in periglacial regions, where water features are sometimes difficult to see from ground level, e.g., water tracks, or where the local hydrology has not yet been confirmed by quantitative data, e.g., a drainage network comprised of sorted stripes.

6.3 Network Analysis of a Sorted Patterned Ground Field

Sorted stripes are characteristic periglacial features that represent subsurface flow pathways for water. Aerial imagery and elevation data can provide insight into the organizational structure of sorted stripes. Flow modeling is a useful tool to identify drainage patterns and to obtain stream parameters such as stream length and number of streams. Stream parameters derived from flow modeling, implemented on a DEM, facilitate the quantitative analysis of the sorted patterned ground field. Horton's laws can be used to characterize its morphology as a drainage network.

The availability of high-resolution orthophotos and a DEM facilitate the application of the D8 flow model on the sorted patterned ground field. Quantitative characterization of it as a drainage network can be conducted once flow models have identified the locations of subsurface flow on the CT tread. Two technical approaches can be used: (1) manual digitizing to identify features; and (2) use of automated flow models to identify stream pathways. Both the manually digitized pathways and those derived from the flow model can be used to characterize the organization of the patterned ground field. The organization of the patterned ground can then be used to in evaluate the geomorphic significance of sorted stripes in cryoplanation terrace formation, specifically in the context of the nivation hypothesis.

6.3.1 Study area. A series of incipient cryoplanation terraces are incised into Frost Ridge, imparting a notched profile appearance to its north-facing flank. A well-expressed patterned ground field occupies a gently sloping CT tread located at the junction between Splinter Peak and the uppermost cryoplanation terrace tread (Figure 6.1). This field of patterned ground is dominated by sorted stripes extending from the scarp-tread junction to the toe of the CT tread. Other types of sorted patterned ground, frost-fractured clasts mantling slopes, solifluction lobes, needle ice creep, and nivation hollows are periglacial features also found on Frost Ridge (Queen, 2018, p. 42). The widths of sorted–stripe units range from 1.7 m to 5.4 m, and are 2.75 m wide on average (Queen, unpublished data). There is no apparent correlation between the lengths and widths of the fine stripes (Nelson 1975, 21), which is inconsistent with Goldthwait's (1976) assertions about regular spacing. The pattern-diameter to depth-of-sorting ratio is 3.44, within the range reported by Uxa et al. (2017). The underlying geology of the site is Paleozoic sedimentary rock (Queen, 2018,56 and references therein). Additional site information is summarized in Table 6.1.

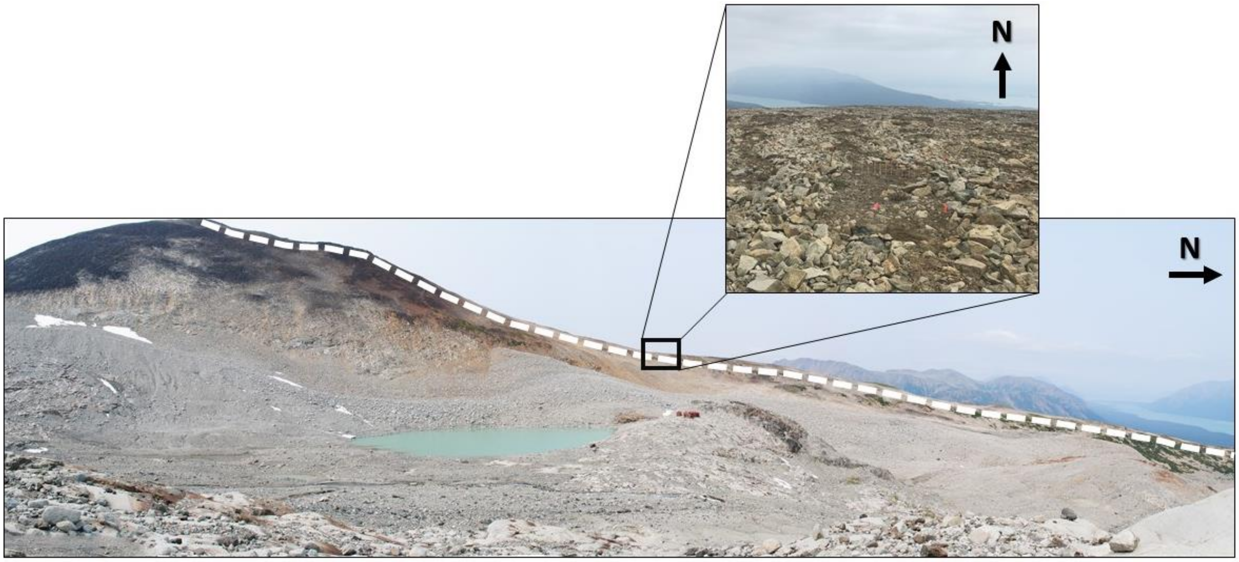

Figure 6.1 Panoramic view of Frost Ridge and inset photo of sorted patterned ground features. *The dashed white line delineates Frost Ridge; the black box indicates the location of the inset photo. Within the inset map, sorted stripes are oriented northward. Dark brown areas are fine-textured sediment, lighter gray, coarse-textured areas are coarse sorted stripes.*

Table 6.1 Field site topographic information.

Total relief (m)	29
Average slope (°)	10
Aspect	North, northeast
Elevation (m)*	1690
CT tread length** (m)	279

*Elevation at the scarp-tread junction
** Tread length is approximated by measuring the horizontal distance from the scarp tread junction to the ridge of the CT scarp immediately downslope.

6.3.2 Study area data acquisition. A DJI Mavic 2 Pro drone was used to survey the patterned ground field, covering a total area of 0.143 km^2 in the fall of 2018 (Figure 6.2). Using DJI mission flight planning software, a double grid flight path was flown with 80° camera angle, 85% front and 82% side overlap. No ground control points were used. The orthomosaic, DEM, and a quality report were generated using Pix4Dmapper Pro version 4.2.27 software (Pix 4D

Inc., San Francisco, California). Areas with 3-5 plus overlapping images were deemed acceptable for analysis. The area outlined in Figure 6.2 was chosen to limit the number of pixels that did not have sufficient overlap to be included in the network analysis. The study area used in the analysis includes the scarp backwall and most of the CT tread extending from the base of the scarp-tread junction. The patterned ground study area lies within areas considered to be of good quality. A spatial resolution of 3.27 cm/pixel was achieved for both the DEM and orthophotos.

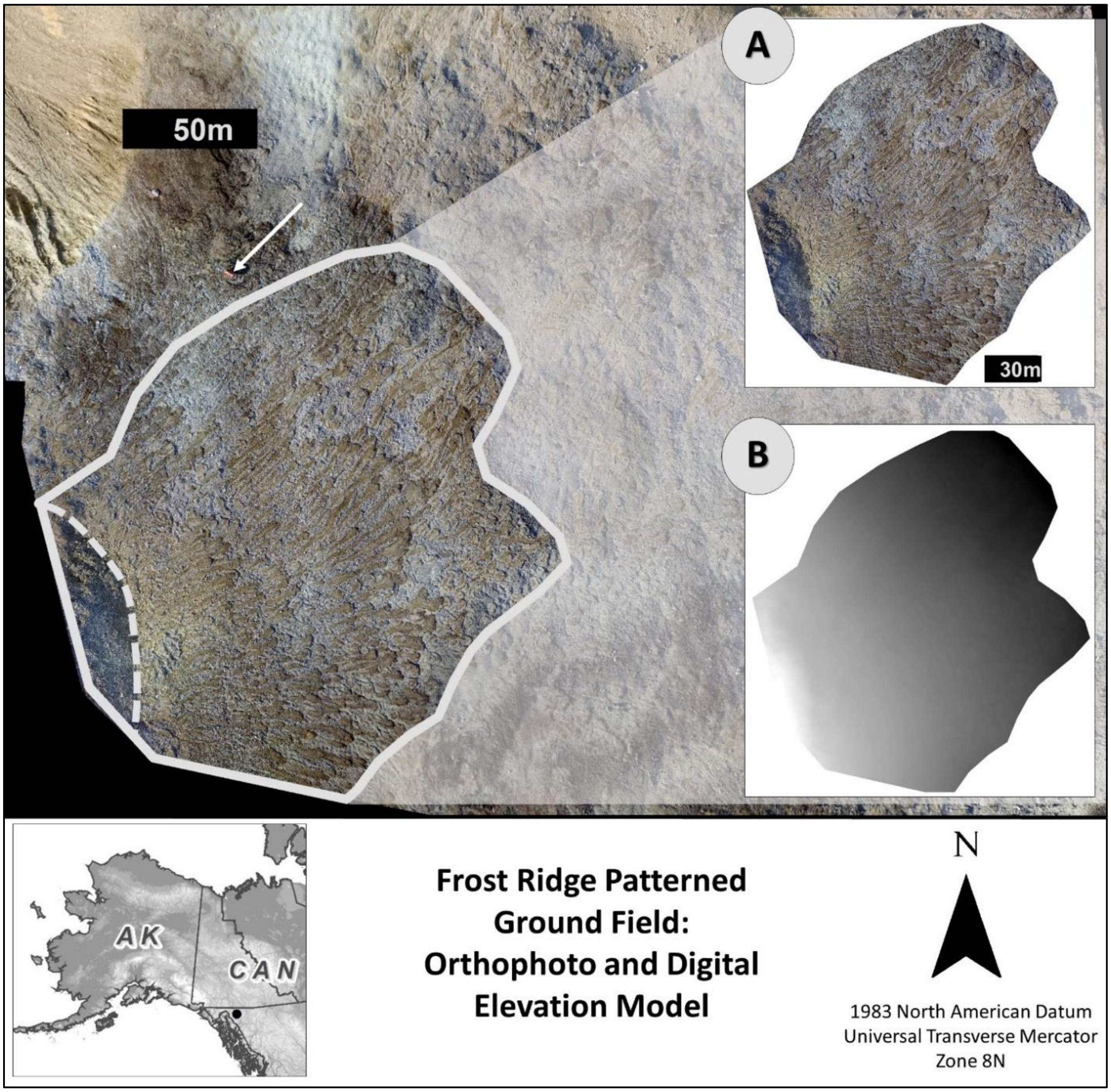

Figure 6.2 Aerial survey data. *A UAV survey flown September 4, 2018 northwest at 80 meters above the takeoff site located in the northwest portion of the map (indicated by an arrow). An orthomosaic (A) and Digital Elevation Model (B) were generated though post-survey processing using Pix4DMapper Pro software. Coarse stripes are light gray, highly textured linear features oriented approximately parallel with the slope. Within the DEM, elevations are represented as a gradient from white (relatively higher elevations) to black (relatively lower elevations). The gradient indicated the north-northeast orientation of Frost Ridge The extent of the field study site is indicated by the solid white outline. The scarp is indicated by a dashed white line, separating it from the outward-extending CT tread. Data quality decreases with increasing distance from the patterned ground field study area. Black areas outside the map area contain no data values. Remote sensing products courtesy of Merlin Geoscience Inc.*

6.3.3 Network analysis inputs. Before flow modeling was implemented in the study area, visual analysis was used for preliminary characterization of the patterned ground field. Using the orthomosaic as a guide, manual digitizing was used to identify coarse portions of the sorted stripes thought to channel water and transported sediment across the CT tread. The polyline tool implemented in ArcMap™ 10.6 (Environmental Systems Research Institute, Inc., 2020) was used to delineate the coarse patterned ground from intervening fine-textured areas. The coarse portions of sorted circles and nets found near the scarp-tread junction were identified by Nelson (1975) as channels for water flow, based upon visual assessment and the sound of water running in them throughout the summer. These features grade into sorted stripes found just downslope. Sorted nets and circles were included in the digitized channel network in addition to sorted stripes. The arrangement of the features revealed a network reminiscent of a drainage basin. The process of digitizing the network was guided by the high-resolution orthomosaic, DEM (indicative of the downslope direction), and expert field knowledge derived from fieldwork conducted during the summers of 2018 and 2019. Other filters applied to the study area DEM and orthomosaic aided in the visual characterization of the sorted patterned ground field (Figure 6.3).

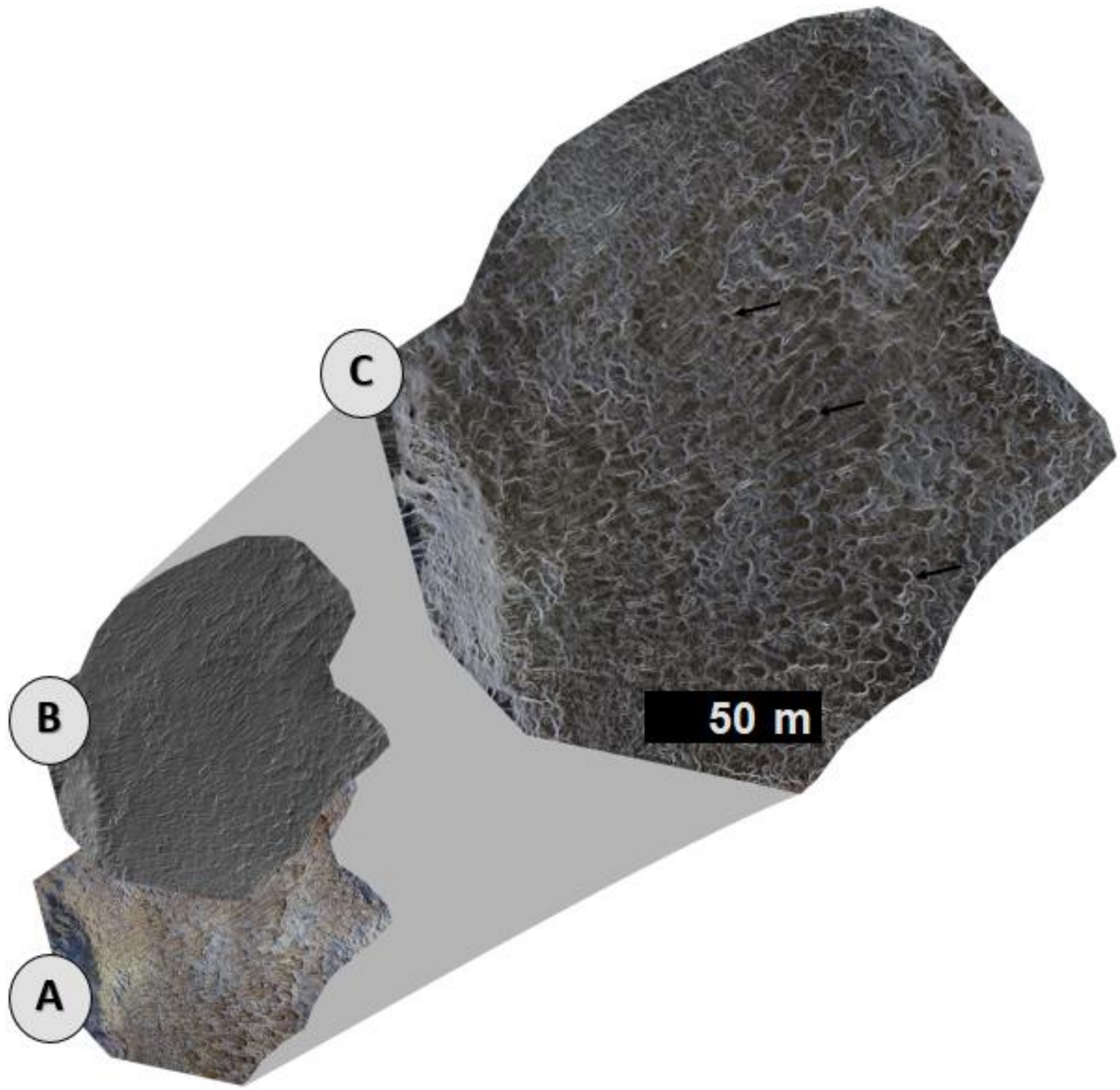

Figure 6.3 Compound filter map. *The hillshade tool implemented within ArcMap™ software creates a shaded relief surface taking the source angle and shadows into consideration, highlighting subtle relief features on the surface. The hillshaded surface was made partially transparent and draped over the orthomosaic map (B) to create a compound map (C). Solifluction lobes—indicated by small black arrows on map C—, linear coarse stripes—light gray areas—, and the scarp backwall are especially prominent in the compound map. Darker features resembling raindrop shapes constitute the fine stripes, which are fine-textured sediment moving as solifluction lobes. From the compound map, solifluction lobes and coarse stripes appear to extend out from the scarp-tread junction to the edge of the study area boundary to the northeast.*

Equations for the dimensionless ratios used for quantitative network analysis require numeric inputs such as stream order, derived from the results of flow algorithms implemented in a GIS. The D8 flow algorithm was used to model flow in the study area, and tabular data were used later to calculate the drainage network parameters. The stream identification process was conducted on the DEM within GRASS GIS version 7.8.1 (GRASS Development Team, 2019) using tools within the Hydrologic Modeling toolset. Following the methodology for stream identification detailed by O'Callaghan & Mark (1985), the DEM was first filled using the *r.fill.dir* tool to remove pits within the area. Using the *r.watershed* tool, flow direction and flow accumulation rasters were generated. Using the raster calculator, a conditional statement, which performs conditional if/else statements set by the user on each of the input cells of an input raster, was used to determine a flow accumulation threshold, set to a value of 100,000. The assumption of this step is that only cells having a certain amount of flow accumulation constitute flow paths on the surface. The chosen flow accumulation threshold excluded noise from the cells with small flow accumulation values that are unlikely to represent drainage channels, while preserving the overall pattern identified by the drainage direction matrix. This threshold identified the dominant flow paths extracted by the flow modeling algorithm. In the context of fluvial geomorphic activity, the flow accumulation value represents the amount of water convergence that must occur to initiate a flow path. Conceptually, this channelization results in the initiation of a sorted stripe on FR. Other workers have also indicated the importance of fluvial processes in sorted patterned ground initiation/formation (e.g., Nelson, 1975; Paquette et al., 2017b). The flow paths identified indicate a minimum estimate of the hydrologic activity atop FR, as many of the minor channels have been excluded from the analysis. Similarly, the flow accumulation threshold chosen for this analysis represents the upper limit of total convergence required to initiate a sorted stripe flow path. The results of the manual digitizing and stream identification processes are shown in Figure 6.4. The goal of this methodology was to identify the coarse portions of the patterned ground network, to identify its overall pattern and orientation as verified by the digitized network, and then to derive the numeric data needed to quantitatively assess the drainage basin and channel network.

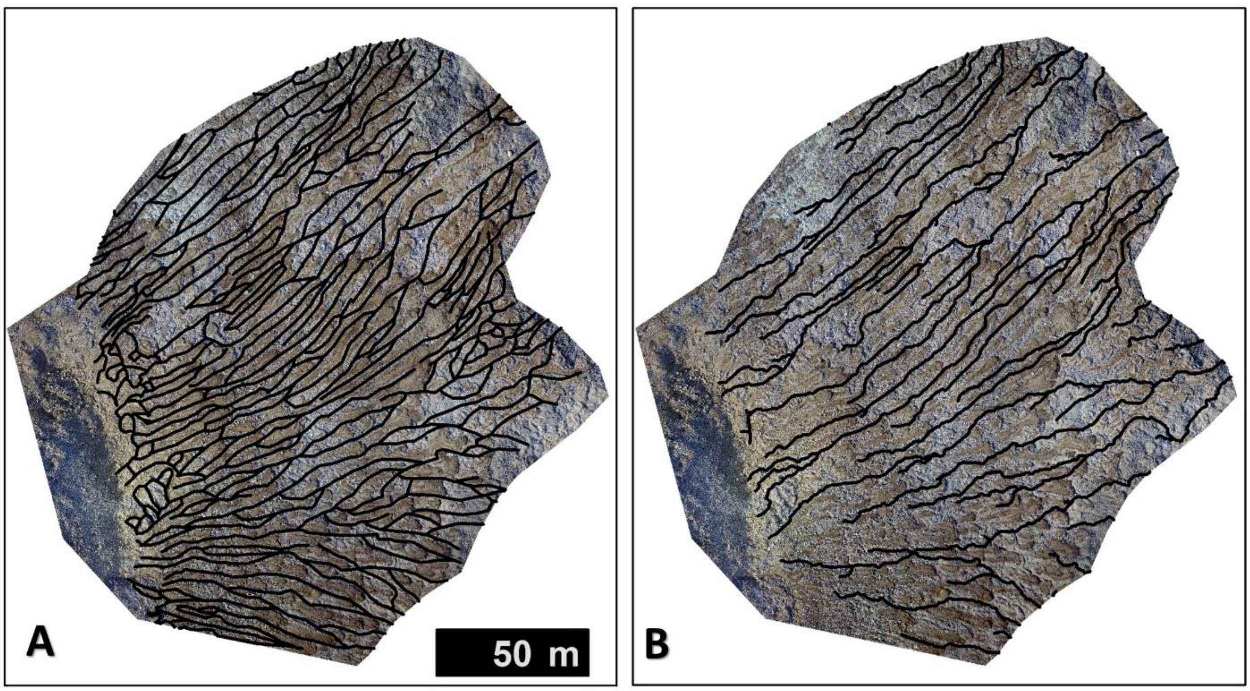

Figure 6.4 Drainage network identification results. (*A) Flow pathways identified through manual digitizing efforts. (B) Flow pathways identified through flow modeling methodology. Both results indicate an interconnected system of coarse components of the patterned ground.*

6.3.4 Comparison of digitized and automated drainage network extractions. The results of both manually digitized and automated stream extraction methods are shown in Figure 6.4. The automated map identifies the most prominent stream channels based on basin topography. Both maps identify areas of accumulation that connect with one another, constituting the stream channels in both networks. Areas of accumulation were identified in the manually digitized map based on the spectral differences between the coarse and fine-textured stripes. The automated channel detection method did not identify the coarse stripes in the same locations as they were identified via manual digitization. This result most likely reflects the microtopography on the seemingly flat CT tread: linear piles of coarse fragments constituting the coarse stripes are topographically higher relative to intervening bands of fine-textured sediment, which function as solifluction lobes. The flow algorithm assumes water flow through topographically low points on the slope, however, water flows within topographic high lineations on FR. The results of the automated channel detection method were channels located at the borders of coarse and fine stripes, as opposed to the interior of coarse stripes. For identifying terrace-level drainage basin organization, the automated methodology was sufficient because the D8 flow algorithm was able to capture large-scale sorted stripe feature organization, based on visual comparison with the manual channel detection method. Both maps depict similar drainage network patterns where stream channels extend outward from the scarp-tread junction--in the southwestern corner of the map—in a northeasterly direction. Generally, streams in both maps follow the northeasterly aspect of the CT tread but at the southeastern edges of the study area, streams assume an easterly flow path. Flow paths on the CT tread probably reflect the slightly convex topography of the tread (Nyland, 2019, 57–58). The predominant orientation of sorted stripes in both maps is reminiscent of a parallel drainage network (Hobbs, 1910; Zernitz, 1932) although the entire CT tread must be analyzed to make conclusive assertions about the organizational structure of the drainage network on Frost Ridge. The predominantly parallel nature of the network depicted in Figure 6.4 is part of a larger distributary network that reflects the slightly convex topography of the CT tread and clearly depicts flow off the side of the treads eastern margin. Visual assessment of the maps in Figure 6.4 is useful for an integrated characterization of the drainage on the entire CT slope. The organization of the network and the slope of the CT tread indicate that the “headwaters” of the network occur near the scarp-tread junction while the network mouth is located near in the CT tread toe. Both the interconnectedness of the patterned ground field and the organization of the stripes into a parallel network extending toward the CT tread’s toe indicates efficient transportation of snowmelt water and sediment across and over CT treads and side slopes.

The stream order of the drainage basin based on flow modeling data is shown in Figure 6.5. Stream ordering was based on the Strahler method. The FR drainage basin is a third-order basin. First-order streams are most numerous and represent the “headwaters” of the network. The network converges into third-order streams near the toe of the CT tread. Overall stream discharge and channelization of water is probably highest in the 3rd order streams. Stream order of the FR drainage network confirms the direction of the flow of water and helps to locate areas of elevated discharge on the CT tread. Comparison of the automated network identification map with the manually digitized map shows that automated methods to delineate a periglacial drainage network can be used to achieve useful flow pathway maps. Automated maps are particularly effective for obtaining drainage parameters such as stream order, whereas manual methods of stream delineation tend to be labor intensive and subject to user error, possibly resulting in biased network parameters.

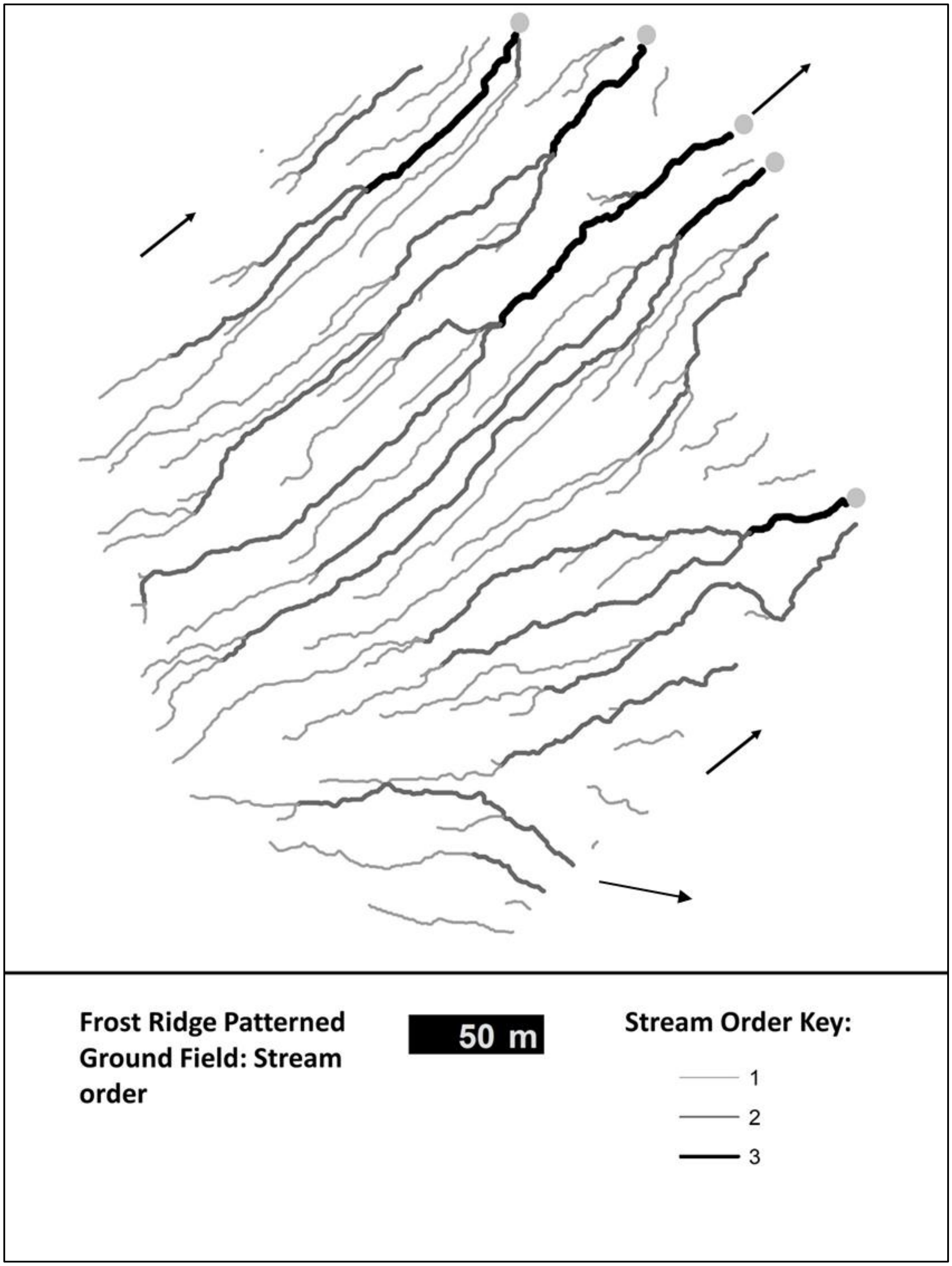

Figure 6.5 Stream ordering results. *The above stream ordering map was generated using the Stream Order tool* (Environmental Systems Research Institute, Inc., 2020) and demonstrates an overall stream order of 3*. The Strahler stream order method (Strahler, 1952) was used. Black arrows indicate the flow direction. Light gray circles represent the main outflow points of the drainage network, or the areas where the most water is thought to be channeled out through based on the high order stream channel.*

6.3.5 Network analysis results. Drainage basin characteristics were quantified using methods presented in Horton (1945), Strahler (1952 & 1964), and Schumm (1956). All numeric information required to calculate the parameters presented in the drainage network analysis was sourced from the DEM of the sorted patterned ground field. Multiple metrics were chosen to capture the breadth of the drainage basin characteristics. Inputs to the chosen morphometric parameters are summarized in Table 6.2. The results of the morphometric parameter calculations are summarized in Table 6.3.

Table 6.2 Ancillary drainage basin data. *Values in this table were derived from a GIS based on the study area DEM. Some values, e.g., basin relief were measured within a GIS using ruler tools. Stream order and number values were calculated following the implementation of the D8 flow algorithm. Values in this table were used in the quantitative drainage basin characterization.*

Parameter	Value	Source
Basin Relief, R, (m)	29	*
Basin Area, A, (m^2)	26,382	*
Basin Perimeter, P, (m)	635	*
Number of 1st Order Streams, N_1	50,085	**
Number of 2nd Order Streams, N_2	31,496	**
Number of 3rd Order Streams, N_3	5,249	**
Total Number of Streams, N_T	86,831	**
Length of the Principal Drainage Line, L_P, (m)	184	*
Total Stream Length, L_T, (m)	3,420	**
Mean Length of 1stOrder Stream, $\bar{L}_1$, (m)	4.1	*
Mean Length of 2nd Order Stream, $\bar{L}_2$, (m)	4.7	*
Mean Length of 3rd Order Stream, $\bar{L}_3$, (m)	19.0	*
Mean Length of all Streams, $\bar{L}_T$, (m)	4.5	*

* Data derived from ArcMap™ v. 10.6 software

** Data derived from GRASS GIS v. 7.8.1 software

Table 6.3 Quantitative drainage basin characterization. *Parameter values were calculated and are organized by parameter types. Stream order ratios are specified for the bifurcation and stream length ratio calculations. For example, the first bifurcation ratio calculation (1st:2nd) indicates that the calculation was performed using the 1st order stream data as the numerator and 2nd order stream data was used as the denominator. A list of sources, indicated by stars, is located below the table. Both Horton (1945) and Strahler (1952) are listed as sources for stream order because Strahler (1952) modified Horton's original stream ordering method; the Strahler method was used for the classification of the drainage basin in this study.*

Parameter	Value	Source
Linear		
Bifurcation Ratio, Rb_1 (1st:2nd)	1.6	**
Bifurcation Ratio Rb_2 (2nd:3rd)	6.0	**
Stream Length Ratio, RL_2 (2nd:1st)	1.2	**
Stream Length Ratio, RL_3 (3rd:2nd)	4.0	**
Stream Order	3.0	**, ***
Areal		
Drainage Frequency, D_f, (m^{-1})	3.3	*
Drainage Density, D_d, (m^{-2})	1.7×10^{-4}	**
Relief		
Relief Ratio, R_r	0.16	****

* Equation from Horton (1932)
** Equation from Horton (1945)
*** Equation from Strahler (1952)
**** Equation from Schumm (1956)

6.4 Discussion

6.4.1 Bifurcation ratio. Bifurcation ratio (R_B) is the ratio of the number of streams of a given order, *N*, to the number of streams of the next highest order, *N+1*, and serves an index of the relief and dissection of a basin and reflect the branching within a drainage basin (Horton, 1945). Bifurcation can also indicate geologic control and degree of disturbance within a drainage basin (Pareta & Pareta, 2011 and references therein). Bifurcation ratios are not constant between order, and values range from 3.0 to 5.0 (Schumm, 1956, 603). In flat or rolling drainage basins, lower bifurcation values are typical (Horton, 1945). Bifurcation values of

3 and greater are typical in highly dissected or mountainous drainage basins (Horton, 1945). The bifurcation ratio value of 1.6 for 1st to 2nd order streams field reflects the flat topography encountered in the interior of the CT tread. Typically, low-relief basins exhibit low bifurcation ratios because the degree of dissection is low in flat areas relative to high-relief areas. Less dissection resulting in a lower bifurcation ratio is especially true between 1st and 2nd order streams in the FR basin, a fact evidenced from the stream-order map (Figure 6.5). The 6.0 bifurcation ratio of 2nd to 3rd order streams reflects large amounts of bifurcation of 2nd order streams into 3rd order streams within the drainage basin. The higher bifurcation value for the 2nd to 3rd order is expected because near the CT toe tread, where the 2nd and 3rd order streams are located, slope tends to be greater than that near the scarp-tread junction. Increases in slope impact the amount of bifurcation due to an increase in stream power, which is related to relief. The bifurcation ratio for the FR drainage accurately reflects the subtle changes in slope that occur across the CT profile. The CT tread drainage basin tends to be more highly dissected closer to the toe and less dissected near the scarp-tread junction, based on inputs from the flow model stream results.

Attention should be paid to the influence of the flow accumulation threshold used in the flow model algorithm. Due to the accumulation threshold chosen for the analysis, the flow algorithm likely underestimated the number of 1st order streams because those streams have less accumulation than 2nd and 3rd order streams and thus may have not been identified. Comparison of the two maps in Figure 6.5 underline this possibility. However, the bifurcation ratios accurately reflect the subtle sloping conditions that exist on the CT tread, suggesting that the bifurcation ratios calculated can be used to quantitatively characterize the FR drainage basin.

6.4.2 Stream length ratio. Stream length ratio is the ratio of the mean stream length of a given order, *L*, to the mean stream length of the next lowest order, *L-1*, and reflects the relationship between surface flow and discharge and the erosion stage of the basin (Hajam et al., 2013 and references therein). Stream length ratios calculated for the FR drainage basin are 1.2 for 2nd to 1st order streams and 4.0 for 3rd to 2nd order streams, falling near the range of typically observed stream length ratios, which range from 0.5-3 (Horton, 1945). For 2nd and 3rd order streams, the high stream length ratio indicates a large jump in average stream length from 2nd to third order. Increasing length with increasing order is typical in most drainage basins. Large flow accumulation values identified within the 3rd order streams indicates inflated discharge rates from higher order streams within the basin.

6.4.3 Drainage frequency. Calculated as the ratio of the total number of all streams, N_T, to the basin area, *A*, drainage frequency reflects the texture of the drainage network and indicates substrate permeability. The drainage frequency value of 3.3 is high relative to results reported by others e.g., (Vittala, Govindaiah, & Honne Gowda, 2004; Hajam et al., 2013; Martins & Gadiga, 2015; Rai, Mohan, Mishra, Ahmad, & Mishra, 2017), which range from 0.3-3.0. The high D_f calculated for the FR drainage basin reflects the large number of water features identified by the flow algorithm. High D_f values have also been attributed to the permeability of the substrate, where a high value indicates low substrate permeability (Reddy, Maji, & Gajbhiye, 2004). In the case of the Frost Ridge drainage network, the existence of a frozen substrate and the depth of sorting within the sorted patterned ground both contribute to low permeability. Frozen material and the depth to fine-textured material would inhibit vertical flow, encouraging the dispersion of flow in a semi-horizontal plane. The dominance of lateral water flow could enhance the formation of sorted patterned ground, which is closely related to moisture availability. Overall, the drainage frequency of the sorted patterned ground field indicates low permeability of the substrate and the abundance of drainage features identified by the flow algorithm.

6.4.4 Drainage density. Drainage density, D_d, is the average length, $\bar{L}_T$, of streams per unit area A, and indicates the degree of drainage within a basin. Rainfall and relief commonly influence drainage density values within a basin but infiltration capacity—the maximum rate that soil can absorb water—and erosivity of the basin substrate are also important (Horton, 1945). A well-drained basin will tend to have a lower drainage density than a poorly drained system. Because drainage density is calculated based on the average stream lengths, drainage density is related to the degree of branching within the basin. Basins with high D_d values rarely exceed 3.0 and in most humid basins where soil erosion is active, D_d varies between 1.0-2.0 (Horton, 1945, 359). The calculated D_d value for the FR sorted patterned ground basin, 1.7×10^{-4} m, is low based on common values presented by Horton (1945). The low drainage density values are likely due to the abundance of short stream lengths identified by the flow algorithm. Although some of the higher-order streams in the basin are long, much of the basin is dominated by relatively shorter stream lengths. The abundance of small features is responsible for the removal of water across the seemingly flat CT tread that is underlain by permafrost. The abundance of sorted stripe features on the CT tread result in a well-drained basin despite basin topography and substrate impermeability.

Low drainage density values are typically associated with youthful drainage basins that are dominated by 1st order streams. This is not the case for the sorted stripes atop FR, which have been developing since the waning stages of the Wisconsinan. In some cases, basins that exhibit low drainage density values may actually be at a mature stage of development if overland flow has not eroded specific areas of the drainage basin due to flat slopes, high infiltration capacity, surface resistance to erosion, or a combination of all those factors (Horton, 1945). In the case of FR, relatively flat slopes and frozen substrate probably contribute to the propagation of the 1st order streams and the low drainage density value. Because of the flatness and resistance to erosion due to frozen ground in the early spring when snowmelt water is abundant, water is unable to erode into well-defined channels. Water is then channeled through the coarse portions of the sorted patterned ground network, which are small forms relative to the total area of the CT tread. The low drainage density of the FR basin indicates that the area is well-drained and when physical characteristics such as slope are considered, the drainage basin may also be characterized as mature. The results of the drainage density calculation suggest that sorted stripes classified as first order dominate the basin and contribute to the drainage of water from the CT tread.

6.4.5 Relief ratio. The relief ratio of a basin is calculated as the ratio of basin relief, R, to the length of the principal drainage line, L_p. Here, the principal drainage line was determined by identifying the longest 3rd order stream and measuring a line parallel to the flow path. A positive relationship between relief ratio and sediment loss was shown in Schumm (1956), suggesting that relief ratio can be used to predict sediment transportation within a drainage basin. The relief ratio of the Frost Ridge patterned ground network is 0.16, which is high based on the values presented by Schumm (1956), which range from 0.009 in low-relief basins to 0.15 in high-relief basins. The high relief ratio in this case is not indicative of a high relief basin, which contradicts the trends found in Schumm (1956). However, the high relief ratio could have been influenced by the small spatial extent that was analyzed in this study compared to the regional/landscape-scale studies from which relief-ratio values have been reported. The high value calculated does provide some support for the occurrence of large amounts of sediment transportation on the slope, following research from Schumm (1956).

6.5 Conclusion

The organization of the sorted patterned ground field on Frost Ridge was evaluated in this chapter through network analysis. Visual assessment of manually digitized and flow modeled drainage maps revealed that, although flow modeling can lead to underestimation of 1^{st} order streams in a basin, both drainage identification methods identified drainage patterns within the network that are reminiscent of a parallel drainage network, with ancillary distributary characteristics near lateral tread margins. The network of soil pipes analyzed by Bernatek (2015) has similar characteristics.

Quantitative analysis of drainage basin characteristics based on flow algorithm inputs confirm trends in microtopography and slope on the CT tread. Calculated bifurcation ratios confirm that relief and slope increase toward the CT tread's toe, supporting sorted stripe development and sorted stripe bifurcation. High stream-length ratios within the drainage basin in addition to the location of 3^{rd} order streams indicate areas of greater stream discharge to exist at the terminus of 3^{rd} order sorted stripes, which occur near the CT tread toe. Drainage frequency and drainage density values conform with the manually digitized map, which shows a high density of sorted stripe features in accordance with the gentle topography shown in the DEM. Drainage frequency and drainage density values indicate that flow is dominantly lateral as vertical percolation is inhibited, owing to the frozen substrate and the depth of patterned ground sorting. The high relief ratio of the FR drainage basin indicates that sorted stripes are related to effective sediment transportation. Three main points are derived from the network analysis of the sorted patterned ground field: 1) the abundance of sorted stripes results in a highly dissected drainage network; 2) the flow of water within the sorted stripe network is likely dominantly horizontal; and 3) the greatest amount of discharge is probably located at the terminus of 3rd order streams, which occur near the CT toe tread.

The agreement of quantitative drainage parameters with the manually digitized map and field observations indicate that flow modeling of a sorted patterned ground network is an appropriate analytic methodology. Quantitative basin characteristics also indicate the operation of phenomena, such as sediment transportation, that are not known based on visual assessment of remotely sensed data. The visual and quantitative assessment of the sorted patterned ground field lend support to the hypothesis that the network of sorted patterned ground atop FR is conducive to the efficient transportation of water and sediment despite the gently sloping conditions on the CT tread. Quantitative parameters help to define the hypothesis that the highly dissected network directs water laterally though the sorted landscape toward the CT toe tread, facilitating the transportation of water and sediment across the tread. Based on these results, the lack of material accumulations on flat CT treads may be attributed to the flow of water within a sorted patterned ground field. The flow of water through the sorted landscape would probably promote further development of sorted stripes while helping to maintain the flatness of the tread through the removal of fines over low permeability substrates. Further analysis of this drainage basin could be improved by confirming the locations of first-order stripes, underlying permafrost conditions, and comparison of morphometric parameters that have been calculated for other sorted stripe drainage basins.

Chapter 7 Synthesis and Conclusions

7.1 Summary of Research

Competing hypotheses of CT formation lie primarily within two distinct groupings. The first group attributes CT form to geologic structure (e.g., French, 2016) whereas the second, and more widely accepted hypothesis, attributes CT formation to climatic influences, particularly from the microclimate in and around late-lying snowpatches. The second formation hypothesis, known as the nivation hypothesis, requires investigation of the capability of periglacial processes to initiate CT formation, (e.g., Lauriol et al., 2006), the existence of active periglacial processes that maintain or further modify CTs (e.g., French, 2016), and the lack of material rampart accumulations on inner CT treads (Ballantyne, 2018). Recent research lends support to the time-transgressive nature of CT tread growth (Nyland, 2019; Matthews et al., 2019; Nyland & Nelson, 2020) the poleward orientation of CTs (Nelson, 1998), the widespread occurrence of CTs in periglacial regions across the globe (Demek, 1969), and repeating assemblages of periglacial features on CTs (Queen, 2018), all pointing to a strong association between CTs and periglacial conditions. However, previous work fails to account for the absence of ramparts of weathered material on CT inner treads, contributing to skepticism about the nivation hypothesis. The work presented in this study focuses on relating periglacial processes to CT formation and also challenges the notion of geomorphic quiescence implied by the occurrence of sorted patterned ground (e.g., Karte 1979, 81; Thorn & Hall, 2002b, 545).

7.1.1 Field-based process investigations. Installation of temperature and hydrologic monitoring equipment on two incipient cryoplanation terraces was undertaken to fulfill the need for process-focused investigations on CTs (e.g., Demek, 1969) that link nivation to CT formation. The short temperature monitoring data records available from Frost Ridge clearly display cyclic diurnal temperature behavior, at distinct scales. At the slope level, a temperature gradient exists between upper and lower positions on the slope, confirming the expected air temperature decreases with increasing elevation. At the terrace level, a temperature gradient extending from the scarp to the CT tread toe is also apparent. At the feature level, distinctive diurnal temperature behaviors were observed in the coarse and fine stripes. Within the coarse stripes, the temperature records demonstrate the impacts of surface albedo, proximity to the snowpatch margin, and non-conductive thermal processes on the thermal regime. Pulses of snowpatch meltwater moving through the coarse stripes, coinciding with the onset of increasing air temperatures, constitute non-conductive heat-transfer processes operating within coarse stripes. These pulses and the large interstitial spaces within coarse stripes contribute to the spiky temperature record observed. Within the fine-textured stripes, temperature records displayed less extreme diurnal amplitudes, except near the toe of the CT tread, indicating the dominance of conductive heat transfer within fine-textured stripes where surface temperatures are largely impacted by larger-scale (terrace-scale) temperature gradients and the dark, low-albedo surfaces. Phase lags and progressively subdued diurnal amplitudes with depth in the vertical temperature profile of a fine stripe confirm that heat transfer in the fine stripes was primarily conductive during the period of observation, although variations in soil moisture at the diurnal scale significantly impact the ground thermal regime.

Sediment troughs and overland flow-collection jugs indicate key outflow points that occur at coarse stripe termini. The duration of the field campaign provides a rough envelope of fill time for the overland flow jugs, which imply flow volumes in excess of 19 liters per day from a single sorted stripe, coinciding with summertime temperatures, upslope snowpatch conditions, and the thermal regime of the coarse stripes. The comparison of coarse stripe termini and snowpatch-margin transported sediment via particle size analysis is strong evidence for sediment transport by fluvial processes, in which suspended particles derived from weathering processes at the snowpatch margin are sorted by texture en route to the CT toe tread. Deposition points of transported material are evidenced by silt fans and turf-banked solifluction lobes.

7.1.2 Sorted patterned ground network analysis. The sorted patterned ground field on the uppermost terrace of Frost Ridge is characterized by alternating coarse boulder stripes and fine-textured solifluction lobes that extend from the scarp-tread junction out toward the CT tread toe and over CT side slopes. Motivated by the well-documented hydrologic activity within coarse stripes (Nelson, 1975), the coarse stripes were manually digitized to outline flow paths on the CT tread. Automated flow modeling confirmed the organization of the manually digitized flow map and provided input data for calculation of quantitative morphometric drainage basin parameters. Results from the morphometric parameters provide convincing evidence for strong hydrologic influence over the organizational structure in the patterned-ground field and quantitative support for the characteristics inferred from the process-focused investigations. The relief ratio, bifurcation ratio, drainage frequency, and stream-order values calculated indicate that basin morphometry is influenced by underlying impermeable conditions, which direct flow along downslope paths toward major outflow points at the toe and sides of the CT tread.

Unusual values calculated for some morphometric parameters are explained through consideration of the periglacial characteristics of the drainage basin. Specifically, the number of streams is influenced both by underlying permafrost conditions, which are related to the depth of the permafrost table, and the consequent depth of particle sorting. The agreement of morphometric analyses with field observations highlights the advantages of applying automated flow modeling in a sorted patterned ground landscape. Based on the morphometric analyses presented here, the organization of the sorted patterned ground field is interpreted as a well-integrated system of flow paths that occupy a gently sloping tread underlain by permafrost. The network of patterned ground thereby connects the snowpatch margin hydrologically to outflow points located near the toe tread. Ancillary drainage paths remove sediment from CT treads along their margins. Results from the automated and manual flow-detection methods presented here both demonstrate that a pattern akin to a parallel drainage network exists over most of the sorted patterned-ground field. Areas on the periphery of the study area were not all included owing to decreased quality of input data, so the quantitative network analysis in this study largely covers the interior of the patterned ground field. Consideration of areas near the periphery of the present study area in the morphometric characterization would clearly reveal feature organization reminiscent of a distributary pattern, which would agree with the slightly convex topographic profile of the CT tread (Nyland, 2019, 57–58). The southwest part of the area with adequate coverage shows drainage pathways leading to the lateral margin of the CT tread.

7.2 Synthesis

7.2.1 The role of fluvial action in cryoplanation terrace formation. Sorted patterned ground features have long been associated with cryoplanation landforms but have rarely been considered in the context of CT formation. On Frost Ridge, the climatic regime, periglacial processes, and fluvial influences combine to impart a distinct hydrologic signature on CT treads that exerts an important control over CT formation. Where snowpatches persist into the summer, the coarse and fine stripes on CT treads constitute dynamic surfaces of transportation over which sediment and water produced at snowbank sites are removed from terrace treads. Contrasting substrate material influences spatial divergences in the ground thermal regime, attributable to diurnal water pulses within coarse stripes, while long-term frost creep and slow flow of saturated soil occurs within fine-textured stripes.

7.2.2 The conveyor system model. Considering CT treads as efficient surfaces of transportation gives rise to a conceptualization of the system as a conveyor-like device for transporting weathered material between the snowbank and tread margins. Rapid transport of water and fine sediment occurs as diurnal pulses of snow meltwater within coarse stripes, which form an interconnected network of features terminating near or extending over the CT tread toe and lateral margins. The intervening fine stripes function as solifluction lobes that move large volumes of sediment at much slower rates across CT treads and side slopes. The underlying frozen ground functions in both the fine and coarse stripes as an impermeable substrate that governs the depth of saturation and sorting, promotes laminar flow in the lobes and turbulent flow in the coarse gutters, and anchors the coarse stripes. Together, these mechanisms work to prevent the construction of rampart-like features at the bases of subjacent scarps. Material removed from the scarp-tread junction is transported over tread toes and lateral margins and moves further downslope. If transported over the distal edge it is recycled to the subjacent CT scarp-tread junction, downslope of which another conveyor transport system operates. If transported over tread margins and onto side slopes, material is rapidly removed from the ridge entirely or incorporated in solifluction lobes (Brunnschweiler, 1965). Cryoplanation terrace side slopes in interior and western Alaska are festooned with solifluction lobes more comprehensively than on Frost Ridge, where Neoglacial moraines dominate.

Under the conveyor-system model of sediment excavation on CT treads, localized weathering near snowpatches is accentuated as material derived from the snowpatch vicinity is subsequently transported away during snowmelt. Fluvial action within sorted patterned ground is a key component of scarp retreat and tread expansion. The coarse stripes function as a "skeleton," anchored in permafrost, that fortifies the tread surface, confines, and directs sediment transport in the fine stripes to "corridors," and acts as channels for rapid transport by flowing water. Other factors, particularly such microclimatic parameters as topographic shadowing and slope aspect, are important for preserving the conveyor system because they promote the maintenance of underlying permafrost and the late-lying snow cover. The erosive power of this system is demonstrated by the time-transgressive back-wasting of scarps through localized weathering and efficient removal of sediment by processes enabled by snow meltwater (Nyland and Nelson 2020; Nyland et al. 2020a, b).

The hydrologic significance of sorted patterned ground has been described in other studies that highlighted the ease with which water flows in boulder gutters (e.g., Caine, 1963;

Nelson, 1975; Wilkinson & Bunting, 1975). The conveyor-system model underlines the importance of periglacial hydrology in the context of geomorphic activity and aligns with the results of previous research on patterned-ground hydrology. The results of this study refute the notion that patterned ground is indicative of geomorphic dormancy and highlight the hydrologic imprint of patterned ground on CT treads. The occurrence of patterned ground is directly related to CT form, i.e., flat treads, and helps to explain formation process attributable to CTs, i.e., prevention of weathered rampart accumulations.

The results presented in this study provide substantial evidence for the hydrologic significance of periglacial assemblages existing as parts of CT treads, and demonstrate the efficacy of periglacial processes in landscape formation, a phenomenon that has been indicated in other periglacial regions, (e.g., Paquette et al., 2014). The hydrologic significance of other fluvial features in permafrost environments, known as water tracks, has also been noted in recent years (Levy et al., 2011; Paquette et al., 2017b, 2018). These smaller periglacial water-related features can impart significant controls on periglacial hillslope hydrology. By considering cryoplanation landforms as integral, functional parts of the periglacial assemblage, an integrated perspective on the upland periglacial environment is obtained. These "most striking features of the landscape" (Prindle 1905, 1913) are equally notable for their ubiquity (Brunnschweiler, 1965; Reger, 1975). Minor periglacial landforms, including sorted patterned ground, blockfields, and solifluction lobes, occupy distinct functional niches in the creation of cryoplanated terrain. *Rather than simply being "superimposed" on terrain, the microforms actively contribute to sculpting it*, imparting both a characteristic geomorphometric signature (Queen, 2018) and a distinctively periglacial appearance to the landscape.

7.2.3 Frost Ridge as the type locality for the "periglacial conveyor system". The uppermost patterned ground field on Frost Ridge exemplifies the conveyor model and highlights the dynamic nature of upland periglacial assemblages (Figure 7.1). The micro- and meso-scale features are integral components of the nivation process suite, the various components of which are represented by photos around the periphery. The tread is a tessellated surface composed of interconnected periglacial microforms functioning as an integrated system for moving weathering products from the snowbank vicinity, across the CT tread, and on to lower elevations. The conveyor-system model of sediment transport on CT treads presents a new and compelling argument in favor of the nivation hypothesis of CT formation.

As noted above, many elements of the periglacial literature describe periglacial microforms as having been *superimposed* atop pre-existing topography (e.g., Berthling & Etzelmüller, 2001). From a process perspective, however, it bears repeating that this term fails to convey what is perhaps the most important consideration for the long-term evolution of upland periglacial geomorphic landscapes: upland periglacial assemblages function as *systems* that interact through scale linkages to create distinctively periglacial topography ("a characteristic periglacial landscape"). This concept is well illustrated by the uppermost cryoplanation terrace on Frost Ridge:

> *From a vantage point midway up Splinter Peak (Figure 7.1) the observer gains a vivid impression of the periglacial processes and landforms that constitute Brunnschweiler's "altiplanorium" concept—terminology presented to describe systems of smaller periglacial forms that comprise landscape-scale features* (Brunnschweiler, 1965). *The fundamental unit of*

the altiplanorium, cryoplanation terraces, are maintained under the influence of minor periglacial features, which provide evidence for the dynamic system of weathered material transport: lobate solifluction tongues, alluvial fan-like silt deposits that extend from coarse stripe termini, audible flowing of water through coarse stripes, the appearance of needle ice, and accumulations of angular fragments on the upslope sides of large immobile boulders. The periglacial features on Frost Ridge form a continuous tessellation with a geometric pattern reminiscent of a distributary drainage system, an organization that operates to remove weathered material from the scarp-tread junction and transport it over the tread. Water flows rapidly through the interstitial spaces of coarse gutters, or slowly as pulses of moisture through fine-textured soil stripes. During periods of diurnal freeze-thaw action, the phase change of water results in the incremental downslope movement of soil via frost creep and the growth and ablation of needle ice. The sorted stripe features on Frost Ridge and associated periglacial processes comprise a system of transport in which material is excavated from the vicinity of the snowpatch margin, exposing new material to the influence of nivation, leading to the retreat of CT scarps and tread extension.

As noted in Chapter 3 of this thesis, the large patterned-ground field at the confluence of Splinter Peak and Frost Ridge had a far less dynamic appearance in the late 2010s than it did in the mid-1970s. This may be attributable to the fact that the snowbank at this location disappears much earlier in recent years than it did in the 1970s. This crossing of a “tipping point” in the intervening years could be reversed by artificial augmentation of the snowpack. A critical experiment will form the next phase of research on Frost Ridge.

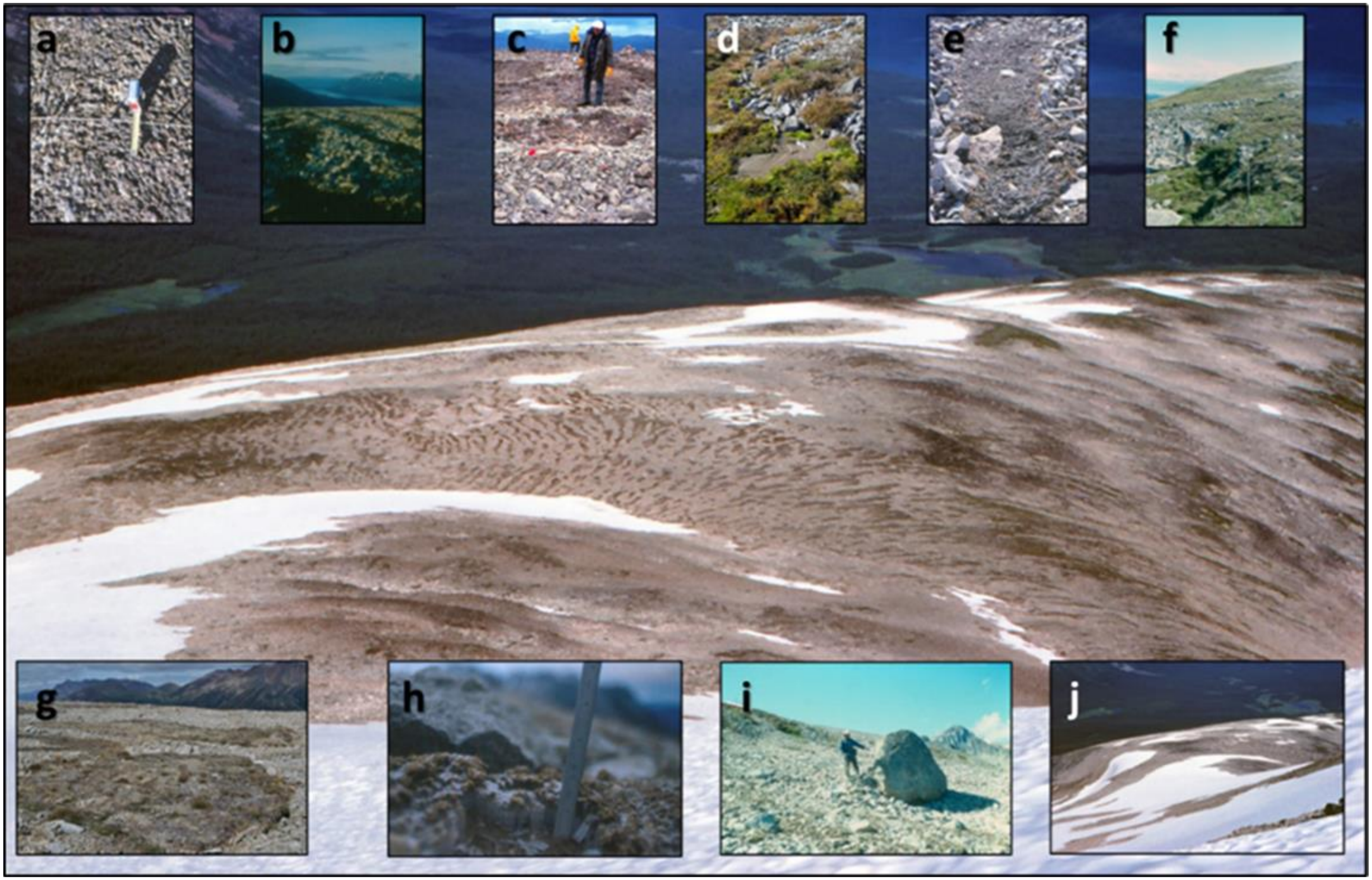

Figure 7.1 "The Conveyor System". *(Seen from mid-slope on Splinter Peak) (a) Movement pegs displaced two years after emplacement in a T1 fine (solifluction) stripe by V. Jones. Pegs were installed in summer 1974 and show 1-2 cm downslope movement. Photo by C. Cialek, August 1976.*

Figure 7.1 (cont'd). *(b) Sorted stripes on T1. Sorting extends to the depth of 80 cm, below which it is inhibited by the presence of permafrost. Water could be heard running in these coarse "gutters" throughout the summers of 1975 and 1976. Photo by F. Nelson, August 1975. (c) Sorted circle near crest of Frost Ridge on flattest part of T1 tread surface. Despite the low gradient, water flowed through the coarse segment of this feature. JIRP Director Maynard M. Miller standing just beyond the sorted circle. See Figure 2.1. Photo by C. Cialek, August 1976. (d) silt fan formed by sediment exiting sorted stripe, near distal edge of T2. Photo by F. Nelson, July 2019. (e) Solifluction lobe flowing in "corridor" created by coarse portions of the sorted stripes atop T1. Note stone-banked front and concentric parabolic furrows pointing downslope, indicative of movement. Photo by C. Cialek, August 1976. (f) Large turf-banked solifluction lobe immediately downslope of distal edge of T1 tread. Robert L. Nichols near center of photo. Photo by F. Nelson, August 1976. (g) Splaying solifluction lobes on T1 tread, formed where the fine stripes encounter a decrease in slope angle. Note that splaying lobes have buried the bounding coarse stripes. Photo by F. Nelson, August 1975. (h) needle ice with superincumbent load formed atop fine stripe on T1 terrace. Photo by F. Nelson, September 1975. (i) Large boulder, possibly rooted in permafrost, in vicinity of T3. Note accumulation of clastic material on upslope side of boulder, probably emplaced by frost creep. (j) Snowpatch at scarp-tread junction of T1. Photo by C. Cialek, August 1976.*

7.3 Conclusions

This study is among the first to relate quantitative field-based and remotely sensed data to cryoplanation terrace formation. One of the primary contributions of this work is the proposition, supported by process-focused investigations, that periglacial patterned ground plays a significant role in water/sediment transportation on CT treads, thereby providing an important dimension to the nivation hypothesis of cryoplanation terrace formation. From this analysis of hillslope hydrology, the main conclusions of this study are derived:

- The presence of sorted patterned ground does not indicate geomorphic quiescence. Well-developed patterned ground networks facilitate geomorphic activity through hydrologic processes.

- Sorted patterned ground constitutes a transportation network that promotes the toe-ward and lateral transmission of water and sediment, despite the seemingly flat microtopography of the CT tread.
- Coarse stripes anchored in permafrost form the “backbone” of CT treads, effectively stabilizing the patterned ground field, and facilitating rapid transmission of water and sediment through boulder gutters. Ancillary sediment evacuation occurs as solifluction in the intervening “corridors,” moving weathered material across and over CT treads and sidewalls.
- Sorted patterned ground, solifluction lobes, and other periglacial microforms are not simply “superimposed” atop broader-scale terrain. These features perform important, interconnected functional roles in sculpting the distinctively periglacial topography typified by cryoplanation terraces.
- The arrangement of sorted stripes on Frost Ridge resembles a fluvial network characterized by interconnected features that extend from the snowpatch to terrace margins. The apparent organization of the sorted-stripe networks underlines their propensity for efficient water transportation and points to a fluvial origin for sorted stripes.

7.4 Recommendations for Future Work

7.4.1 Long-term process investigations. Process investigations conducted for this study can be extended and enhanced through continued monitoring efforts and through installation of additional loggers on Terraces 2 and 4. The short-term temperature and soil moisture records established in this study would be complemented by continued data collection at similar temporal resolutions, i.e., 5-minute logging intervals, to capture both long-term patterns and short-term pulses in the fine and coarse stripe records. The resulting highly detailed records would contribute substantially to future exploration of the ground thermal regime and for establishing data for long-term monitoring studies. Temperature sensors should be installed at additional depths on both Terrace 2 and Terrace 4 to characterize the thermal processes operating in fine and coarse stripes. Based on the initial results derived from this study, continued monitoring of patterned ground on active CT terraces through repeat UAV survey and process measurements would complement efforts to define more precisely the role of patterned ground in periglacial hydrology, an association that has been indicated in previous research, but has yet to be widely embraced (Paquette, 2017). Mapping of the permafrost table via ground-penetrating radar (GPR) at key locations on Frost Ridge would confirm underlying permafrost conditions, complementing the morphometric characterization of the patterned ground network.

7.4.2 Broader implications of Frost Ridge periglacial studies. The work reported in this study has potential to assist in the resolution of some outstanding questions in Quaternary studies. Continued monitoring efforts of the periglacial activity on Frost Ridge, such as those established in this study, are critical in developing an extensive body of quantitative data to achieve a definitive theory of cryoplanation terrace formation. Both relict cryoplanation terraces and sorted patterned ground have been reported widely in the Appalachian Mountains south of the glacial border (e.g., Braun, 1989; Clark & Ciolkosz, 1988; Clark & Hedges, 1992; Clark & Schmidlin 1992), but the periglacial affinities of some of these features has been challenged (e.g., Kerwan, 2001). Application of the fluvial morphometric methods employed in Chapter 6 to fields of relict sorted stripes could help to resolve such differences.

Future mapping and monitoring efforts focused on the permafrost of Frost Ridge would also contribute to efforts related to investigating the response of areas affected by permafrost to warming global temperatures, and contributing to a growing area of research in periglacial geomorphology (Ballantyne, 2018, 2). The response of underlying permafrost conditions and snow accumulation to warming temperatures has the capacity to impact the formation and distribution of sorted stripes, which have been shown to influence the distribution of vegetation, nutrient transport, and hillslope-scale hydrologic connectivity (Paquette et al., 2017; 2018). Continued monitoring of sorted stripe morphology and underlying permafrost are therefore critical to assess changes in CT response to warming temperatures and will provide input for climate and geomorphic modeling that result in improved assessments of the effects of environmental change.

APPENDIX

Table A.1 Chapter 5 data logging equipment information.

Tool	*Purpose/description*	*Specifications*	*URL*
Hobo® TidbiT® MX Temp 400 (MX2203)	Measure temperatures in water bodies and soil environments	• Temperature range: -20° to 70°C • Accuracy: ± 0.25 °C from -20° to 0°C; ±0.2°C from 0° to 70°C • Resolution: 0.01°C • Dimensions: 4.45 x 7.32 x 3.58 cm	https://www.onsetcomp.com/products/data-loggers/mx2203/
Soil Moisture Smart Sensor (S-SMx-M005)	Measure soil water content	• Measurement range: 0 to 0.550 m^3/m^3; Temperature range 0° to 50°C • Accuracy: ±0.031 m^3/m^3 • Resolution: 0.0007 m^3/m^3 • Probe dimensions: 89 x 15 x 1.5 mm	https://www.onsetcomp.com/products/sensors/s-smd-m005/
HOBO® Micro Station (H21-USB)	Store data recorded from temperature and soil moisture sensors	• Operating Range: -20° to 50°C • Time accuracy: ±5 seconds per week at 25°C	https://www.onsetcomp.com/products/data-loggers/h21-usb/
12-Bit Temperature Smart Sensor 9s-TMB-M0xx)	Temperature monitoring	• Temperature range: -40° to 100°C • Accuracy: < ±0.2° from 0° to 50°C • Resolution: <0.03°C from 0° to 50°C • Probe Dimensions: 5.1 x 33 mm	https://www.onsetcomp.com/products/sensors/s-tmb-m0xx/

Table A.2 Chapter 6 GIS tools information.

Tool	*Source*	*Information/operation*	*URL*
Stream Order	ArcMap	Stream ordering- assign a numeric order to links in a stream network using the Strahler (1957) method which assigns an order of 1 to all links without any tributaries	https://desktop.arcgis.com/en/arcmap/10.3/tools/spatial-analyst-toolbox/how-stream-order-works.htm#ESRI_SECTION1_332E8909620C461B9B991A7FC1A5E843
Polyline	ArcMap	Digitizes coarse patterned ground—constriction template tool implemented within the *Create Features* window	https://desktop.arcgis.com/en/arcmap/10.3/manage-data/editing/what-is-editing-.htm#ESRI_SECTION1_8E30256BC6C5408C832128CF45C36C5B
Hillshade	ArcMap	Reveals minor periglacial features- a grayscale representation of the surface that takes the sun's relative position into account to shade the image. Default azimuth; 315°, and sun height; 45°, were used.	https://desktop.arcgis.com/en/arcmap/10.3/manage-data/raster-and-images/hillshade-function.htm
r.fill.dir	GRASS	Fill DEM—generates a depressionless elevation map, and flow direction map. All depressions within the input elevation raster are filled, subsequent filling occurs if the flow direction algorithm identifies additional pits.	https://grass.osgeo.org/grass78/manuals/r.fill.dir.html
r.watershed	GRASS	Flow direction (using D8method) and flow accumulation	https://grass.osgeo.org/grass78/manuals/r.watershed.html#description
r.mapcalc	GRASS	Defines flow accumulation threshold- raster map calculator that performs user-defined arithmetic expressions	https://grass.osgeo.org/grass78/manuals/r.mapcalc.html

REFERENCES

REFERENCES

Arnold, J. G., Srinivasan, R., Muttiah, R. S., & Williams, J. R. (1998). Large area hydrologic modeling and assessment part I: Model development. *JAWRA Journal of the American Water Resources Association*, *34*(1), 73–89.

Andersson, J. G. (1906). Solifluction, a component of subaërial denudation. *The Journal of Geology*, *14*(2), 91–112.

Ballantyne, C. K. (2018). *Periglacial Geomorphology* (1st ed.). Hoboken, NJ: John Wiley & Sons.

Beckinsale, R.D. & Chorley, R.J. (1991). *The History of the Study of Landforms or the Development of Geomorphology, Volume 3: Historical and Regional Geomorphology 1890-1950.* London and New York: Routledge, 496 pp.

Benedict, J. B. (1970). Downslope soil movement in a Colorado alpine region: Rates, processes, and climatic significance. *Arctic and Alpine Research*, *2*(3), 165–226.

Berthling, I., & Etzelmüller, B. (2011). The concept of cryo-conditioning in landscape evolution. *Quaternary Research*, *75*(2), 378–384.

Bernatek, A. (2015). Visualizing morphometric changes in a piping system using DEM and GIS analysis: the Bieszczady Mts., Poland. *In:* Jasiewicz, J., Zwoliński, Zb., Mitasova, H. & Hengl, T. (eds.). *Geomorphometry for Geosciences* Poznan, Poland: International Society for Geomorphometry, 157-160.

Beven, K. J., & Kirkby, M. J. (1979). A Physically Based, Variable Contributing Area Model of Basin Hydrology. *Hydrological Sciences Journal*, *24*(1), 43–69. Taylor & Francis.

Boyd, D. S. (2009). Remote sensing in physical geography: A twenty-first-century perspective. *Progress in Physical Geography*, *33*(4), 451–456.

Bradshaw, M. (1982). Process, time and the physical landscape: Geomorphology today. *Geography*, *67*(1), 15–28.

Braun, D.D. (1989). Glacial and periglacial erosion of the Appalachians. *Geomorphology* 2(1): 233-256.

Brunn, S. D., Cutter, S. L., & Harrington Jr, J. (2004). *Geography and Technology* (1st ed.). New York: Springer Science & Business Media.

Bryan, K. (1946). Cryopedology, the study of frozen ground and intensive frost-action, with suggestions on nomenclature. *American Journal of Science*, *244*(9), 622–642.

Büdel, J. (1948) Das System der klimatischen Geomorphology. *Verhandl. Deutscher Geographie* 27: 65-100. English translation: The climatic geomorphic system. *In:* Derbyshire, E. (ed.), *Climatic Geomorphology*. London, The MacMillan Press, 104-130.

Büdel, J. (1948b). Die klima-morphologischen Zonen der Polarländer. *Erdkunde* 2(1/3): 22-53

Büdel, J. (1977). *Klima-Geomorphologie*. Berlin: Gebrüder Borntraeger, 304 pp. English translation: *Climatic Geomorphology.* Princeton, NJ: Princeton University Press, 443 pp.

Brunnschweiler, D. (1965). The morphology of altiplanation in interior Alaska. Unpublished report to US Army Cold Regions Research and Engineering Laboratory, Hanover NH. 48 pp.

Caine, T. N. (1963). The Origin of Sorted Stripes in the Lake District. Northern England. *Geografiska Annaler*, *45*(2/3), 172–179.

Cairnes, D. D. (1912). Differential erosion and equiplanation in portions of Yukon and Alaska. *Bulletin of the Geological Society of America*, *23*(1), 333–348.

Campbell, J. B., & Wynne, R. H. (2011). *Introduction to Remote Sensing, Fifth Edition* (5th ed.). New York: Guilford Press.

Christiansen, H. H. (1996). Effects of nivation on periglacial landscape evolution in western Jutland, Denmark. *Permafrost and periglacial processes*, *7*(2), 111–138.

Clark, G.M. and Schmidlin, T.W. 1992. Alpine periglacial landforms of eastern North America: A review. *Permafrost and Periglacial Processes*, 3: 225-230.

Clark, G.M. and Ciolkosz, E.J. (1988). Periglacial geomorphology of the Appalachian Highlands and interior highlands south of the glacial border - a review. *Geomorphology*, 1: 191-220.

Clark, G.M. and Hedges, J. (1992). Origin of certain high-elevation local broad uplands in the central Appalachians south of the glacial border, U.S.A. - A peleoperiglacial hypothesis. *In:*Dixon, J.C. and Abrahams, A.D. (eds.)*, Periglacial Geomorphology*. John Wiley & Sons, Chichester, New York, Brisbane, Toronto, Singapore, 31-61.

Colpron, M., & Nelson, J. (2011). A Digital Atlas of Terranes for the Northern Cordillera, Yukon Geological Survey. Retrieved May 23, 2020, from http://yukon.maps.arcgis.com/apps/webappviewer/index.html?id=b7fa3a4a0ad94ed19412bbad5ec6ab72

Colwell, R. N. (1966). Uses and limitations of multispectral remote sensing. *Proceedings of the 4th International Symposium on Remote Sensing*. University of Michigan, Ann Arbor, MI.

Czeppe, Z. (1961) Participation of flowing water in creation of the periglacial microrelief. *In*: International Association for Quaternary Research (INQUA), 6th Congress, Warsaw, Poland, August-September 1961: 8g.

Davis, W.M (1909). *Geographical Essays*, Boston: Ginn and Company.

Demek, J. (1968). Cryoplanation terraces in Yakutia. *Biuletyn Peryglacjalny* 17: 91-16.

Demek, J. (1969). Cryoplanation terraces, their geographical distribution, genesis and development. *Rozpravy Ceskoslovenski Akademi ved, Rada, Matematickych a Prirodnich*, *79*(4), 80.

Dixon, J.C., Thorn, C.E., and Darmody, R.G. (1984). Chemical weathering processes on the Vantage Peak nunatak, Juneau Icefield, southern Alaska. *Physical Geography* 5(2): 111-131.

Eakin, H. M. (1916). The Yukon-Koyukuk region, Alaska. *U.S. Geological Survey Bulletin* 631, 88 pp.

Eichel, J., Draebing, D., Katenborn, T., Senn, J.A., Klingleil, L., Wiel, M., and Heinz, E. (2020). Unmanned aerial vehicle-based mapping of turf-banked solifluction lobe movement and its relation to material, geomorphometric, thermal and vegetation properties. *Permafrost and Periglacial Processes* 31:97-109. DOI: 10.1002/ppp.2036

Embleton, C., & King, C. A. M. (1975). *Periglacial Geomorphology*. New York: John Wiley & Sons.

Environmental Systems Research Institute, Inc. (2020). *ArcGIS*. Redlands, CA: Environmental Systems Research Institute Inc.

Evans, D.J.A., Kalyan, R., & Orton, C. (2017). Periglacial geomorphology of summit tors on Bodmin Moor, Cornwall, SW England. *Journal of Maps*. 13(2): 342-349. DOI: 10. 1080/17445647.2017.1308283

Fernandez, E., Garfinkel, R., & Arbiol, R. (1998). Mosaicking of aerial photographic maps via seams defined by bottleneck shortest paths. *Operations Research*, *46*(3), 293–304.

Field, W. O., & Miller, M. M. (1950). The Juneau Ice Field Research Project. *Geographical Review*, *40*(2), 179.

French, H. M. (2016). Do periglacial landscapes exist? A discussion of the upland landscapes of northern interior Yukon, Canada. *Permafrost and Periglacial Processes*, *27*(2), 219–228.

French, H. M. (2017). *The Periglacial Environment* (4th ed.). Hoboken, NJ: John Wiley & Sons.

Gerloch Trough Runoff Sediment Sampler. (2018). *Rickly Hydrological Co., Inc.* Retrieved April 10, 2020, from https://rickly.com/gerloch-trough-runoff-sediment-sampler/

Gleyzer, A., Denisyuk, M., Rimmer, A., & Salingar, Y. (2004). A Fast Recursive Gis Algorithm for Computing Strahler Stream Order in Braided and Nonbraided Networks1. *Journal of the American Water Resources Association*, *40*(4), 937–946.

Godin, E., Osinski, G.R., Harrison, T.N., Pontefract, A., and Zanetti, M. (2019). Geomorphology of gullies at Thomas Lee Inlet, Devon Island, Canadian high Arctic. *Permafrost and Periglacial Processes* 30: 19-34. DOI: 10.1002/ppp. 1992.

Goldthwait, R. P. (1976). Frost sorted patterned ground: a review. *Quaternary Research*, *6*(1), 27–35.

Goudie, A. (1990). *Geomorphological Techniques* (2nd ed.). London, UK: Unwin Hyman Ltd.

GRASS Development Team. (2019). *GRASS GIS*. Open Source Geospatial Foundation. Retrieved from https://grass.osgeo.org

Hamelin, L.-E. (1964). Le périglaciare du Massif Juneau en Alaska. *Biuletyn Peryglacjalny*, 13: 5-14.

Hajam, R. A., Hamid, A., & Bhat, S. (2013). Application of morphometric analysis for geo-hydrological studies using geo-spatial technology–a case study of Vishav Drainage Basin. *Hydrology Current Research*, *4*(3), 1–12.

Hallet, B. (1990). Spatial self-organization in geomorphology: from periodic bedforms and patterned ground to scale-invariant topography. *Earth-Science Reviews*, *29*(1–4), 57–75.

Heusser, C. (2007). *Juneau Icefield Research Project (1949-1958)*. Oxford, UK: Elsevier.

Hobbs, W.H. (1910). Soil stripes in cold humid regions, and a kindred phenomenon. *12th Report, Michigan Academy of Science*, 51-53.

Hodgson, R., & Young, K. L. (2001). Preferential groundwater flow through a sorted net landscape, Arctic Canada. *Earth Surface Processes and Landforms*, *26*(3), 319–328.

Horton, R. E. (1945). Erosional development of streams and their drainage basins; hydrophysical approach to quantitative morphology. *Geological society of America bulletin*, *56*(3), 275–370.

Hövermann, J. and Oberbeck, G. (eds., 1972). Hans-Poser-Festschrift. *Göttinger Geographicsche Abhandlungen*, 60, 571 pp. + maps, diagrams.

Humlum, O. (2008). Alpine and polar periglacial processes: The current state of knowledge (p. 8). Presented at the Ninth International Conference on Permafrost, University of Alaska Fairbanks.

Jayawardena, A. W. (2014). *Environmental and Hydrological Systems Modelling*. Boca Raton, FL: CRC Press.

Jensen, J. R. (1995). Issues involving the creation of digital elevation models and terrain corrected orthoimagery using soft-copy photogrammetry. *Geocarto International*, *10*(1), 5–21. Taylor & Francis.

Johnson, R. F. (1983). *Ice movement and structural characteristics of the Cathedral Glacier system, Atlin Provincial Park, British Columbia* (M.S. Thesis). Department of Earth Sciences, Montana State University, Bozeman, Montana.

Johnston, G.H., Ladanyi, B., Morgenstern, N.R., and Penner, E. (1981). Engineering characteristics of frozen and thawing soils. *In:* Johnston, G.H. (ed.), *Permafrost: Engineering Design and Construction*. Toronto: John Wiley & Sons, 73-147.

Jones, V. K. (1975). *Contributions to the Geomorphology and Neoglacial Chronology of the Cathedral Glacier System, Atlin Wilderness Park, British Columbia.* (M.S. Thesis), Department of Geology, Michigan State University, East Lansing, MI.

Kamp, U., Bolch, T., & Olsenholler, J. (2005). Geomorphometry of Cerro Sillajhuay (Andes, Chile/Bolivia): comparison of digital elevation models (DEMs) from ASTER remote sensing data and contour maps. *Geocarto International*, *20*(1), 23–33. Taylor & Francis.

Karte, J. (1979). Räumliche Abgrenzung und regionale Differenzierung des Periglaziärs. *Bochumer Geographische Arbieten*, 35, 211 pp.

Karte J. (1982). Development and present state of German periglacial research in Arctic and alpine environments. *Biuletyn Peryglacjalny*, 29, 183-201.

Kerwan, M.L. (2001). *Origin and evolution of High Elevation Southern Appalachian Plateaus*. (M.S. Thesis), Department of Geology, The College of William and Mary.

Kessler, M. A. (2003). Self-organization of sorted patterned ground. *Science*, *299*(5605), 380–383.

Kessler, M.A., Murray, A., Werner, B., & Hallet, B. (2001). A model for sorted circles as self-organized patterns. *Journal of Geophysical Research: Solid Earth*, *106*(B7), 13287–13306.

Křížek, M., Krause, D., Uxa, T., Engel, Z., Treml, V., & Traczyk, A. (2019). Patterned ground above the alpine timberline in the high Sudetes, central Europe. *Journal of Maps* 15(2): 563-569. DOI: 1080/17445647.2019.1636890

Lauriol, B., Lamirande, I., & Lalonde, A. E. (2006). The giant steps of Bug Creek, Richardson Mountains, NWT, Canada. *Permafrost and Periglacial Processes*, *17*(3), 267–275. Wiley Online Library.

Levy, J. S., Fountain, A. G., Gooseff, M. N., Welch, K. A., & Lyons, W. B. (2011). Water tracks and permafrost in Taylor Valley, Antarctica: Extensive and shallow groundwater connectivity in a cold desert ecosystem. *GSA Bulletin*, *123*(11–12), 2295–2311.

von Lozinski, W. (1909). *Über die Mechanische Verwitterung der Sandsteine im Gemässigten Klima*. *Acad Sci, Cracovie Bull. Internat. cl. sci. math et naturelles.* 1, 1-25 (English Translation: On the Mechanical Weathering of Sandstones in Temperate Climates.

MacIntyre, D., Villeneuve, M., & Schiarizza, P. (2001). Timing and tectonic setting of Stikine Terrane magmatism, Babine-Takla lakes area, central British Columbia. *Canadian Journal of Earth Sciences*, *38*(4), 579–601. NRC Research Press.

Martins, A. K., & Gadiga, B. L. (2015). Hydrological and morphometric analysis of upper Yedzaram catchment of Mubi in Adamawa state, Nigeria usingg eographic information system (GIS). *World Environment*, *5*(2), 63–69.

Martonne, E. de (1913). Le climat-facteur du relief. *Scientia* 1913: 339-355. English translation: Climate: Factor of relief. *In:* Derbyshire, E. (ed.), *Climatic Geomorphology*. London, The MacMillan Press, 61-75.

Martz, L. W., & Garbrecht, J. (1992). Numerical definition of drainage network and subcatchment areas from digital elevation models. *Computers & Geosciences*, *18*(6), 747–761.

Matthes, F. E. (1900). Glacial sculpture of the Bighorn Mountains, Wyoming. *US Geological Survey Twenty-first Annual Report Part II*, 167–190.

Matthews, J., Wilson, P., Winkler, S., Mourne, R., Hill, J., Owen, G., Hiemstra, J., et al. (2019). Age and development of active cryoplanation terraces in the alpine permafrost zone at Svartkampan, Jotunheimen, southern Norway. *Quaternary Research*, *92*, 641–664.

McCann, S., Howarth, P., & Cogley, J. (1972). Fluvial processes in a periglacial environment: Queen Elizabeth Islands, NWT, Canada. *Transactions of the Institute of British Geographers*, 69–82. JSTOR.

McNamara, J., Kane, D., & Hinzman, L. (1998). An analysis of streamflow hydrology in the Kuparuk River basin, Arctic Alaska: A nested watershed approach. *Journal of Hydrology*, *206*(1–2), 39–57.

McNamara, J., Kane, D., & Hinzman, L. (1999). An analysis of an arctic channel network using a digital elevation model. *GEOMORPHOLOGY*, *29*(3–4), 339–353.

Melton, M. A. (1957). *An Analysis of the Relations among Elements of Climate, Surface Properties, and Geomorphology* (Technical Report No. 11) (pp. 100). Office of Naval Research, Department of Geology, Columbia University, New York, NY.

Mertie, J. B. (1937). *The Yukon-Tanana Region, Alaska* (p. 276). U.S. Geological Survey Bulletin 872.

Miller, M. M. (1975). *Mountain and Glacier Terrain Study and Related Investigations in the Juneau Icefield Region, Alaska-Canada* (No. AD-A019 703) (p. 265). Seattle, Washington: Foundation for Glacier and Environmental Research.

Mithan, H.T., Hales, T.C., & Cleall, P.J. (2019). Supervised classification of landforms in Arctic mountains. *Permafrost and Periglacial Processes* 30: 131-145. DOI: 10.1002/ppp2015

Monger, J. (1977). *Upper Paleozoic rocks of the Atlin Terrane, northwestern British Columbia and South-Central Yukon.* (No. 77–1A) (pp. 255–262). Geological Survey of Canada.

Monger, J., Souther, J., & Gabrielse, H. (1972). Evolution of the Canadian Cordillera; a plate-tectonic model. *American Journal of Science*, *272*(7), 577–602. American Journal of Science.

Mortensen, H. (1930). Einige Oberflächenformen in Chile und auf Spitsbergen im Rahmen einer vergleichenden Morphologie der Klimazonen. *Petermanns Geographische MittelungenErgänzungscheft* 209: 147-156.

Mulvaney, T. J. (1851). On the use of self-registering rain and flood gauges in making observations of the relations of rainfall and flood discharges in a given catchment. *Proceedings of the institution of Civil Engineers of Ireland*, *4*, 19–31.

Nelson, F. E. (1975). *Periglacial Features on the Cathedral Massif, northwestern British Columbia: A Preliminary Investigation* (Open File No. 75). Seattle, Washington: Juneau Icefield Research Program and The Foundation for Glacier and Environmental Research, 36 pp.

Nelson, F. E. (1979). *Patterned Ground in the Juneau Icefield Region, Alaska-British Columbia* (M.S. Thesis). Department of Geography, Environment, and Spatial Sciences, Michigan State University, East Lansing, MI.

Nelson, F. (1982a). Sorted-circle macrofabrics. *Polarforschung* 52(1/2): 43-53.

Nelson, F. (1982b). Sorted-stripe macrofabrics. *Geografiska Annaler* 64A(1-2): 25-33.

Nelson, F. E. (1989). Cryoplanation terraces: Periglacial cirque analogs. *Geografiska Annaler: Series A, Physical Geography*, *71*(1–2), 31–41.

Nelson, F. E. (1998). Cryoplanation terrace orientation in Alaska. *Geografiska Annaler: Series A, Physical Geography*, *80*(2), 135–151.

Nelson, F. E., & Nyland, K. E. (2017). Periglacial cirque analogs: Elevation trends of cryoplanation terraces in eastern Beringia. *Geomorphology*, *293*, 305–317.

Nelson, F., Outcalt, S., Goodwin, C., & Hinkel, K. (1985). Diurnal thermal regime in a peat-covered palsa, Toolik Lake, Alaska. *Arctic*, 310–315. JSTOR.

Nyland, K.E., & Nelson, F. E. (2020). Time-transgressive cryoplanation terrace development through nivation-driven scarp retreat. *Earth Surface Processes and Landforms*, *45*(3), 526–534. Wiley Online Library.

Nyland K.E., & Nelson, F. E. (2020). Long-term nivation rates, Cathedral Massif, northwestern British Columbia. *Canadian Journal of Earth Sciences*. DOI: 10.1139/cjes-2019-0176

Nyland, K. E. (2019). *Stairways to Heaven: Origins and Development of Cryoplanation Terraces* (Ph.D Thesis). Department of Geography, Environment, and Spatial Sciences, Michigan State University, East Lansing, MI.

O'Callaghan, J. F., & Mark, D. M. (1984). The extraction of drainage networks from digital elevation data. *Computer vision, graphics, and image processing*, *28*(3), 323–344.

Onset HOBO and InTemp Data Loggers. 470 MacArthur Blvd. Bourne, MA 02532: Onset Computer Corporation.

Paquette, M., Fortier, D., & Vincent, W. F. (2014). *The geomorphic and hydrologic relation between water tracks development and patterned ground on a High Arctic slope.* Presented at the Fourth European Conference on Permafrost, Evora, Portugal. Retrieved from https://www.researchgate.net/publication/271645193_The_geomorphic_and_hydrologic_relation_between_water_track_development_and_patterned_ground_on_a_High_Arctic_slope/comments

Paquette, M., Fortier, D., & Vincent, W. F. (2017). Water tracks in the High Arctic: A hydrological network dominated by rapid subsurface flow through patterned ground. *Arctic Science*, *3*(2, SI), 334–353.

Paquette, M., Fortier, D., & Vincent, W. F. (2018). Hillslope water tracks in the High Arctic: Seasonal flow dynamics with changing water sources in preferential flow paths. *Hyrological Processes*, *32*(8), 1077–1089.

Pareta, K., & Pareta, U. (2011). Quantitative morphometric analysis of a watershed of Yamuna basin, India using ASTER (DEM) data and GIS. *International Journal of Geomatics and Geosciences*, *2*(1), 248–269.

Penck, A. (1905). Climatic features in the land surface. *American Journal of Science* (4th Series), 109: 165-174.

Porter, C., Morin, P., Howat, I., Noh, M.-J., Bates, B., Peterman, K., Keesey, S., et al. (2018). ArcticDEM. Harvard Dataverse. Retrieved May 19, 2020, from https://doi.org/10.7910/DVN/OHHUKH

Poser, H. (1931). Beiträge zur Kenntnis der Arktischen Bodenformen. *Geologische Rundschau* 22: 200-231.

Poser H. (ed., 1977). Formen, Formengesellschaften, und Untergrenzen in den heutigen Periglazialen Höhenstufen der Hochgebirge Europas und Africas zwischen Arktis und Äquator: Bericht über eine Symposium. *Abhandlungen der Akademie der Wissenschaften in Göttingen, Mathematische-physikalische Klasse*, Dritte Folge, 31: 354 pp.

Prindle, L. M. (1905). *The gold placers of the Fortymile, Birch Creek, and Fairbanks regions, Alaska*. U.S. Geological Survey Bulletin, 251, 89 pp.

Prindle, L.M. (1913). A geologic reconnaissance of the Circle Quadrangle, Alaska. *U.S. Geological Survey Bulletin 538*, 82 pp.

Queen, C. W. (2018). *Large-Scale Mapping and Geomorphometry of Upland Periglacial Landscapes in Eastern Beringia* (M.S. Thesis). Department of Geography, Environment, and Spatial Sciences, Michigan State University, East Lansing, MI.

Quinn, P., Beven, K., Chevallier, P., & Planchon, O. (1991). The prediction of hillslope flow paths for distributed hydrological modelling using digital terrain models. *Hydrological processes*, *5*(1), 59–79.

Quinton, W. L., & Marsh, P. (1999). Image analysis and water tracing methods for examining runoff pathways, soil properties and residence times in the continuous permafrost zone. *IUGG 99 Symposium HS4* (pp. 257–264). Presented at the Integrated Methods in Catchment Hydrology--Tracer, Remote Sensing and New Hydrometric Techniques, Birmingham: IAHS PRESS-INTERN ASSOC HYDROLOGICAL SCIENCE.

Rai, P. K., Mohan, K., Mishra, S., Ahmad, A., & Mishra, V. N. (2017). A GIS-based approach in drainage morphometric analysis of Kanhar River Basin, India. *Applied Water Science*, *7*(1), 217–232. Springer.

Rajeev, P. & Kodikara, J. (2016). Estimating apparent thermal diffusivity of soil using field temperature time series. *Geomechanics and Geoengineering* 11(1): 28-46. DOI: 10.1080/17486025.1006266

Reddy, G. P. O., Maji, A. K., & Gajbhiye, K. S. (2004). Drainage morphometry and its influence on landform characteristics in a basaltic terrain, Central India–a remote sensing and GIS approach. *International Journal of Applied Earth Observation and Geoinformation*, *6*(1), 1–16. Elsevier.

Reger, R. D. (1975). *Cryoplanation Terraces of Interior and Western Alaska* (Ph.D. Thesis). Arizona State University, Tempe, Arizona.

Reger, R. D., & Péwé, T. L. (1976). Cryoplanation terraces: Indicators of a permafrost environment. *Quaternary Research*, *6*(1), 99–109.

Rhoads, B. L. (2004). Whither physical geography? *Annals of the Association of American Geographers*, *94*(4), 748–755. Taylor & Francis.

Roels, J. M., & Jonker, P. J. (1983). Probability sampling techniques for estimating soil erosion. *Soil Science Society of America Journal*, *47*(6), 1224–1228.

Sack, D. (1992). New wine in old bottles: The historiography of a paradigm change. *Geomorphology*, *5*(3–5), 251–263.

Salomon, W. (1929). Arktisch Bodenformen in den Alpen. *Sitzber. Heidelberg Akademie Wissenschaften, Math.-Naturw Klasse*, 5: 1-31.

Schumm, S. A. (1956). Evolution of drainage systems and slopes in badlands at Perth Amboy, New Jersey. *Geological society of America bulletin*, *67*(5), 597–646. Geological Society of America.

Short, N. M., & Blair, R. W. (1986). *Geomorphology from space: A global overview of regional landforms*. Washington, DC: Scientific and Technical Information Branch, National Aeronautics and Space Administration.

Singh, V. P. (2018). Hydrologic modeling: Progress and future directions. *Geoscience Letters*, *5*(1: 1-18).

Slupetzky, H., & Krisai, R. (2009a). Indications of late glacial to Holocene fluctuations of Cathedral Massif Glacier, Coast Range (Northern British Columbia, Canada). *Zeitschrift für Gletscherkunde und Glazialgeologie*, *43*(44), 187–212.

Smart, J. (1978). The analysis of drainage network composition. *Earth Surface Processes*, *3*(2), 129–170. Wiley Online Library.

Smith, H.T.U. (1968). "Piping" in relation to periglacial boulder concentrations. *Biuletyn Peryglacjalny* 17: 204.

Smith, M., & Pain, C. (2009). Applications of remote sensing in geomorphology. *Progress in Physical Geography*, *33*(4), 568–582. Sage Publications Sage UK: London, England.

Statistics Canada. (2018, May). Stikine Region. British Columbia Statistics. Retrieved from https://www2.gov.bc.ca/assets/gov/british-columbians-our-governments/local-governments/governance-powers/stikine_region_map.pdf

Strahler, A. N. (1952). Dynamic basis of geomorphology. *Geological Society of America Bulletin*, *63*(9), 923–938.

Tallman, A. M. (1975). *The Glacial and Periglacial Geomorphology of the Fourth Of July Creek Valley, Atlin Region, Cassiar District, northwestern British Columbia* (Ph.D. Thesis). Department of Geology, Michigan State University, East Lansing, MI.

Tarboton, D. (1989). *The Analysis of River Basins and Channel Networks using Digital Terrain Data* (Ph.D Thesis). Massachusetts Institute of Technology, Cambridge, MA.

Taylor, B. (1955). Terrace formation on Macquarie Island. *The Journal of Ecology*, 133–137. JSTOR.

Thorn, C. E. (1976). Quantitative evaluation of nivation in the Colorado Front Range. *Geological Society of America Bulletin*, 87(8), 1169–1178.

Thorn, C. E., & Hall, K. (1980). Nivation: An Arctic-alpine comparison and reappraisal. *Journal of Glaciology*, *25*(91), 109–124.

Thorn, C. E., & Hall, K. (2002). Nivation and cryoplanation: The case for scrutiny and integration. *Progress in Physical Geography*, *26*(4), 533–550.

Thornbury, W.D. (1969). *Principles of Geomorphology*. New York: John Wiley & Sons, Inc., 594 pp.

Tricart, J. & Cailleux, A. (1972). *Introduction à la Géomorphologie Climatique*. Paris: Société d'Édition d'Enseignement Supérieur. English translation: *Introduction to Climatic Geomorphology*. New York: St. Martin's Press, 295 pp.

Troll C. (1944). Strukturböden, Solifluction und Frostklimate der Erde. *Geologische Rundschau* 34: 545-694. English translation: Structure Soils, Solifluction, and Frost Climates of the Earth. U.S. Army Snow Ice and Permafrost Research Establishment, Wilmette, IL., 1958, 121 pp.

Ule, W. (1911). Glazialer Karree -- eder Polygonenboden. *Zeitschrift Ges. Erkunde*, 253-262.

Uxa, T., Mida, P. & Křížek, M. (2017). Effect of climate on morphology and development of sorted circles and polygons. *Permafrost and Periglacial Processes* 28: 663-674. DOI: 10.1002/ppp.1949

Vittala, S., Govindaiah, S., & Honne Gowda, H. (2004). Morphometric analysis of sub-watersheds in the pavagada area of Tumkur district, South India using remote sensing and GIS techniques. *Journal of the Indian Society of Remote Sensing*, *32*(4), 351–362.

Washburn, A. L. (1956). Classification of patterned ground and review of suggested origins. *Geological Society of America Bulletin*, *67*(7), 823.

Washburn, A. L. (1969). *Weathering, frost action, and patterned ground in the Mesters Vig district, Northeast Greenland*. CA Reitzels.

Wilkinson, T. J., & Bunting, B. T. (1975). Overland transport of sediment by rill water in a periglacial environment in the Canadian high Arctic. *Geografiska Annaler. Series A, Physical Geography*, *57*(1/2), 105–116.

Williams, P. J., & Smith, M. W. (1989). *The Frozen Earth: Fundamentals of Geocryology*. Cambridge, UK: Cambridge University Press.

Wolock, D. M., & McCabe, G. J. (1995). Comparison of single and multiple flow direction algorithms for computing topographic parameters in TOPMODEL. *Water Resources Research*, *31*(5), 1315–1324.

Woo, M.-k. (1986). Permafrost hydrology in North America. *Atmosphere-Ocean*, *24*(3), 201–234.

Woo, M.-k. (2012). *Permafrost hydrology*. Berlin Heidelberg: Springer-Verlag.

Woo, M.-k., Kane, D. L., Carey, S. K., & Yang, D. (2008). Progress in permafrost hydrology in the new millennium. *Permafrost and Periglacial Processes*, *19*(2), 237–254.

Woo, M.-k., & Sauriol, J. (1980). Channel development in snow-filled valleys, Resolute, NWT, Canada. *Geografiska Annaler: Series A, Physical Geography*, *62*(1–2), 37–56. Taylor & Francis.

Woo, M.-k. (1976). Hydrology of a small Canadian High Arctic basin during the snowmelt period. *Catena*, *3*(2), 155–168. Elsevier.

Woo, M.-k. (2012). *Permafrost Hydrology*. Berlin Heidelberg: Springer-Verlag.

Zernitz, E. R. (1932). Drainage patterns and their significance. *Journal of Geology*, *40*(6), 498–521. JSTOR.

Zhang, W., & Montgomery, D. R. (1994). Digital elevation model grid size, landscape representation, and hydrologic simulations. *Water Resources Research*, *30*(4), 1019–1028. Wiley Online Library.